DANMARKS OG GRØNLANDS GEOLOGISKE UNDERSØGELSE RAPPORT 2012/63

Timing of deformation and structural styles along Fracture Zone/Transfer Zone in East Greenland and Faroese area: impact on plate tectonics, implications for inversion structures and basin architechture

Report for the SINDRI Group
Project C46-53-01

Pierpaolo Guarnieri, John R. Hopper
& Morten S. Andersen

GEOLOGICAL SURVEY OF DENMARK AND GREENLAND
DANISH MINISTRY OF CLIMATE, ENERGY AND BUILDING

GEUS

DANMARKS OG GRØNLANDS GEOLOGISKE UNDERSØGELSE RAPPORT 2012/63

Timing of deformation and structural styles along Fracture Zone/Transfer Zone in East Greenland and Faroese area: impact on plate tectonics, implications for inversion structures and basin architechture

Report for the SINDRI Group
Project C46-53-01

Pierpaolo Guarnieri, John R. Hopper
& Morten S. Andersen

Released 01.07.2012

GEOLOGICAL SURVEY OF DENMARK AND GREENLAND
DANISH MINISTRY OF CLIMATE, ENERGY AND BUILDING

G E U S

Table of contents

Abstract

The main task of the project was to evaluate the presence and importance of strike-slip structures in southern East Greenland to compare it with the Faroe margin, starting from an area in Kangerlussuaq (southern East Greenland). The overall aim of this project is to better define the tectonic evolution of the conjugate continental margins in the Faroe-Shetland area and southern East Greenland during the continental break-up and subsequent oceanic spreading. During fieldwork in 2009-2010 in southern East Greenland, structural analysis of major faults was carried out to better understand the tectonic setting of the Kangerlussuaq Basin and the structural significance of major NW-SE trending faults analogue to the transfer zones described in the Faroe-Shetland area. Fault-slip data collected along major fault systems document two episodes of strike-slip faulting in Middle-Late Paleocene and Late Eocene-Early Oligocene. The present study shows that the complex tectono-magmatic and sedimentary evolution of this area is related to four tectonic stages:

- The first documented faults activity (achieved from stratigraphic evidence eg. deepening of basin, erosion and major unconformities) is Late Cretaceous-Early Paleocene. This stage of rifting corresponds to a pull-apart formation along with NE-SW oriented rift faults and NW-SE transfer faults. The NE-SW oriented maximum horizontal stress derived from fault-slip data inversion together with the evidence of NNE-SSW right-lateral shear along the Agtertia Shear Zone are interpreted in relation with rotation and NE-ward motion of Greenland during the initial opening of the Labrador Sea;
- During Middle-Late Paleocene re-activation of former rift faults with strike-slip component, together with the en-echelon geometry and magmatic segmentation of macrodykes intruded at 55.8 Ma, are interpreted as evidence of oblique rifting during NW-SE extension and the activation of the left-lateral ENE-WSW oriented Kangerlussuaq Fracture Zone that linked the South East Greenland and the Norwegian Sea breakup;
- The Early Eocene breakup around 55.4 Ma is associated with coastal flexure and thermal subsidence during the emplacement of a thick sequence of Plateau Basalts. This tectonic stage is associated with intrusion of a sheeted dyke complex parallel to the present-day coastline together with land-ward dipping normal faults that accommodate the NW-SE extension;
- Post-breakup deformation is related to an E-W maximum horizontal stress. This strike-slip tectonic regime is interpreted as responsible for basin inversion and uplift of the area in Late Eocene-Early Oligocene in response to plate re-organization related to separation of the Jan Mayen micro-continent.

Finally, the onshore study in Kangerlussuaq indicates that this area can be considered a structural analogue to the Judd High, Judd Fault and Foinaven Basin in the Faroe-Shetland Chanel.

1. Introduction

1.1 The project

To fully understand the origin of potential trapping structures along the East Greenland and Faroes conjugate margins, a more complete model of the tectonic evolution of the North Atlantic along the Greenland-Iceland-Faroes Ridge is required. In particular, the final rifting and early breakup phase had a strong impact on prospective basins. The structures that developed during these stages likely controlled the subsequent evolution of the offshore basins.

In this project, we will:

- *carry out 3D-photogeology mapping and structural analysis of strike-slip faults oblique to the coast, from Kangerlussuaq up to Nansen Fjord;*
- *evaluate the offshore prolongation of these structures based on the available geophysical data (gravity, magnetics, seismic);*
- *compare and correlate these structures to the well documented transfer zones in the Faroes area;*
- *define a new tectonic framework to constrain the timing and kinematics of North Atlantic opening along the Greenland-Iceland-Faroes Ridge.*

By working with data from the East Greenland margin and combining the onshore structural data with offshore marine geophysical data, we can establish the regional importance of these strike-slip structures and determine the extent to which they can be correlated to similar features that have been studied in detail both onshore and offshore along the conjugate Faroes margin. This will enable a better understanding of the timing and mechanisms of their formation will give insight into the influence of various structures on basin architecture, including the interaction between lava sequences and the basin sediments.

Plate tectonic reconstructions during rifting and continental breakup of North Atlantic show the proximity of the Faroe Islands and the Blosseville Kyst (East Greenland). These areas are now situated about 1000 km apart, but in Paleocene time they were no more than 100-120 km apart (Fig. 1-1). Thus the evolution of the major basins in the two areas is closely linked. In addition, it is well documented that final breakup along this conjugate margin pair was accompanied by extremely voluminous volcanism. The relationship between sedimentary distribution systems and basin development during rifting, including the interplay between volcanic processes and sediments, has been the focus of a significant amount of work. Typically, onshore outcrop data are used as an analogue to better understand intrabasaltic sandstone in the offshore areas.

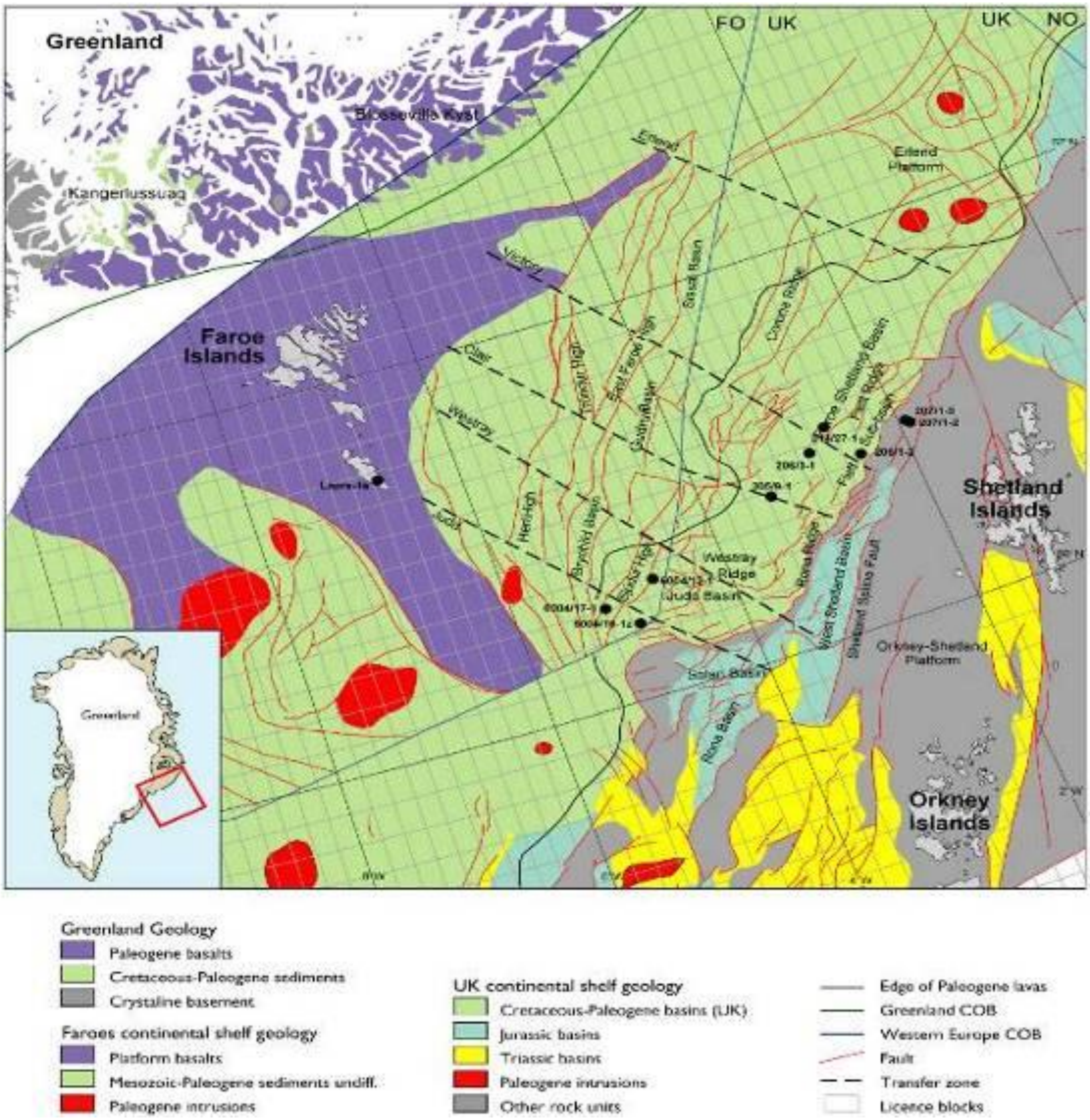

Fig. 1-1. *Location map of East Greenland and the Faroe-Shetland region depicting the paleogeography prior to the onset of seafloor spreading in the Late Paleocene-Early Eocene. After Larsen et al. (2005).*

In the Faroe-Shetland basin, recent studies have documented the presence of NW-SE oriented tectonic lineaments that are observed in seismic data and mark a series of transfer zones (Fig. 1-1). However, there remain significant unanswered questions regarding the kinematics and ages of these regional structures and their influence on basin development.

The presence of regional structures of similar orientation oblique to the main rift axis in East Greenland and in the Faroes link these two areas and is the starting point for this tectonic study. There is currently a significant lack of structural and tectonic studies on the East Greenland margin that can help to define the kinematics and relationships between these major fault systems and their importance during continental break-up and subsequent oceanic spreading. The origin and evolution of these structures have important implications for understanding the formation of possible trapping structures in prospective basins in the region as well as for understanding the structural controls on volcanic intrusion and extrusion during breakup and seafloor spreading and the impact of volcanic processes on the basin sediments.

The purpose of this project is to establish a new tectonic framework for breakup between East Greenland and the Faroes with the aim of defining the timing and style of deformation, as well as the relationships between faults, volcanic intrusions and sedimentation.

This structural/tectonic study that links the Faroes area and East Greenland will include:

- *constraining the timing of faulting;*
- *establishing the relationship between strike-slip tectonics and dike intrusion;*
- *determining the kinematics of transfer zones and fracture zones and their importance for regional tectonic models;*
- *defining the structural styles related to strike-slip tectonics and the formation of traps;*
- *documenting uplift and inversion structures (transpression);*
- *establishing the relationship between fault activity and sandstone units in basins;*

2. Geologic background and state-of-the-art

2.1 South East Greenland Volcanic Rifted Margin

The South East Greenland is a type example of a volcanic rifted margin. Based on the volume and production rates of volcanism, East Greenland marks breakup over a warmer than normal mantle (White and McKenzie, 1989; Nielsen and Hopper, 2002, 2004). Volcanic margins show distinctive genetic and structural features. High-rate extension of the lithosphere is associated with large scale mantle melting that is responsible for the accretion of a thick igneous crust. Distinctive structural features of volcanic margins are syn-magmatic and continent-ward dipping crustal faults accommodating the seaward flexure of the igneous crust (Fig. 2-1). Volcanic margins present along-axis magmatic and tectonic segmentation with wavelengths similar to adjacent slow-spreading ridges. Their 3D organisation suggests a connection between loci of mantle melting at depths and zones of strain concentration within the lithosphere. Break-up would start and propagate from localized thermally-softened lithospheric zones. These ‘soft points’ could be localized over small-scale convection cells found at the bottom of the lithosphere, where decompression mantle melting would occur (this is highly speculative and should be referenced). The particular structure of the brittle crust at volcanic passive margins could be influenced by active and sudden oceanward flow of both the unstable hot mantle and the ductile part of the lithosphere during the break-up stage (Geoffroy, 2005).

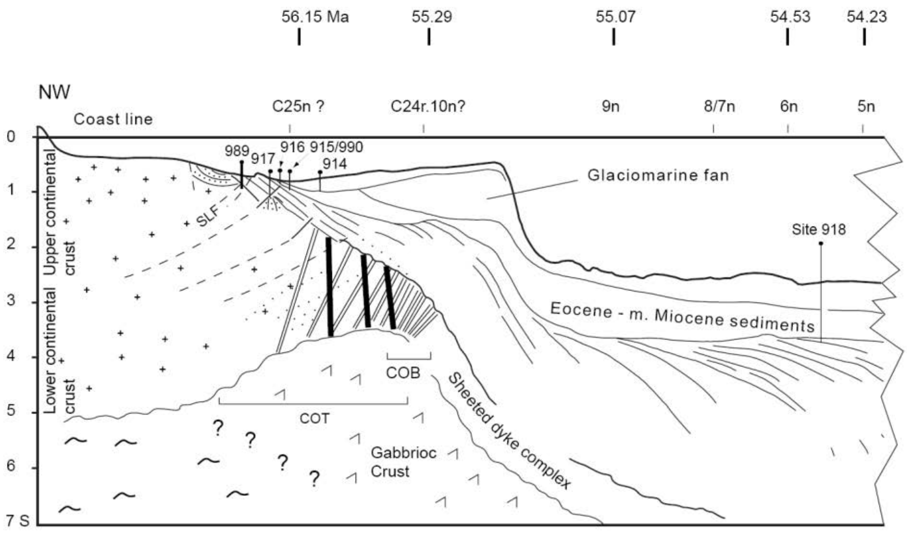

Fig. 2-1. *Crustal section of South East Greenland. The margin is characterized by Seaward-Dipping Reflector Sequence (SDRS) that “onlaps” continental crust to the west and terminates eastward in oceanic crust (Larsen and Saunders, 1998).*

2.2 The Blosseville Kyst (Kangerlussuaq-Scoresby Sund)

Along the Blosseville Kyst from Kangerlussuaq to Scoresby Sund, a thick sequence of flood basalts and the equivalent mafic intrusions (layered gabbro and dolerite sill complexes) crops out (Fig. 2-2). The lavas and many of the intrusions are synchronous with continental break-up at 55 Ma (Tegner et al., 1998). The processes that led to the onset and evolution of the North Atlantic Igneous Province (NAIP) have been a subject of much debate. The most commonly accepted hypothesis is that a mantle plume (the 'Ancestral Iceland' hot spot) impinged on the base of the lithosphere during the Late Cretaceous/Early Tertiary and initiated the first outbursts of lava, eventually culminating in breakup and seafloor spreading in the North Atlantic area in Early Palaeogene times (Saunders *et al.* 1997).

The Kangerlussuaq Basin developed in response to Mid-Cretaceous rifting that preceded North Atlantic opening (Larsen et al., 2005). This continental extension and rifting is also observed in the Faroe-Shetland, Møre and Vøring Basins (Larsen et al., 1999). Deep-marine conditions prevailed in the Kangerlussuaq Basin during the Upper Cretaceous, but in the Paleocene, a change to shallow marine and fluvial conditions occurred (Larsen et al. 1999). The fluvial succession forms a marker bed over the entire Kangerlussusaq area and may define the breakup unconformity in the region (Larsen et al., 1998). It formed as a consequence of a regional uplift that was probably related to doming and thermal uplift as the Iceland mantle plume impinged on the base of the lithosphere prior to break-up (Larsen et al. 1999).

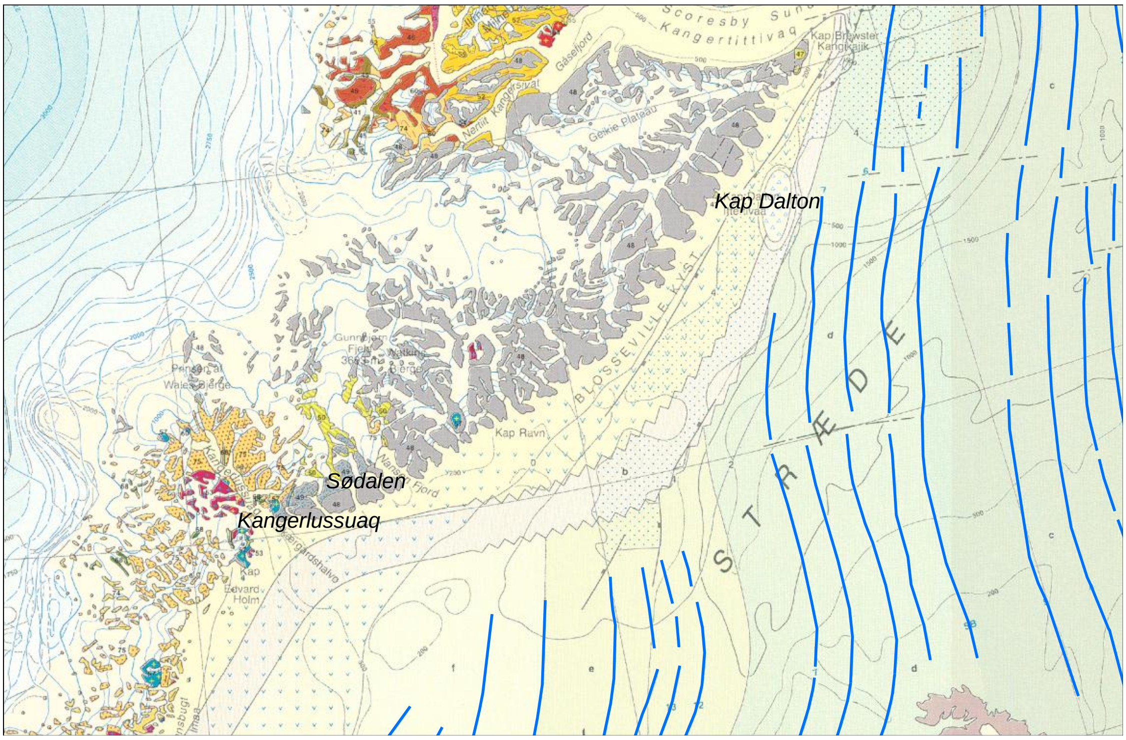

Fig. 2-2. Geological Map of Greenland 1:2500000 scale. (modify after Escher and Pulvertaft, 1995).

Along the southern part of the Blosseville Kyst between Kangerlussuaq and Nansen Fjord (Fig. 2-2), pre-basaltic sediments belonging to the Kangerlussuaq basin and the lower part of the Blosseville Group crop out. The stratigraphy of these formations was originally described by Wager (1934, 1947) It was subsequently refined by Soper et al. (1976) and mapped by Nielsen et al. (1981). Detailed sedimentological studies (Larsen et al., 1999) demonstrate the presence of four major facies units in the Kangerlussuaq basin sequence: (1) late Aptian alluvial and shallow marine deposits, (2) early Paleocene offshore and submarine fan deposits, (3) middle Paleocene fluvial deposits making up the Vandfaldsdalen Formation, and (4) a late Paleocene volcanic assemblage. The lavas of the Blosseville Group have been divided into two main series based on their stratrigraphy, geochemistry, and petrography: the Lower Basalts, which range in composition from picrites to evolved basalts that formed in a continental rift environment between 61-57 Ma. and have a total thickness of 2 km (the Vandfaldsdalen, Mikis and Hægenfjeldet Formations; Nielsen et al., 1981); and the Plateau basalts, which formed in association with final breakup and early seafloor spreading between 57-54 Ma. and have a total thickness of 6 km (the Milne Land, Geikie Plateau, Rømer Fjord and Skrænterne formations;Larsen et al., 1989; Pedersen et al., 1997).
The Blosseville Kyst is characterised by the presence of several generations of dikes and sills, related to both the break-up as well as the post break-up history (Wager, 1947; Nielsen, 1978; Nielsen and Brooks, 1981; Hanghøj, 2003). The presence of coast-parallel swarms of dikes in East Greenland suggests that continental break-up and the formation of oceanic crust (~55 Ma) was parallel to the coast south of Kangerlussuaq and to the Blosseville Kyst. Dikes of the East Greenland Tertiary dike swarm can be divided into pre- and syn-break-up tholeiitic dikes and post-break-up transitional dikes. Of the pre- and syn-break-up dikes, the most abundant group (tholeiitic series; TS) has major element compositions similar to the main part of the East Greenland flood basalts. A group of high-MgO tholeiitic dikes (picrite-ankaramite series; PAS) are much less common and are equivalent to some of the oldest lavas of the East Greenland flood basalts. The post-break-up transitional series (TRANS) dikes are isotopically distinct from Iceland and MORB, and are interpreted to be the product of contamination of Iceland plume melts with continental crust (Hanghøj et al., 2003).
During and after the emplacement of the thick sequence of basalts of the Blosseville Group, subsidence related to lithospheric flexure took place.This may be associated with the development of northward dipping normal faultsthat are well documented along the coast (Fig. 2-2). The flexure may also be linked to loading of the crust by lava flows during early spreading and the formation of seaward dipping reflector sequences.
Along the Blosseville Kyst post-basaltic sediments exposed at Kap Dalton and Savoia Halvø (Fig. 2-2) represent the scattered remains of a much more widespread, fluvial to shallow-marine succession. Deposition in the late Paleocene–Eocene was governed by a complex interplay between loading, thermal contraction of the oceanic crust, passage of the hotspot and eustatic sea-level changes (Larsen et al., 2005). At Kap Dalton, extrusion of Early Eocene, Chron C21r flood basalts was followed by subaerial erosion, creating an irregular relief dissected by fluvial channels. Together with the results from ODP leg 152 off the SE Greenland margin (Saunders et al. 1998), the Kap Dalton-Savoia Halvø areas provide important evidence that may correlate to the early post-volcanic

(Eocene) sedimentary development of the western Faroes. The sediments at Kap Dalton are preserved in a downfaulted 3km wide, N–S-trending graben and represent the remains of a much more widespread sedimentary succession that covered the coastal areas of East Greenland during Eocene times (Larsen et al., 2005).

2.3 Cenozoic uplift and inversion structures

Cenozoic uplift and inversion structures are common along most parts of the Greenland-Europe Rift System, and several major petroleum discoveries are found in such structures. Uplift and inversion structures are often associated with four-way closures and can be recognised in the post-basaltic section. They are thus important for intra-basalt and sub-basalt play models, and most uplift and inversion structures in the Faroe sector of the Faroe-Shetland Basin are now located.

While it is easy to locate and map the Cenozoic expression of uplift and inversion structures, it is difficult to assign precise ages to the structures, and little work has been carried out distinguishing between uplift and inversion structures. The uplift structure would potentially have a thin Mesozoic drape above a pre-existing structure, which could be Precambrian basement or a tilted horst. Inversion structures could have thick Mesozoic successions with a potential for stacked reservoirs. Therefore a geological model that can distinguish between uplift and inversion structures in the Faroe sector of the Faroe-Shetland Basin will be of great value for focusing future sub-basalt exploration.

2.4 Geophysics offshore East Greenland

Geophysical data sets available off the East Greenland margin from Kangerlussuaq to Scoresby Sund include magnetic, gravity, and seismic data. The EASTMAR magnetic survey, which covers the area from Scoresby Sund to south of Sermilik fjord is the most recent available and was collected in 1980-81. It is included in the publicly available global databases. The line spacing is course and thus will not provide high resolution details of offshore structure. However, it is currently the best available for this part of East Greenland.

Figure 2-3 shows the seismic lines offshore East Greenland. There are 9 2D surveys that are potentially relevant. These data sets vary in age from 1976 to 1997 and include both high resolution shallow surveys as well as deep reflection profiles. As part of this project, all the data sets will be examined to determine the extent to which the structures mapped onshore can be observed offshore. Because the data quality is highly variable, we do not propose a comprehensive interpretation at this stage. As a first approach, we will evaluate and confirm that the correlation between structures in the onshore and offshore areas. If promising, a more comprehensive project that possible includes re-processing the older data sets will be developed.

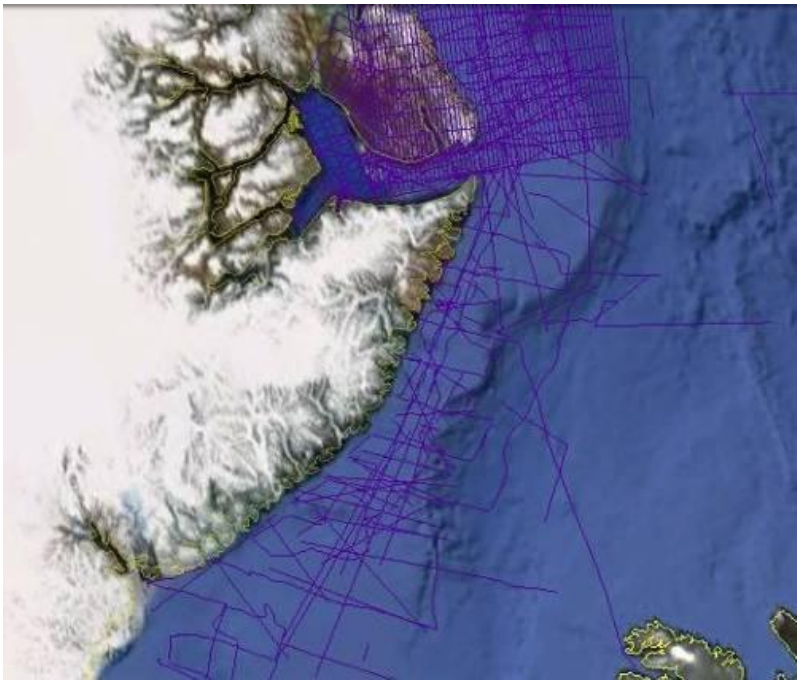

Fig. 2-3. *Geophysical dataset available in East Greenland offshore.*

2.5 Faroe Islands area

The Faroe–Shetland Basin comprises a series of NE–SW-trending sub-basins (Fig. 2-4) that formed during a sequence of rift events following the end of the Caledonian orogeny (Coward 1990). The sub-basins are separated by horst blocks that are cored by metamorphic basement rocks. Collapse of the Caledonian orogen in the Devonian led to the formation of several 'Old

Red Sandstone' basins in the proto-North Atlantic region (Roberts et al. 1999). Renewed rifting during the Permo-Triassic was associated with the development of strongly asymmetrical half-graben basins (Herries et al. 1999). Fluvial and alluvial environments gave way to marine conditions in the early Jurassic, with a regional unconformity removing much of the middle Jurassic succession (Booth et al. 1993). Jurassic extension in NW Europe (Doré et al. 1999) was characterized by the formation of mainly north–south-trending rifts, including the North Sea and Porcupine Basins and parts of the Halten Terrace. Early Cretaceous rifting has been inferred based on packages of coarse-grained, Early Cretaceous clastic sediments that thicken towards the hanging walls of NE–SW-trending normal faults within the Faroe–Shetland Basin (Booth et al. 1993). The dominant

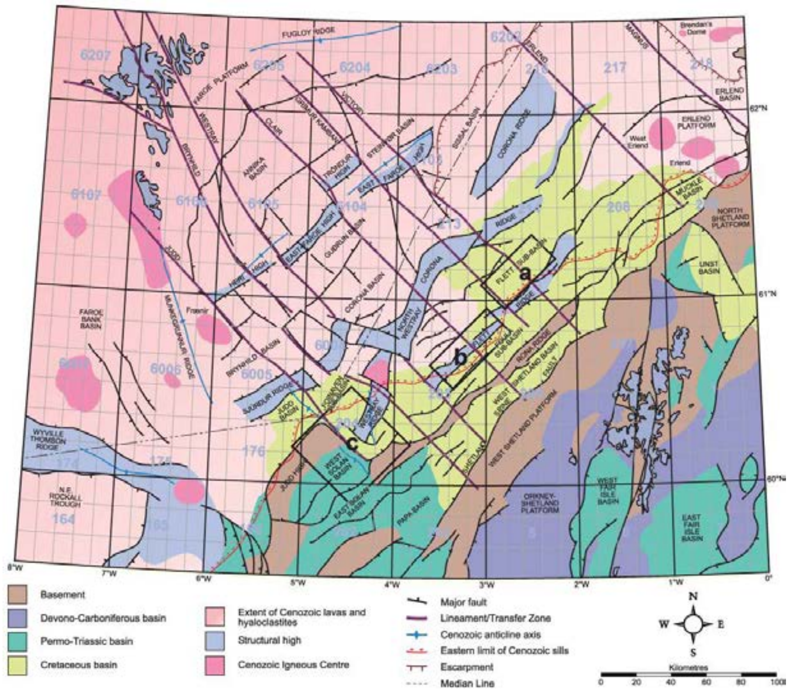

Fig. 2-4. *Structural elements of the Faroe–Shetland Basin with the location of Transfer Zones (after Ellis et al. 2009). Map projection is WGS84, UTM 30N.*

NE–SW trend of the Faroe–Shetland Basin was established by the end of the Cretaceous, by which time rifting had ceased and basin flank uplift gave rise to deposition of a regressive Paleocene succession (Smallwood & Gill 2002). Paleocene rifting in the SW part of the Faroe–Shetland Basin has been inferred by Dean et al. (1999) based on Cretaceous normal faults that appear to have been reactivated. Alternatively, fault initiation and/or reactivation at this time may have been associated with differential compaction of sediments over structural highs (Færseth & Lien 2002).

Current models for the development of the NE Atlantic margin imply a progressive north-westward migration in the locus of active rifting, towards the eventual zone of continental break-up (Lundin & Dore´ 1997). Thus, evidence for a Paleocene rift event may primarily exist beneath, and be largely obscured by, the thick Palaeogene lava pile in the NW part of the present-day Faroe–Shetland Basin (Fig. 2-4). Continental break-up (Eldholm & Grue 1994) was associated with widespread basin uplift and magmatism across the NE Atlantic region, in the form of continental flood basalts, sill and dyke complexes, igneous centres, magmatic underplating and the deposition of regional tuff horizons (White & McKenzie 1989; Naylor et al. 1999; Lundin & Doré 2005). Following continental break-up in the early Eocene, the tectonic evolution of the Faroe–Shetland Basin has been dominated by thermal subsidence and the growth of large-scale Cenozoic anticlines (Boldreel & Andersen 1993; Davies et al. 2004; Stoker et al. 2005; Ritchie et al. 2008). These folds have been attributed to a variety of mechanisms including ridge push, sedimentary draping and reactivation of basement structures (Doré et al. 2008).

On a more regional scale, transfer faults and accommodation zones have been identified at many locations along the Greenland-Europe Rift System (Andersen and Neish, 2009 and references herein). Some of these, such as the Judd Fault, have a significant impact on Paleocene sediment distribution. These transfer faults, or accommodation zones, are typically short and transfer strain between *en echelon* rift basins with basin bounding faults of opposite dip. Most of the transfer zones across the Greenland-Europe Rift System, are sub-parallel to SE-NW trending lineaments across the Faroe-Shetland Basin and are recognisable as faults or accommodation zones over fairly short distances on the order of a few tens of kilometres. They show little indication of being true strike-slip faults in a strict sense. However, some transfer faults or accommodation zones follow other trends. In the Slyne Trough and Porcupine Basin, strain is transferred along NE-SW trending faults, some of which apparently are splays of Great Glenn Fault.

3. Structural Geology and 3D-photogeology

3.1 Fieldwork objectives

The fieldwork was carried out in an area around 68ºN and included reconnaissance from helicopter and visits to locations along the Sødalengletsher, Vandfaldsdalen, Uttental Plateau, Kremer Island, Miki Fjord, Kap J. C. Jacobsen, Nunap Isua, Nansen Fjord (West) and Christian IV Gletscher (West) (Fig. 3-1). The investigations were performed from a base camp on Sødalen and from daily reconaissance flights with the helicopter. The presence of polar bears along the coast and inland areas, as documented by the numerous incursions on the main base camp at Sødalen (unfortunately one was shot) inhibits the opportunity to have extra camps around the area. For this reason we moved daily with the helicopter along with the camera to collect oblique photos and land in several places to collect structural data (Fig. 3-1).

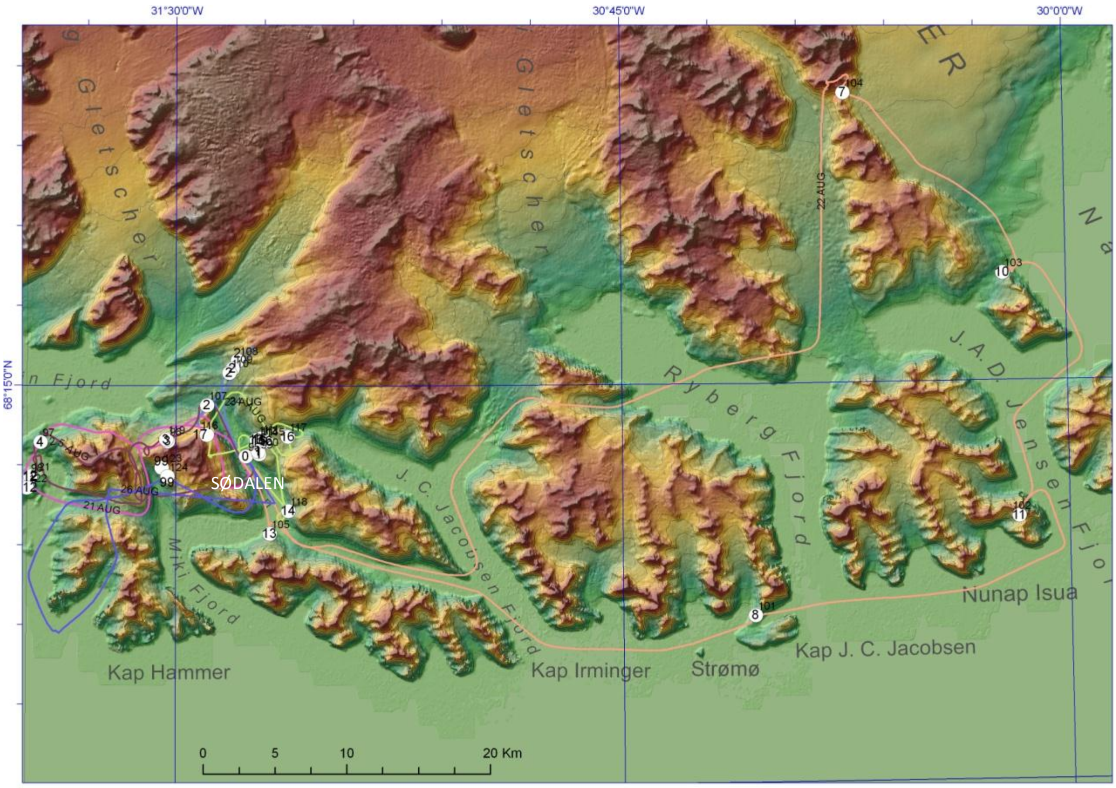

Fig. 3-1. Flight lines and sites location.

The objectives of the fieldwork were

- to make general geological observations,
- to gather structural data along major fault systems,
- to take reconnaissance photographs of major outcrops from helicopter to be used in 3D-photogeology.

The only Geological Maps available are the Kangerlussuaq Sheet 1:500,000 scale, the Geology of the Miki Fjord area 1:20,000 scale (Nielsen et al. 1981) and the Geological Map of the Skaergaard intrusion 1:20,000 scale (McBirney 1989).

More than 250 fault slip data were collected on 16 sites and used for inversion to obtain paleostress. The paleostress analysis of the heterogeneous fault slip data set is performed using integrated software for structural analysis (T-Tecto 3.0 Zalohar 2009). The Gauss Method associated with the visualization of P&T Dihedra (Angelier & Mechler 1977) allowed us to distinguish different superimposed tectonic regimes in this area.

Around 1500 oblique photos were taken along the more than 400 km-long reconnaissance flights with helicopter. Selected oblique photos will be triangulated with aerial photos and analyzed in a stereo plotter for 3D-photogeology interpretation to evaluate the geometry of faults, to reconstruct stratigraphic boundaries (such as the basal contact of the Palaeogene basalts) and to evaluate the vertical/lateral offset along major faults.

3.2 Structural Analysis

The fault-slip datum should be measured at a relatively planar part of the fault which is at least subparallel to the main orientation of the fault. Collection of field data for fault-slip analysis ideally would include measurement of several parameters for each of the faults studied:

- fault plane orientation,
- slip direction,
- sense-of-slip,
- local bedding orientation,
- average displacement, and
- fault surface area.

The first three are all that is required for the dynamic analysis techniques and for graphical kinematic methods, and usually those are all that are measured. To get considerably more out of the data however, the final three should also be measured or estimated. It is commonly impossible to reliably measure average displacement and fault surface area in the field due to inadequate exposure and our inability to see through rocks. Alternatively, *fault gouge thickness* and/or *fault width* can be used to estimate average displacement and fault surface area, and hence the magnitude of fault-slip deformation.

3.2.1 Shear Direction and Sense of movement on a fault plane

The slip direction of a fault is usually determined from slickensides developed in the fault zone (Hancock & Barka 1987; Means 1987). Generally, a fault exposure must be excavated in several places in order to ensure that representative slickensides are chosen for measurement. Slickensides commonly vary locally in orientation by 10-20°. Distinct sets of slickensides, which differ by greater angles, may indicate fault reactivation. Slip direction can also be determined from offset clasts and from offset piercing points defined by intersecting planar markers. Fault scarps, stratigraphic relations, drag folding, vein-bearing fault steps, and offset clasts, veins and faults are the simplest and most reliable indicators. Fault plane surface indicators of sense-of-slip include tails and scratches produced by asperity ploughing (Means 1987), slickolite spikes (Arthaud & Mattauer 1972), and crescentic marks formed by the intersection of the fault plane with secondary fractures (Petit 1987). Many secondary fractures are useful sense-of-slip indicators, such as R, R', P, and T fractures (Petit 1987), bridge structures (Gamond 1987), and foliation in clay fault gouge (Chester & Logan 1987). However, their formation depends on the mechanical properties of the fractured rock and the physical conditions of deformation, so they can be ambiguous. Nevertheless, careful study of secondary fractures at faults of independently known sense-of-slip can identify criteria useful for observing other faults that formed under similar conditions in the same rock. Each fault should be carefully inspected for as many indicators as possible because interpretation of these subtle features can be difficult and contradictory indicators are commonly the only field evidence for a reactivated fault. It is also useful to develop a confidence scale, similar in concept to that used by seismologists to rank the quality of earthquake locations, to give one specific reason to retain or reject specific data.

3.2.2 Sense-of-shear indicators for brittle faults

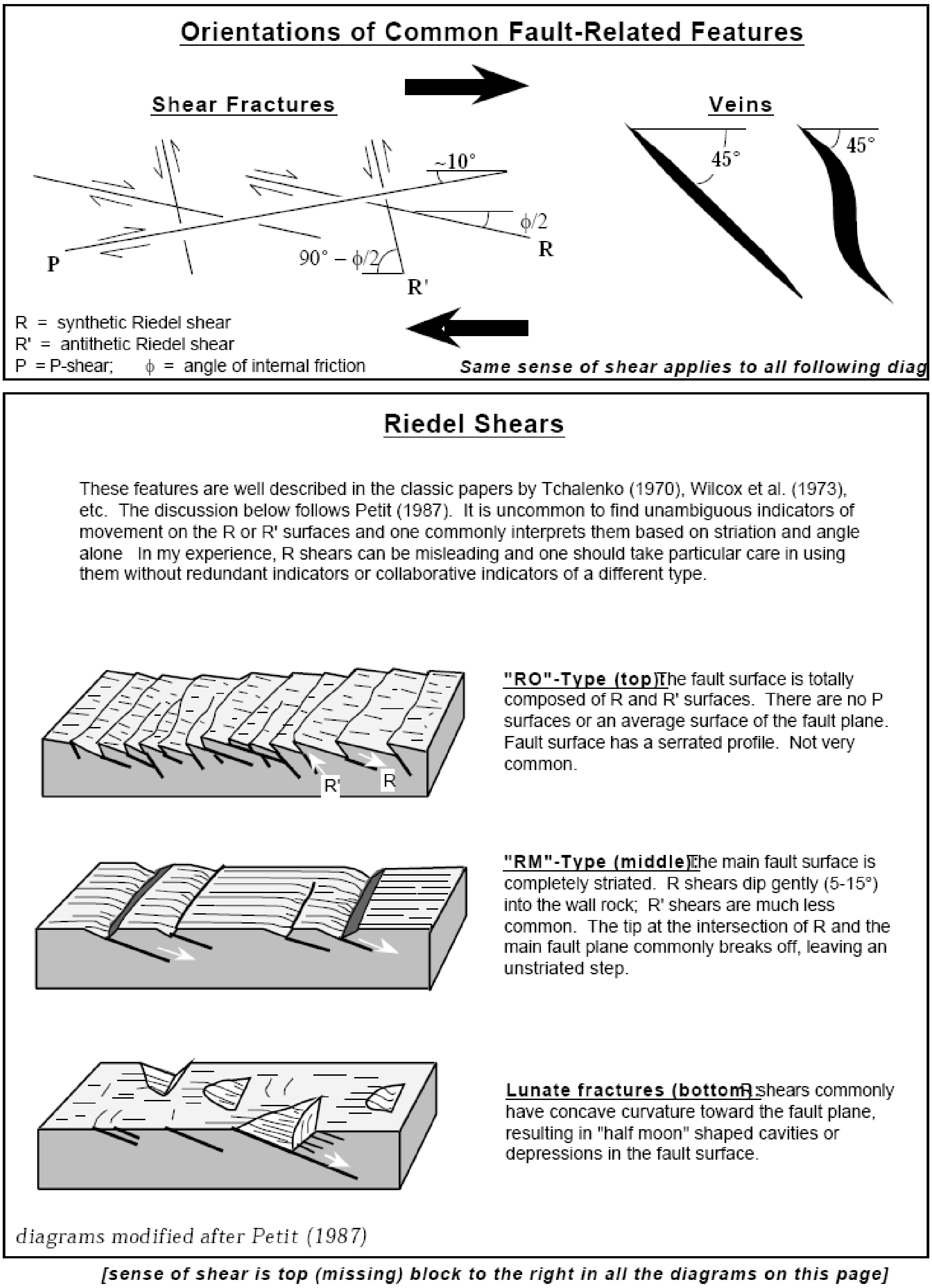

Fig. 3-2 Possible sense-of-shear indicators for brittle faults, after Marret & Allmedinger (1990)

Striated P-Surfaces

These features were first described by Petit (1987). The fault plane is only partially striated, and the striations only appear on the up-flow sides of asperities.

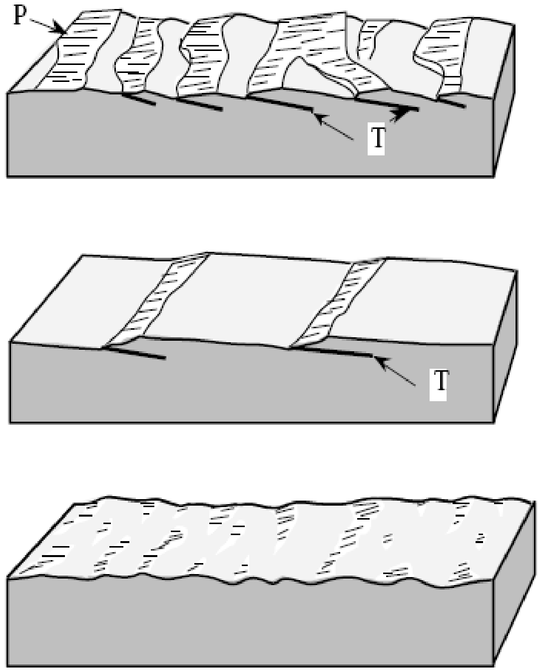

"PT"-Type (top & middle): planar, *non-striated* surfaces dip gently into the wall rock. Petit (1987) calls these "T" surfaces because of lack of evidence for shear, but they commonly form at angles more appropriate for R shears. Striated P surfaces face the direction in which that block moved. Steep steps developed locally at intersection between P and T. P surfaces may be relatively closely spaced (top) or much farther apart (middle).

"PO"-Type (bottom): T surfaces are missing entirely. Striated P surfaces face in direction of movement of the block in which they occur. Lee side of asperities are unstriated.

diagrams modified after Petit (1987)

Unstriated Fractures ("T fractures")

Although "T" refers to "tension" it is a mistake to consider these as tensile fractures. They commonly dip in the direction of movement of the upper (missing) block and may be filled with veins or unfilled.

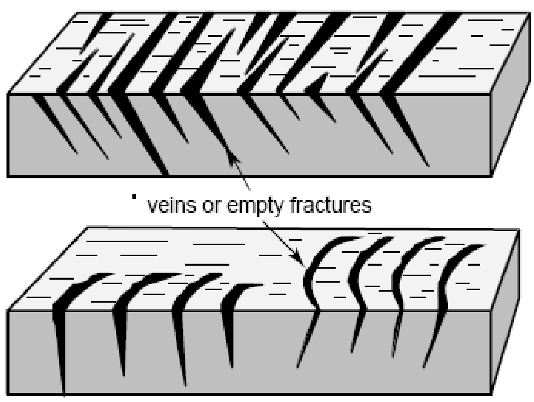

"Tensile Fractures" (top): If truely tensile in origin and formed during the faulting event, these should initiate at 45° to the fault plane and then rotate to higher angles with wall rock deformation. Many naturally occuring examples are found with angles between 30° and 90°. They are referred to as "comb fractures" by Hancock and Barka (1987).

Crescent Marks (bottom): Commonly concave in the direction of movement of the upper (missing) block. They virtually always occur in sets and are usually oriented at a high angle to the fault surface. They are equivalent the "crescentic fractures" formed at the base of glaciers.

diagrams modified after Petit (1987)

[sense of shear is top (missing) block to the right in all the diagrams on this page]

Fig. 3-3 Possible sense-of-shear indicators for brittle faults, after Marret & Allmedinger (1990)

"S-C" Fabrics

Although commonly associated with ductile shear zones, features kinematically identical to S-C fabrics also occur in brittle fault zones. There are two types: (1) those that form in clayey gouge in clastic rocks and (2) those that form in carbonates. They have not been described extensively in the literature. This is somewhat odd because I have found them one of the most useful, reliable, and prevalent indicators.

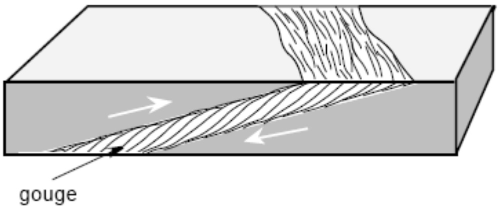

Clayey Gouge fabric (top): Documented by Chester and Logan (1987) and mentioned by Petit (1987). Fabric in the gouge has a sigmoidal shape very similar to S-surfaces in type-1 mylonites. This implies that the maximum strain in the gouge and displacement in the shear zone is along the walls. Abberations along faults may commonly be related to local steps in the walls.

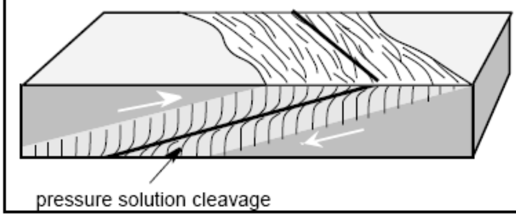

Carbonate fabric (top): This feature is particularly common in limestones. A pressure solution cleavage is localized in the walls of a fault zone. Because maximum strain and displacement is in the center of the zone rather than the edges, the curvature has a different aspect than the clayey gouge case. The fault surface, itself, commonly has slip-parallel calcite fibers.

Mineral Fibers & Tool Marks

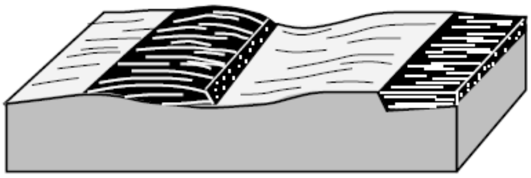

Mineral Fibers and Steps (top): When faulting occurs with fluids present along an undulatory fault surface or one with discrete steps, fiberous minerals grow from the lee side of the asperities where stress is lower and/or gaps open up. These are very common in carbonate rocks and less so in siliceous clastic rocks.

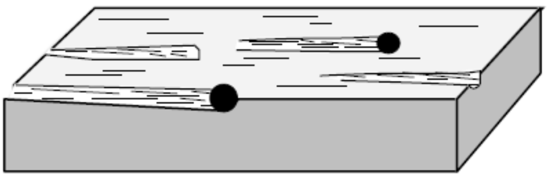

Tool Marks (bottom): This feature is most com- mon in rocks which have clasts much harder that the matrix. During faulting, these clasts gouge the surface ("asperity ploughing" of Means [1987]), producinig trough shaped grooves. Although some attempt to interpret the grooves alone, to make a reliable interpretation, one must see the clast which produced the groove as well. Other- wise, it is impossible to tell if the deepest part of the groove is where the clast ended up or where it was plucked from.

[sense of shear is top (missing) block to the right in all the diagrams on this page]

Fig. 3-4 Possible sense-of-shear indicators for brittle faults, after Marret & Allmedinger (1990)

3.2.3 Paleostress analysis

The main goal of the paleostress analysis is to find the stress tensor capable of explaining the direction of slip on most of the faults observed in the studied rock mass. Generally this problem is referred to by structural geologists as *the inverse problem*. The methods of paleostress analysis proposed by many authors, while different in approach, are all based on similar basic assumptions: (1) the direction of movement on the faults parallels the shear stress on those faults; (2) the faults do not interact (the movement along one fault is independent of the movement on the other faults); (3) the blocks bounded by the fault planes do not rotate; and (4) the stress field activating the faults is time-independent and homogeneous. From these assumptions follows the basic hypothesis of paleostress analysis: the direction of slip on a set of differently oriented faults can be explained by a single stress tensor.
To perform the inversion of the fault-slip data collected during fieldwork, the T-TECTO 3.0 computer program (Zalohar 2009) is used. This software enables classical analysis of heterogeneous fault-slip data using several different numerical methods. The program is based on the classical philosophy of fault-slip data inversion which involves the concept of the best-fitting stress and strain tensors. The defined *compatibility measure* and *compatibility function* verify the compatibility of a given strain or/and stress tensor with observed fault-slip data. In order to constrain inversion results to mechanically acceptable solutions, the program additionally considers the ratio between the normal and the shear stress on the fault plane, since it is assumed that the results of paleostress and strain inversion should be in agreement with the Amontons's law. The optimal solution for stress and strain tensors related to the observed faults are found by searching for the global and highest local maxima of the *object function F* defined as a sum of compatibility functions for all fault-slip data.

3.3 3D-Photogeology

The 3D-Photogeological method (Guarnieri et al., 2009; Vosgerau et al., 2010; Weibel et al., 2010) was developed at the Geological Survey of Denmark and Greenland (GEUS) (Fig. 3-5) and builds on earlier work by Dueholm & Pedersen (1992) and Dueholm & Olsen (1993). The method allows the acquisition of geological data from vertical and oblique aerial photographs, with a three-dimensional overview of the outcrops. The oblique photographs (1:15 000–1:17 000 scale) are triangulated, aerial photographs (1:40 000-1:150 000 scale) using a 3D stereo-plotter coupled with stereo- mirror technology. The mapping of geological features includes determination of strata thickness, strike direction and dip values working on a 3D high resolution vision of the cliffs. The resolution of sedimentary beds and geological features is c. 10 cm. All the mapped features are stored in a GIS database and 3D polylines can be exported as shape files suitable for 3D modeling (Fig. 3-5). Moreover, using 3D feature databases in ArcGIS, geological cross-sections can be generated automatically to obtain real representations of outcrops, and then projected onto a topographic profile, where the accuracy is as high as the resolution in the photographs. The 3D-photogeology consists of integrated analysis from a large range of spatial scales. At large scales (kilometre to metre) 3D-photogeology can be used to study the extent, geometry and interfingering of sedimentary units and to map faults. At an intermediate scale (metre to millimetre), sections describing the sedimentary facies can be logged in the field. The 3D-photogeology is also applied on an intermediate scale, where it is used to map lateral variations of sedimentary units between logged sections. At a fine scale (millimetre to micrometre) biostratigraphical analyses can eventually provide information on age and palaeo-environment. During fieldwork in 2010 a series of small-frame colour photographs were taken for multi-model photogrammetric studies. The photographs were taken out of the open window of an helicopter flying at cruising speeds between 60 and 120 km per hour. A Canon EOS-1Ds Mark III digital camera with a 36mm x 24mm CMOS sensor with 21 MP and a 35 mm Canon lens was used for the photography. The oblique photographs were taken by orienting the camera so the image plane was approximately parallel to the slope of interest. The pilot was instructed to fly in straight lines approximately parallel to the photographed slope at the same altitude and photographs were typically taken with 60 to 80% overlap. While taking the photographs the focus of the camera was set on infinity. In order to reduce image blur caused by image movement due to helicopter vibration and relative movement of the camera with respect to the scene a fixed exposure time of 1/250 seconds was used while the aperture setting was put on automatic. In some cases with good light condition shorter exposure times was used.

Fig. 3-5. The 3D-stereo plotter with polarized screens and glasses together with a perspective view of a 3D-polylines dataset

3.4 Structural data

This paragraph describes the structural data collected during fieldwork in 2010 and similar data collected during summer 2009. Fault-slip data were collected in 23 different localities separated on 12 sites in 2010 and 5 sites in 2009 (Fig. 3-6). For each site there is a short introduction of the outcrop, a detailed geological map, oblique photo of the area, detailed photos showing fault planes and diagrams describing the statistical parameters of fault trends as rose diagram, stereoplot of pole to the plane, kinematics and the paleostress. Faults are represented in a lower-hemisphere Wulff net as great circle or pole to plane, and the kinematics as arrow when known. A rose diagram is used to evaluate the mean direction of fault strike. The paleostress plots show the orientation of the maximum/minimum horizontal stress (black arrows) and the orientation of the stress tensor: σ1 (□), σ2 (□), σ3 (□). All the raw data are presented in Appendix-1.

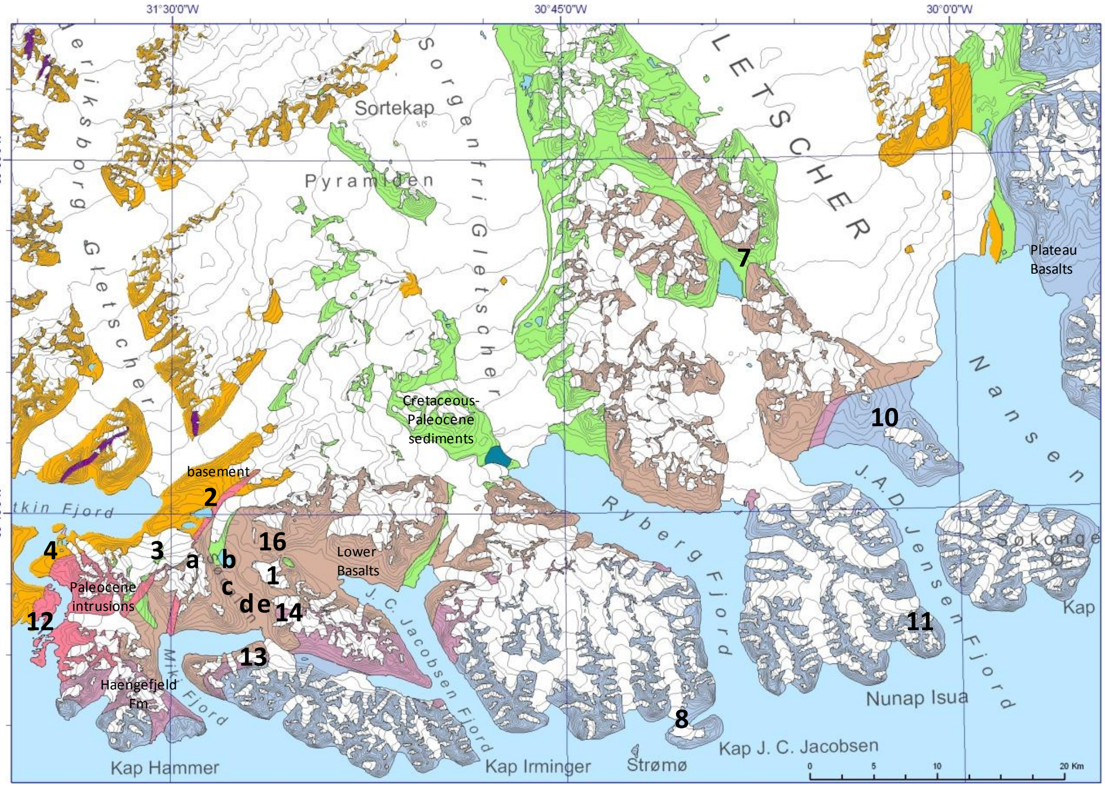

Fig. 3-6. *Location map of the structural sites. Sites numbered 1 to 16 fieldwork 2010, sites labeled with letters a to e, fieldwork 2009 . (Geological map 1:500000 scale, sheet 13 Kangerlussuaq. GEUS, 1988)*

3.4.1 Site1

The site is represented by two waypoints 99 and 100. This locality was investigated to describe the kinematics of a structural trend well visible from aerial photos. The stratigraphic sequence belongs to the Vandfaldsdalen Fm and it is represented by lava flow, hyaloclastites and pillow breccias (Fig. 3-7).

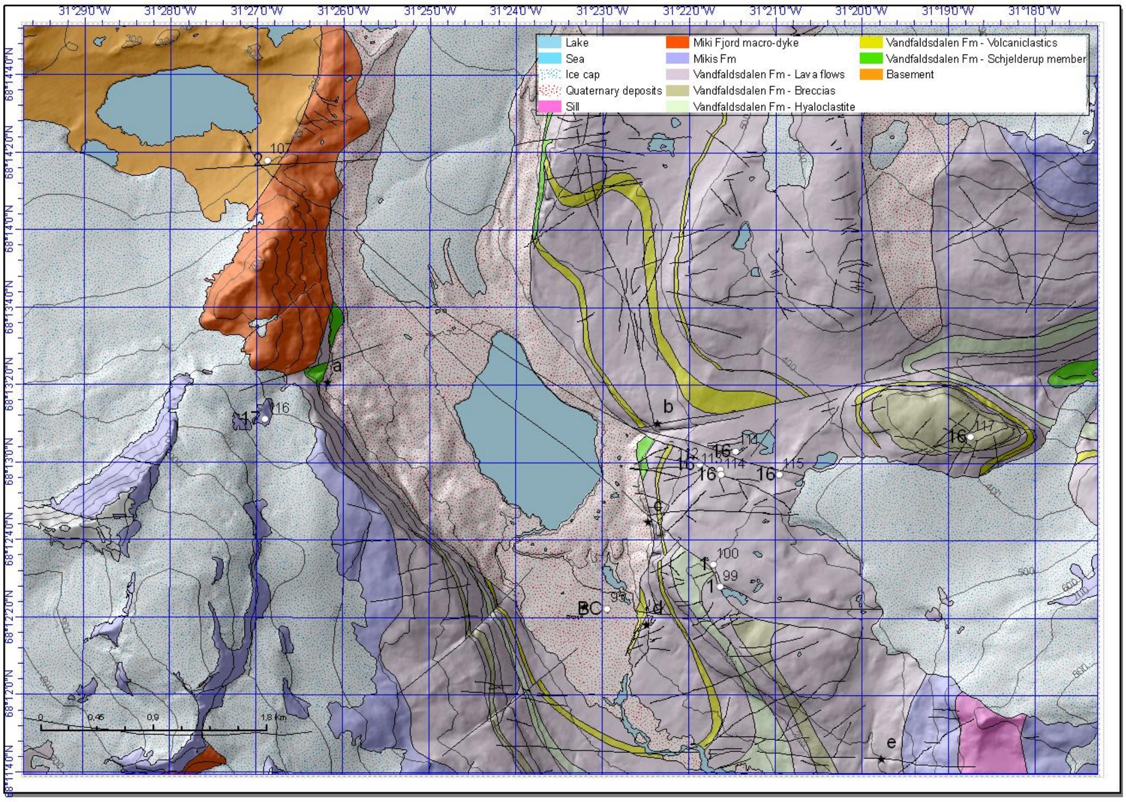

Fig. 3-7. *Shaded Geological map of the Sødalen area. (modified after Nielsen et al., 1981). BC=Base Camp; letters=sites 2009; numbers= sites 2010.*

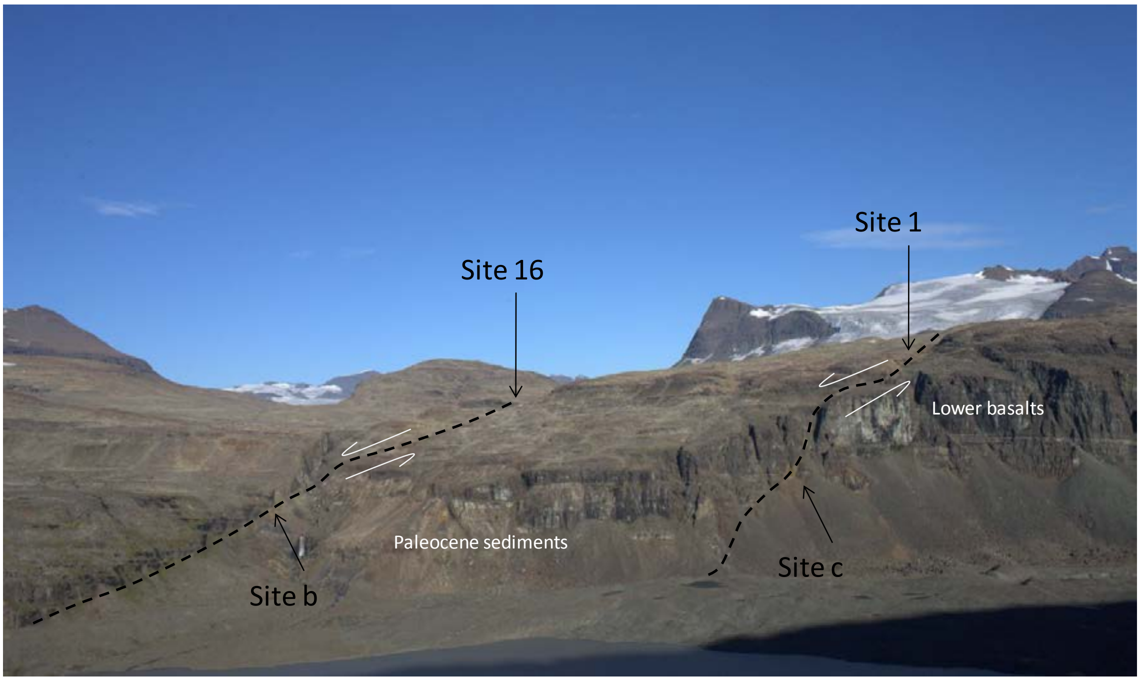

Fig. 3-8. Oblique photo along the east side of Sødalen. Dotted lines represent left-lateral dip oblique faults.

Fig. 3-9. Slickenside along a fault plane with dip oblique left-lateral kinematics at site 1.


Fig. 3-10. Re-crystallized calcite along the fault zone at site 1.

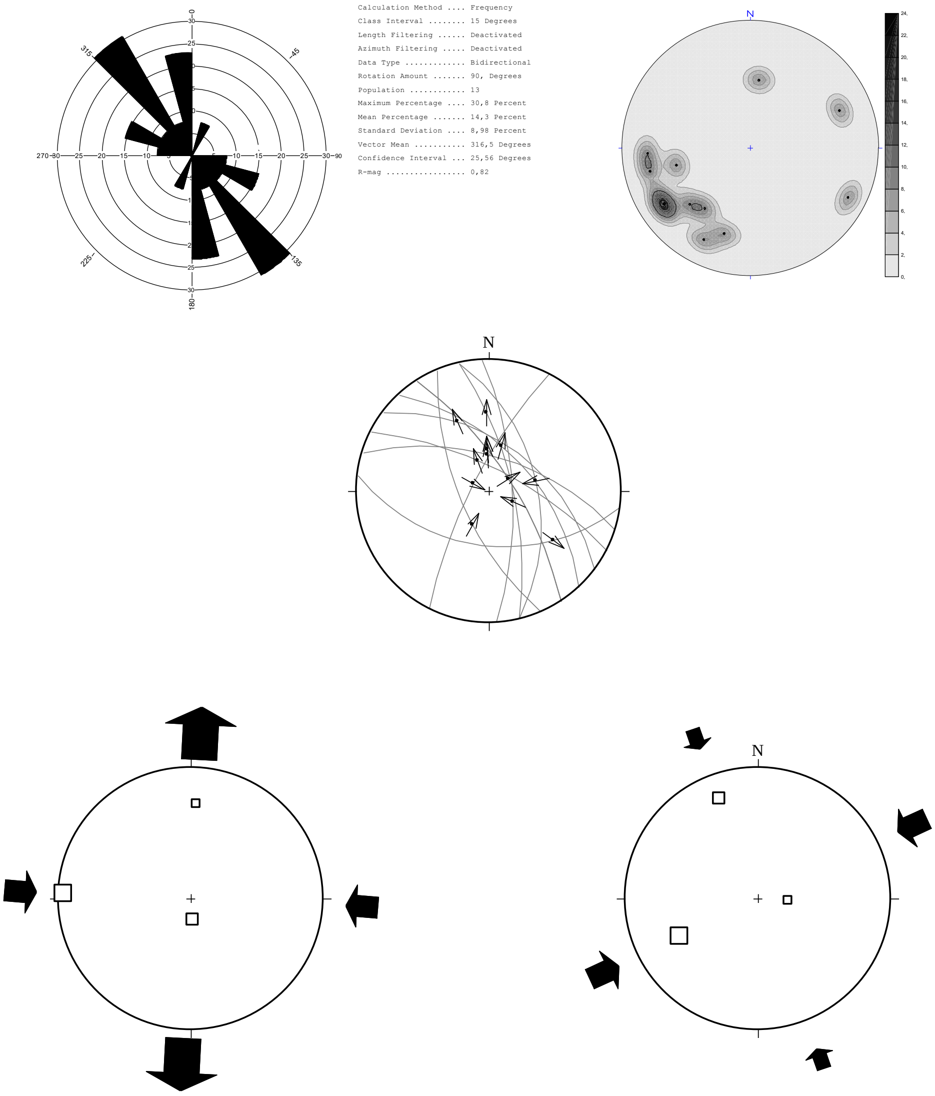

Fig. 3-11. *Structural data Site 1-99. Rose diagram, pole to plane, fault-slip vector and paleostress analysis (black arrows maximum horizontal stress; □σ1>□σ2>□σ3).*

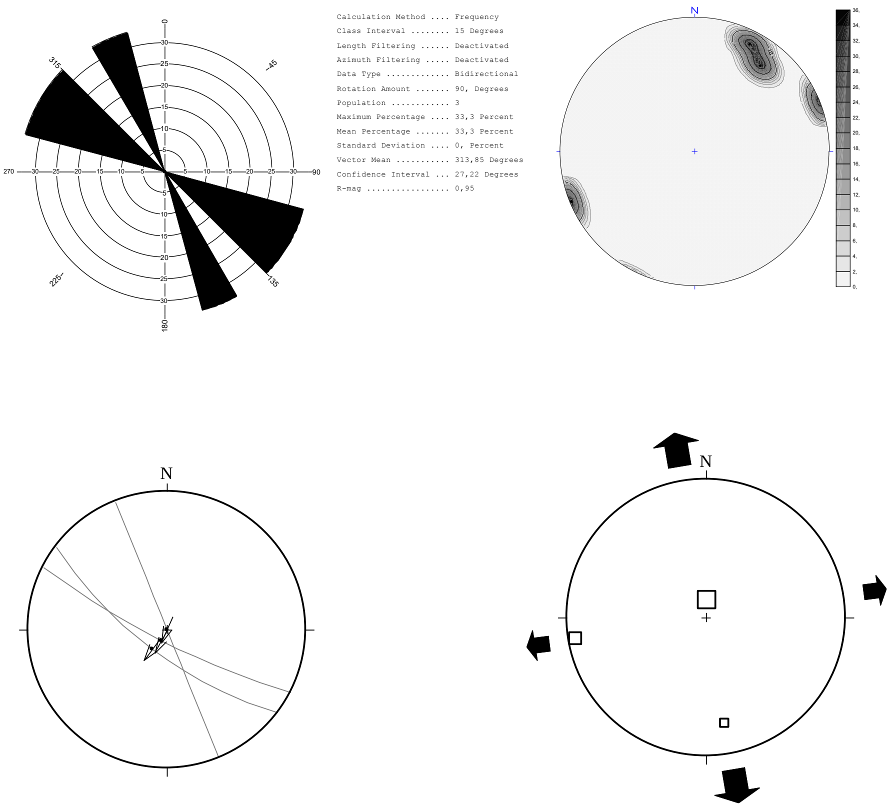

Fig. 3-12. *Structural data Site 1-100. Rose diagram, pole to plane, fault-slip vector and paleostress analysis (black arrows maximum horizontal stress;* □σ1>□σ2>□σ3).

3.4.2 Site 2

The site is represented by four waypoints (107-108-109 and 110). This locality was visited to investigate the contact between the Miki Fjord macro-dyke and basement rocks and to verify the presence of strike-slip faults cross-cutting the macro-dyke. The latter is a layered gabbro presumably 55 Ma old intruded along Paleocene rift faults (Fig. 3-7).

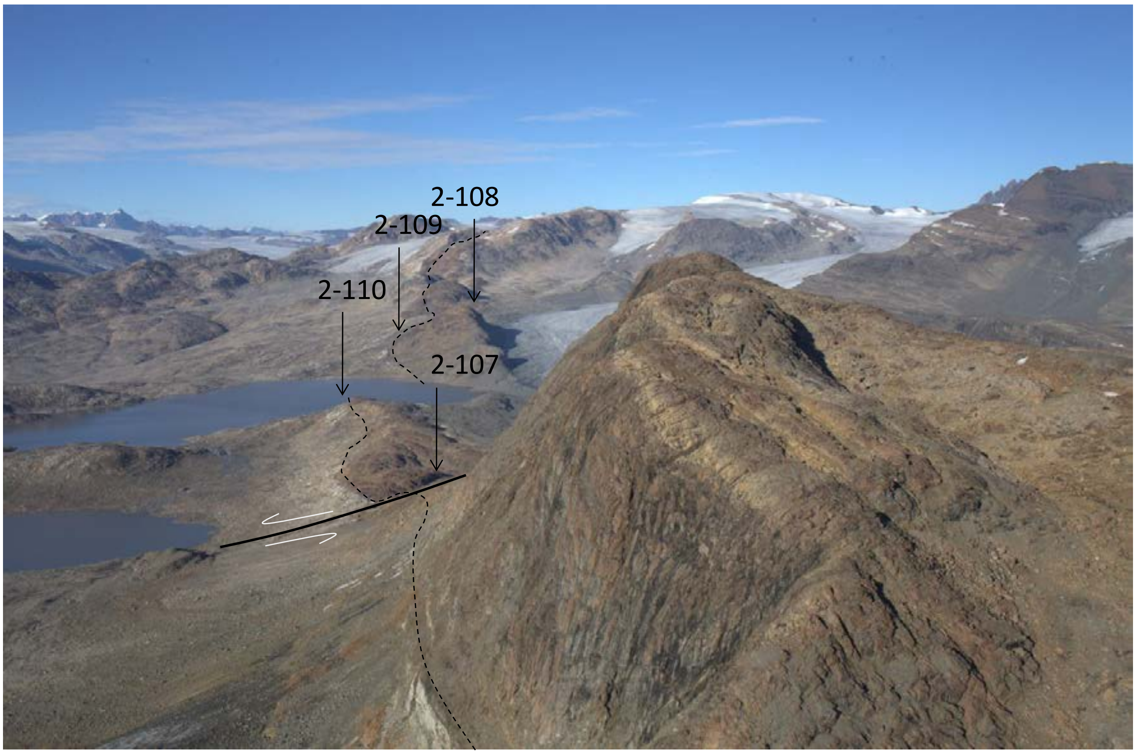

Fig. 3-13. *Oblique photo of the northern contact of the Miki Fjord macrodyke (dashed line) looking NE-ward*.

Fig. 3-14. *Dip oblique slickenside at site 2-107*.

Fig. 3-15. *Left-lateral fault plane with slickenside and P-T type features at site 2-109.*

Fig. 3-16. *Right-lateral fault plane with slickenside and calcite steps at site 2-110. Arrows point on striations with different pitch suggesting multiple re-activation of the fault plane.*

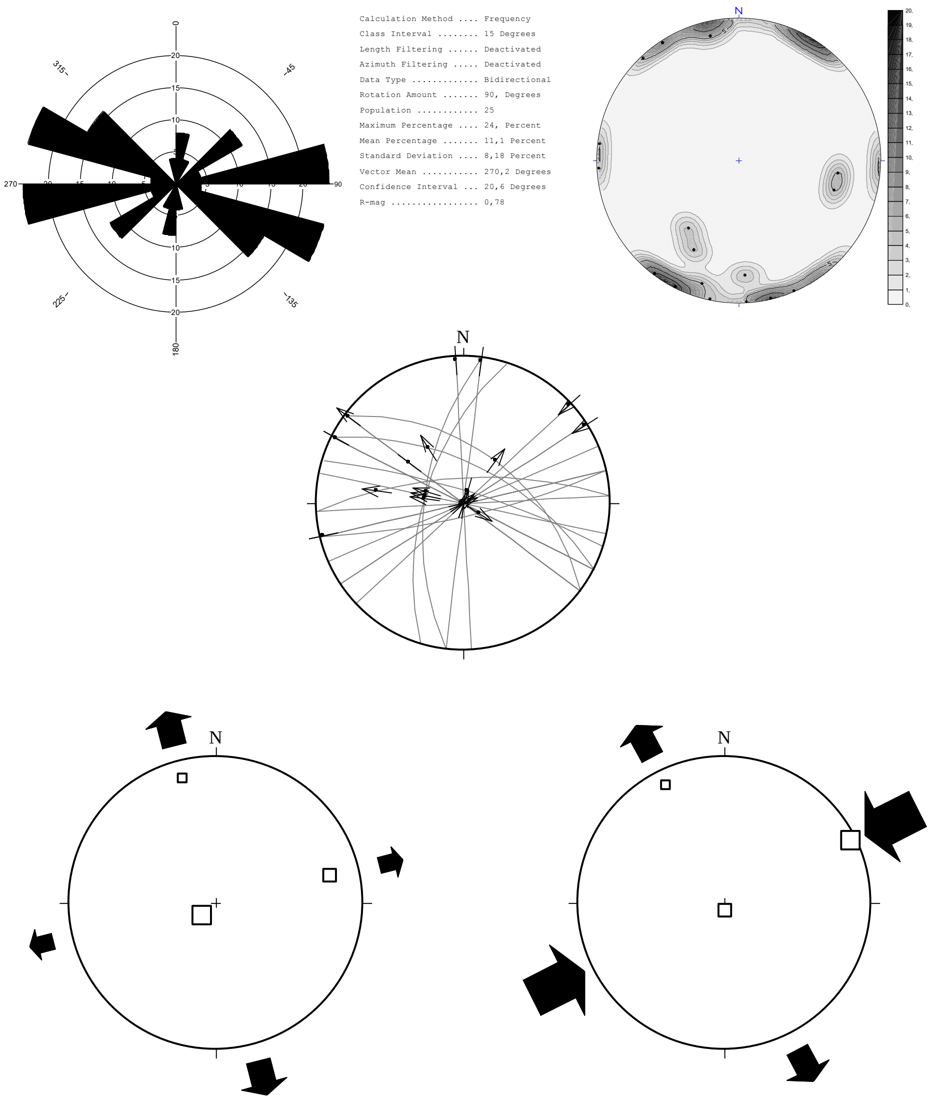

Fig. 3-17. *Structural data Site 2-107. Rose diagram, pole to plane, fault-slip vector and paleostress analysis (black arrows maximum horizontal stress; □σ1>□σ2>□σ3).*

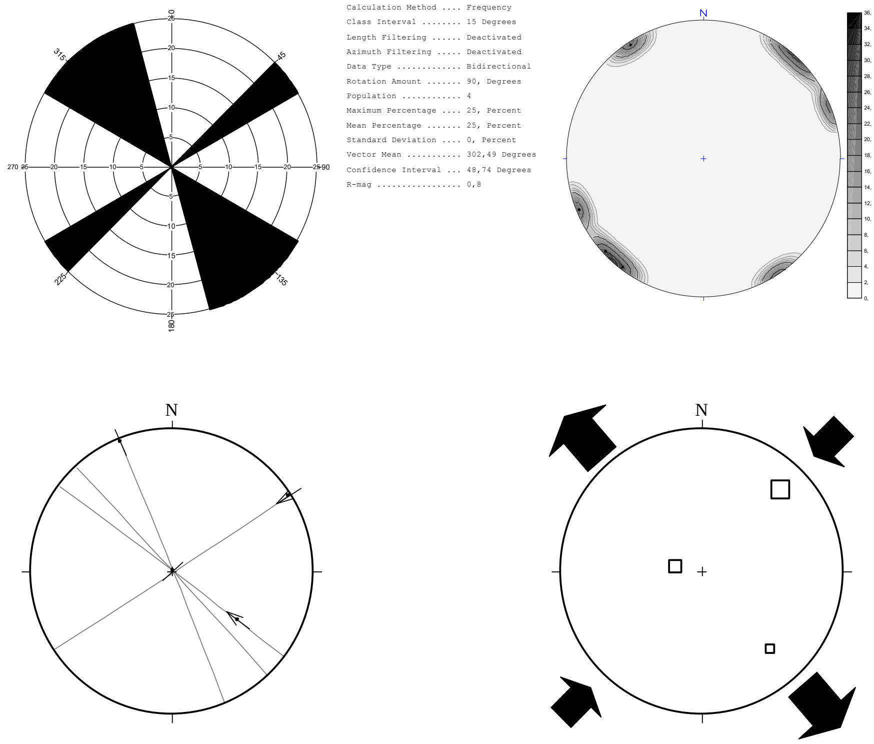

Fig. 3-18. *Structural data Site 2-108. Rose diagram, pole to plane, fault-slip vector and paleostress analysis (black arrows maximum horizontal stress; □σ1>□σ2>□σ3).*

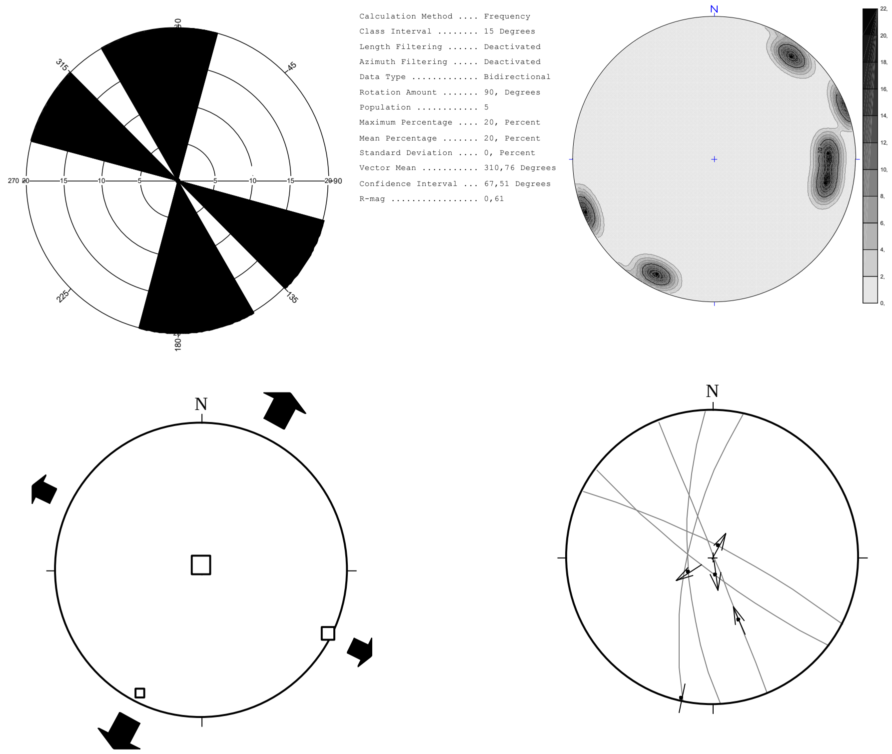

Fig. 3-19. *Structural data Site 2-109. Rose diagram, pole to plane, fault-slip vector and paleostress analysis (black arrows maximum horizontal stress; □σ1>□σ2>□σ3).*

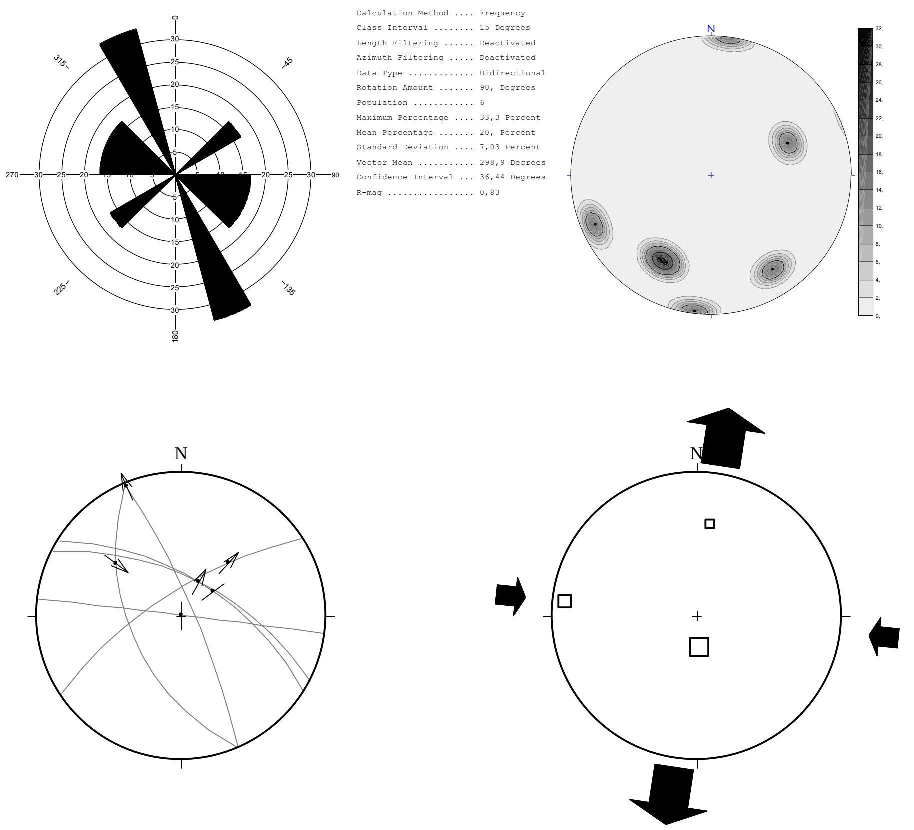

Fig. 3-20. *Structural data Site 2-110. Rose diagram, pole to plane, fault-slip vector and paleostress analysis (black arrows maximum horizontal stress; □σ1>□σ2>□σ3).*

3.4.3 Site 3

This locality is characterized by a small outcrop of Paleocene sandstone (Klitterhorn member) rests unconformably on top of basement rocks (Fig. 3-6). Landing on to this small peak was extremely difficult and only few measurements were collected together with sampling of sandstone and gabbroic intrusion.

Fig. 3-21. *Dip oblique slickenside and calcite fibers at site 3.*

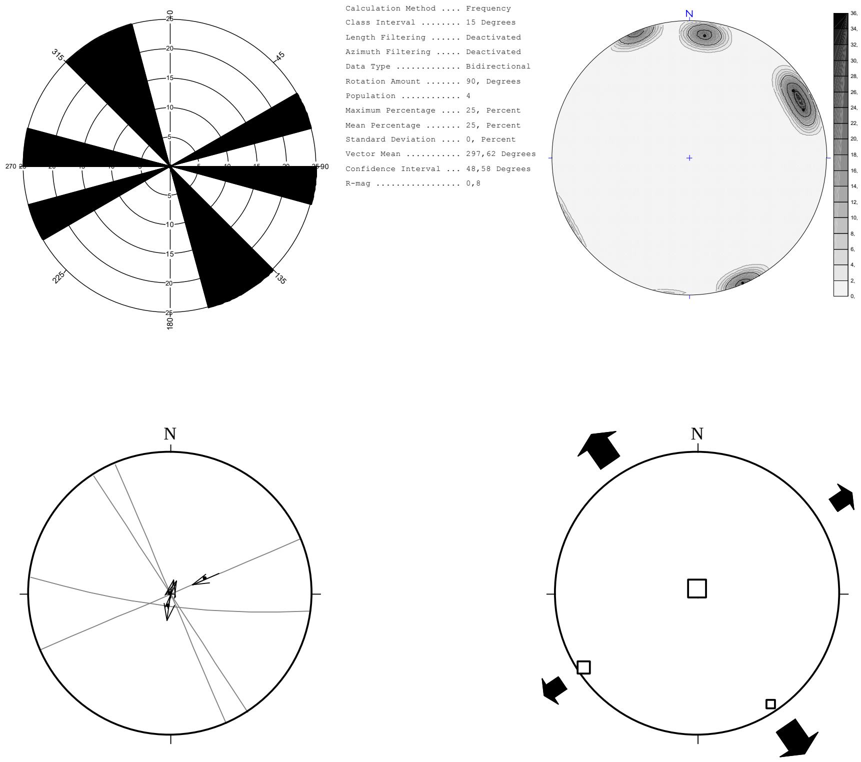

Fig. 3-22. *Structural data Site 3-96. Rose diagram, pole to plane, fault-slip vector and paleostress analysis (black arrows maximum horizontal stress;* □σ1>□σ2>□σ3).

3.4.4 Site 4

The aim to visit site 4 on the Uttental Plateau together with site 12 at Kraemer Ø (Fig. 3-23) was to investigate the presence of brittle deformation post-magmatic, along the contact between the gabbroic Skaergaard intrusion and the basement as described by Nielsen (2004).

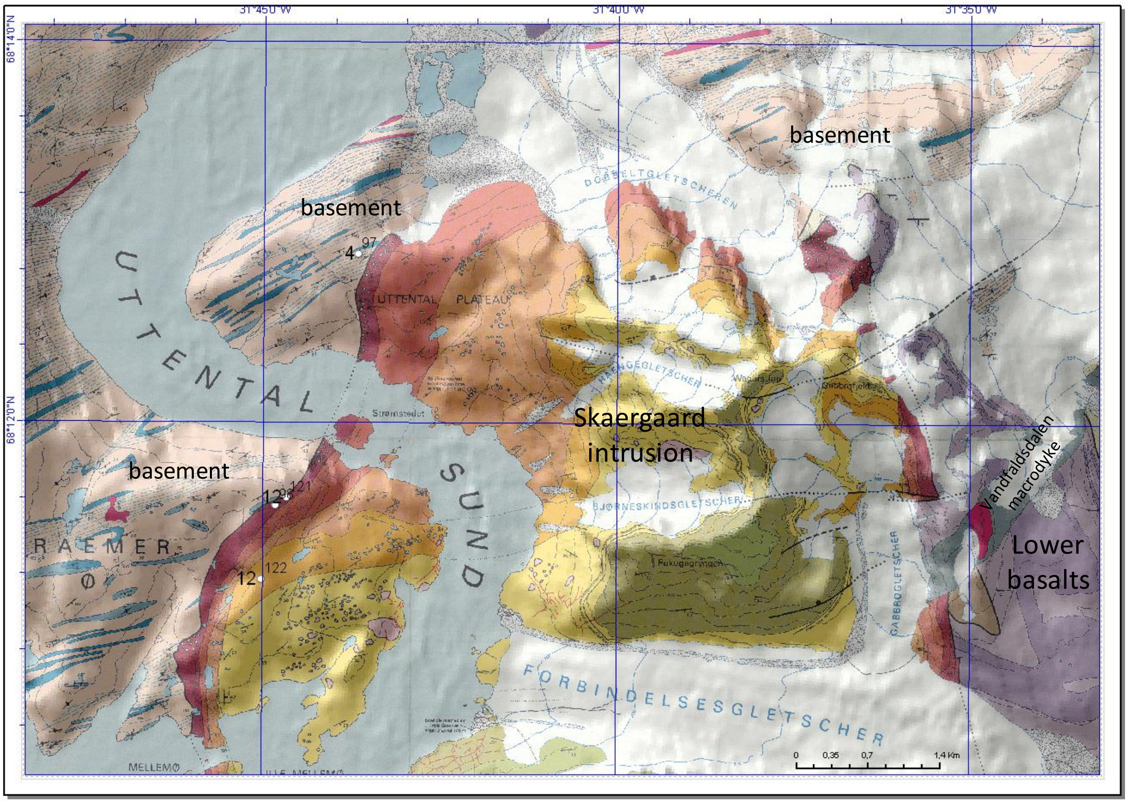

Fig. 3-23. Geological map of the Skaergaard intrusion (after McBirney, 1989) and site location.

The intrusive body was tilted SSE-ward by the coastal flexure as testified by the SSE-ward dipping of the magmatic layering (Nielsen, 2004). The presence of nowadays reverse faults along the contact at site 4 (Fig. 3-24), could be interpreted as rotated rift-related normal faults (Fig. 3-25).

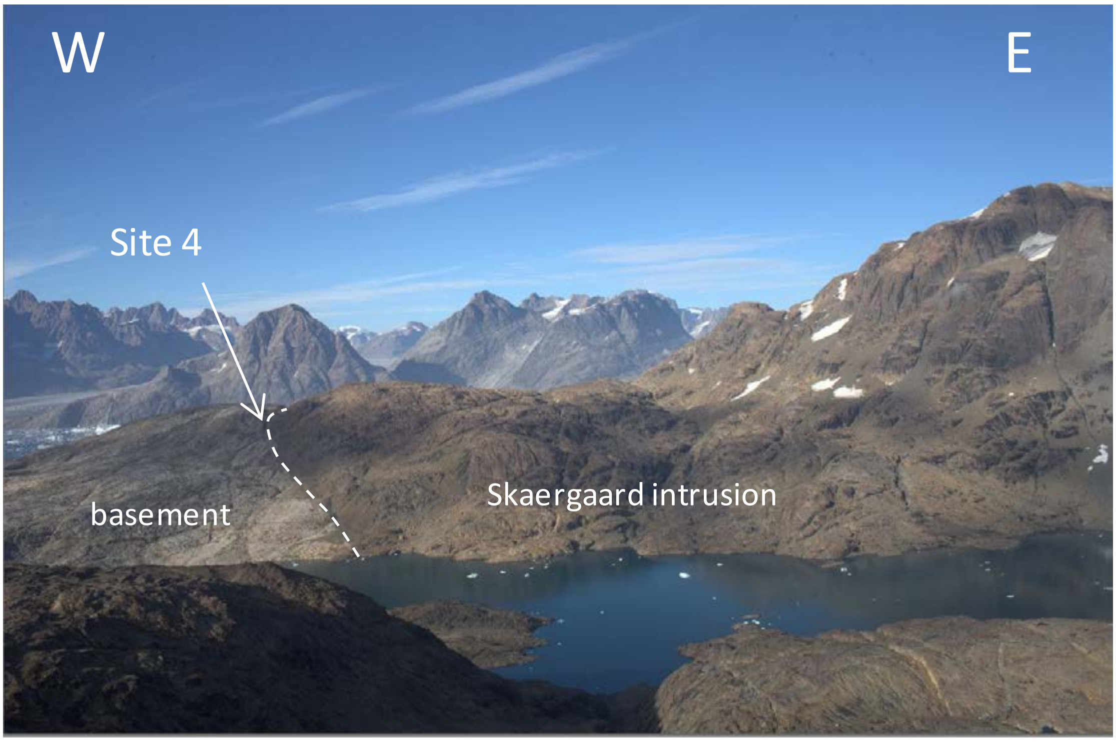

Fig. 3-24. Oblique photo of the Uttental Plateau looking from Kraemer Ø toward North.

Fig. 3-25. NW-ward dipping fractures and faults close to the contact between gabbro and basement at site 4.

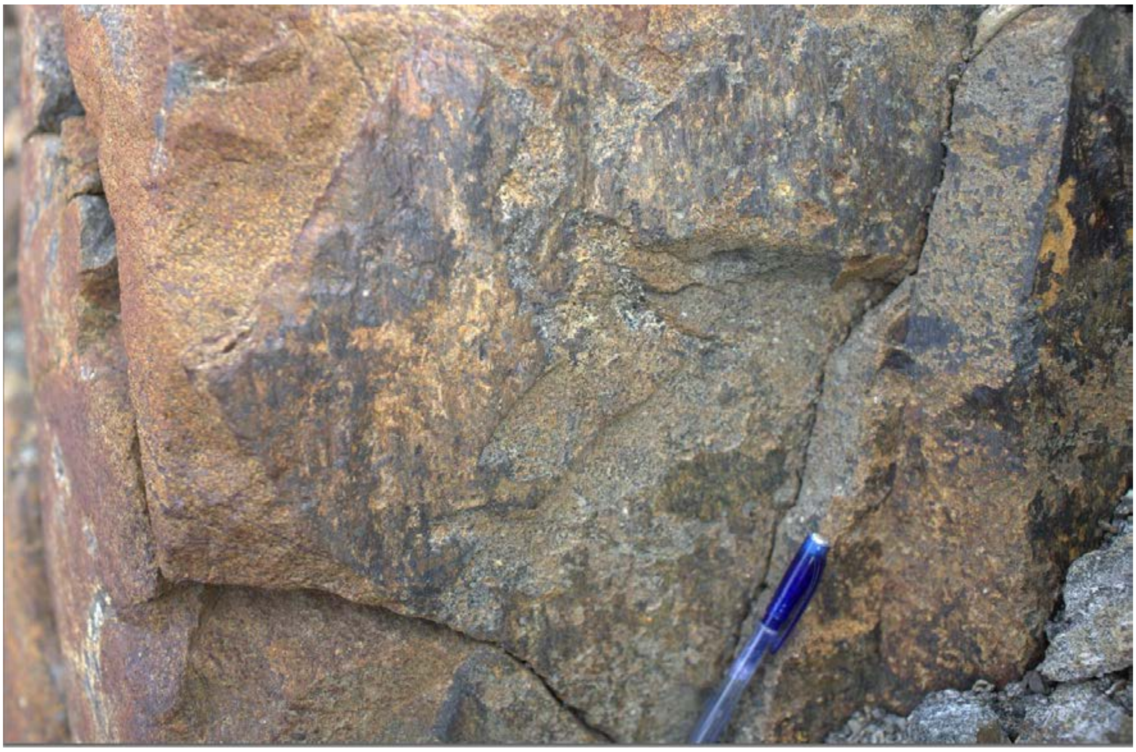

Fig. 3-26 Dip-slip slickenside along a NW-ward dipping fault at site 4.

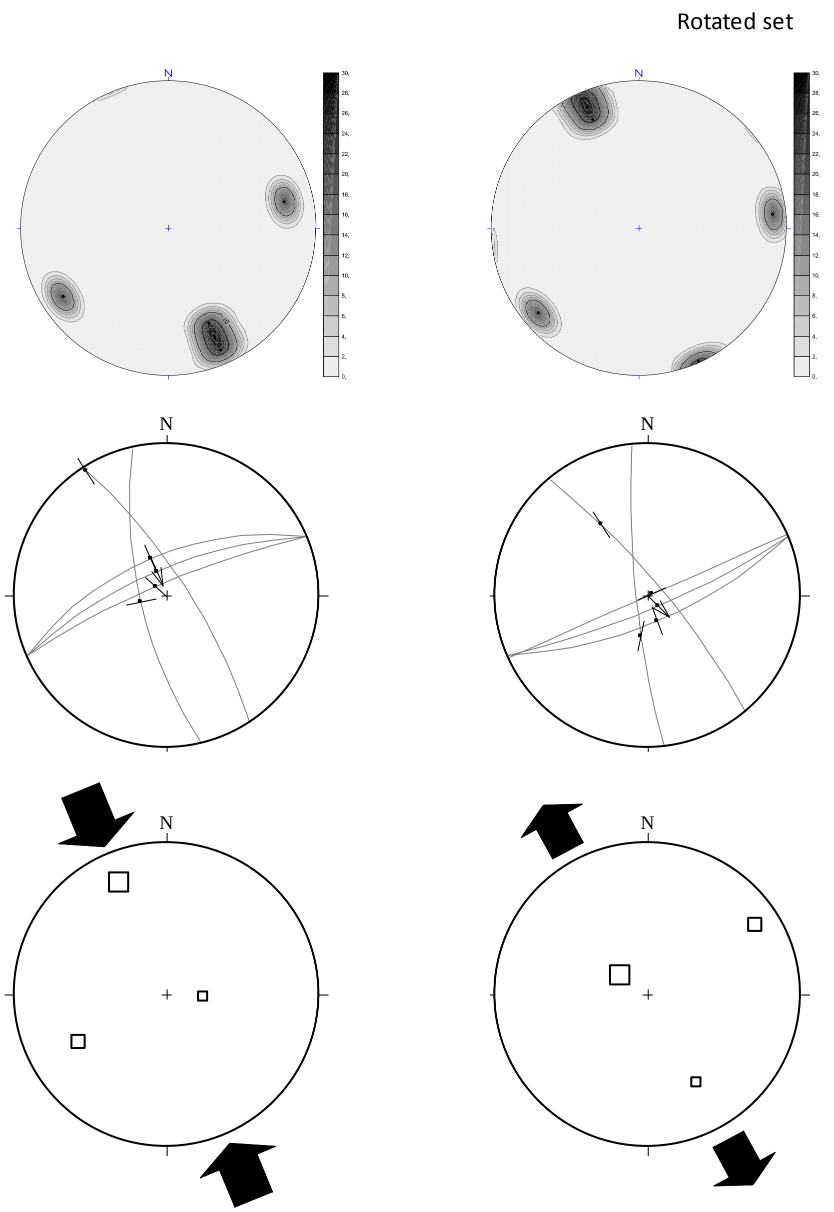

Fig. 3-27. *Left column, structural data at Site 4-97. Pole to plane, fault-slip vector and paleostress analysis (black arrows maximum horizontal stress; □σ_1>□σ_2>□σ_3). Right column show the results after data rotation.*

3.4.5 Site 7

This site represents the farthest point visited during fieldwork. The aim was to collect oblique photos along the western side of the Christian IV Gletscher and to collect structural data along a rift fault mapped at the end of the Fairy Tale Valley (Fig. 3-6). The lithology is represented by Paleocene mudstones and sandstones gently dipping SSE-ward covered by volcanics.

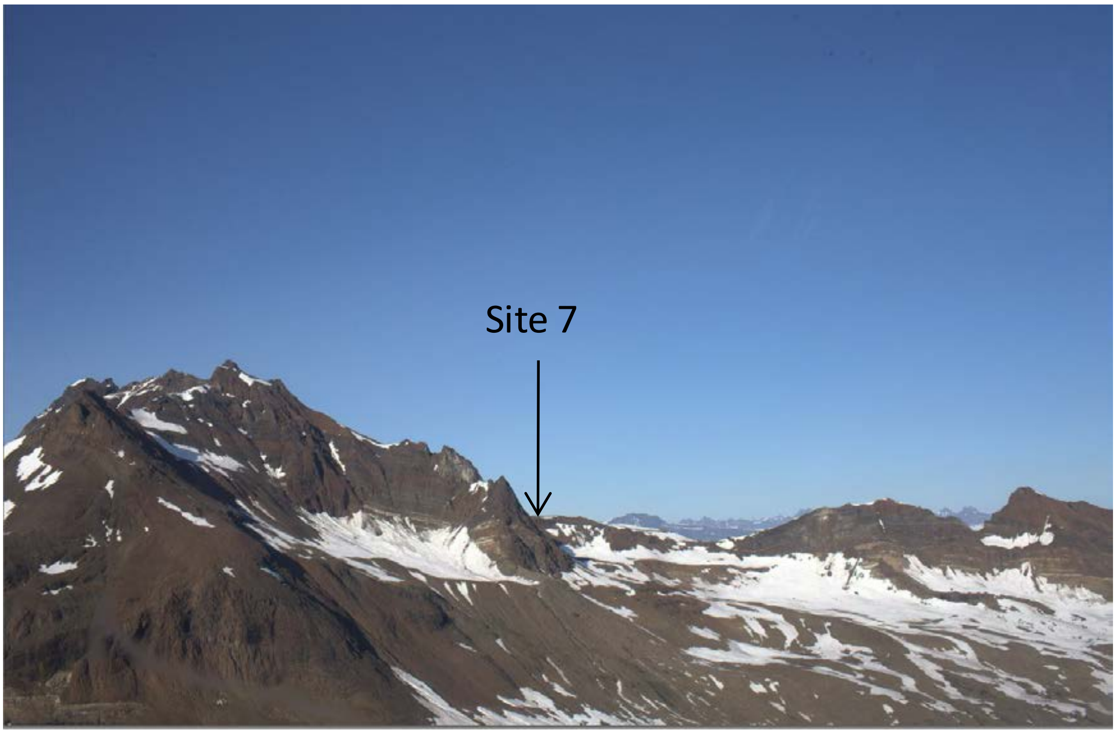

Fig. 3-28. Panoramic view of site 7.

Fig. 3-29. Dip oblique slickenside and calcite fibers along a fault plane at site 7.

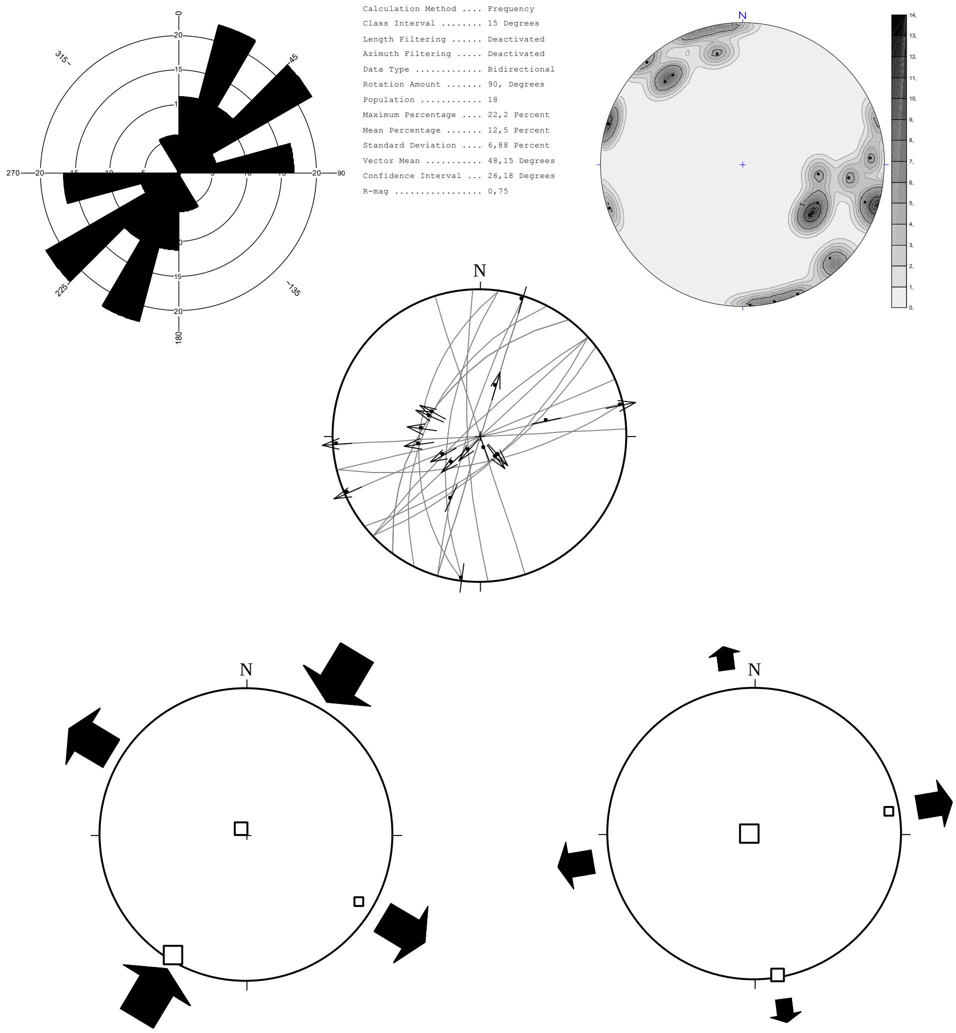

Fig. 3-30. *Structural data Site 7-104. Rose diagram, pole to plane, fault-slip vector and paleostress analysis (black arrows maximum horizontal stress;* □σ1>□σ2>□σ3).

3.4.6 Site 8

The site is located at Kap J.C. Jacobsen (Fig. 3-6) where Plateau Lavas crop out. This area was visited to collect oblique photos for 3D-photogeology and structural data along the coastal flexure.

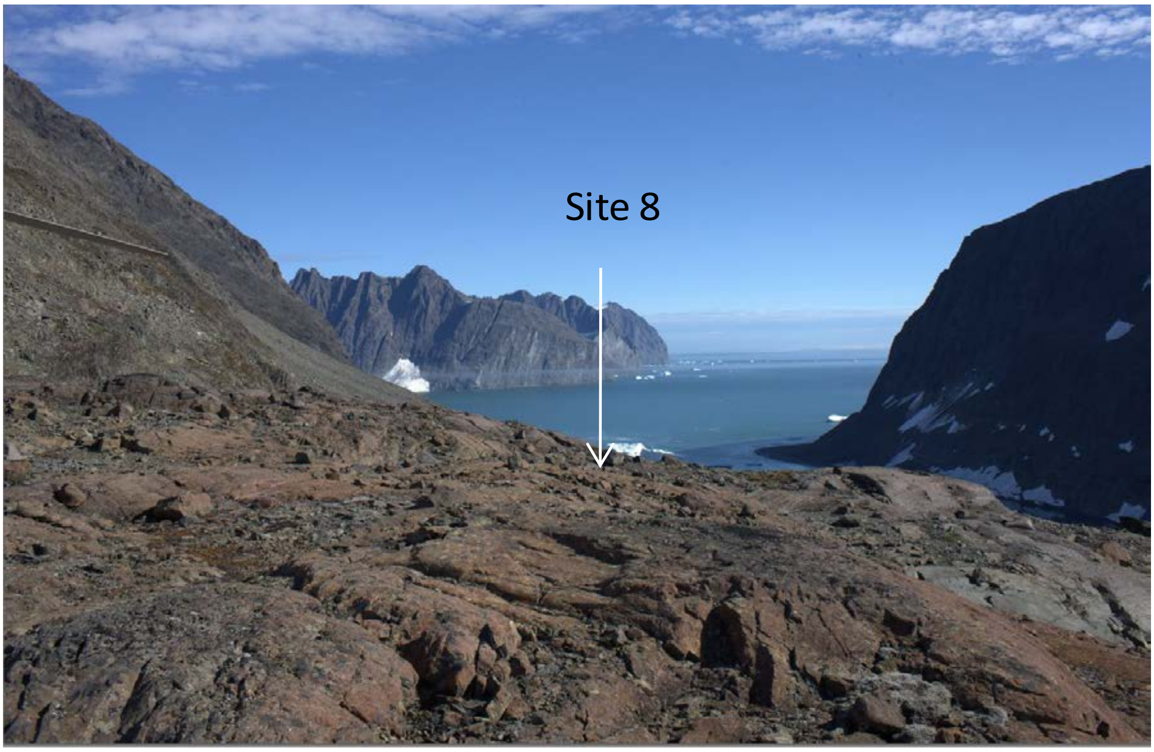

Fig. 3-31. Panoramic view at site 8.

Fig. 3-32. Left-lateral slickenside along a fault plane cutting the basalts at site 8.

Fig. 3-33. E-W oriented dyke cutting through the basalts at site 8.

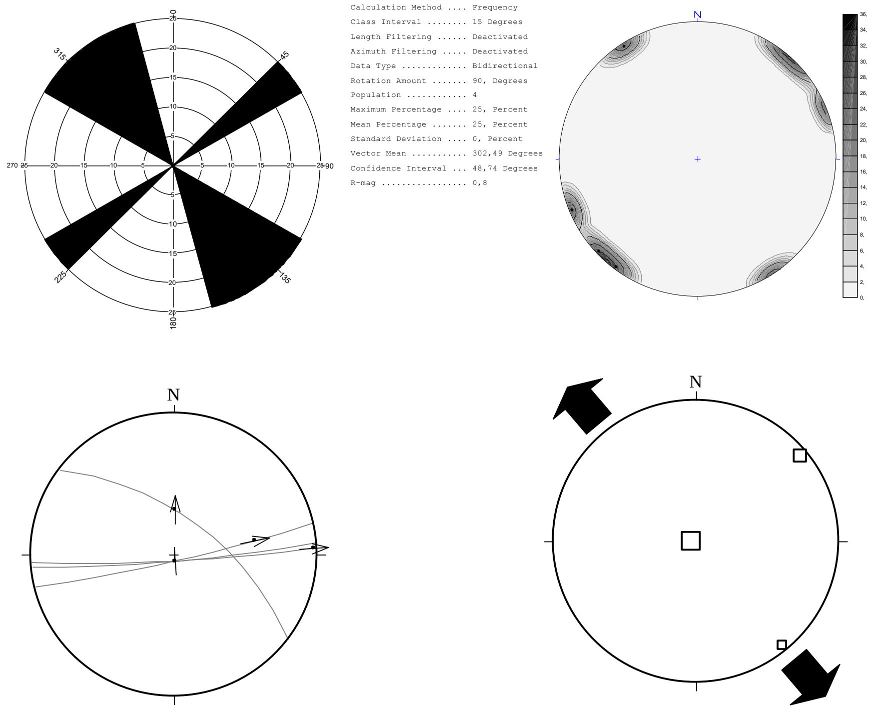

Fig. 3-34. *Structural data Site 8-101. Rose diagram, pole to plane, fault-slip vector and paleostress analysis (black arrows maximum horizontal stress;* □σ1>□σ2>□σ3).

3.4.7 Site 10

The site is located between J.C. Jensen Fjord and Nansen Fjord (Fig. 3-6). The aim to visit this site was the investigation of a NE-SW oriented fault between the volcaniclastic deposits of the Haengefjeld Fm and the Milne Land plateau lavas (Fig. 3-35).

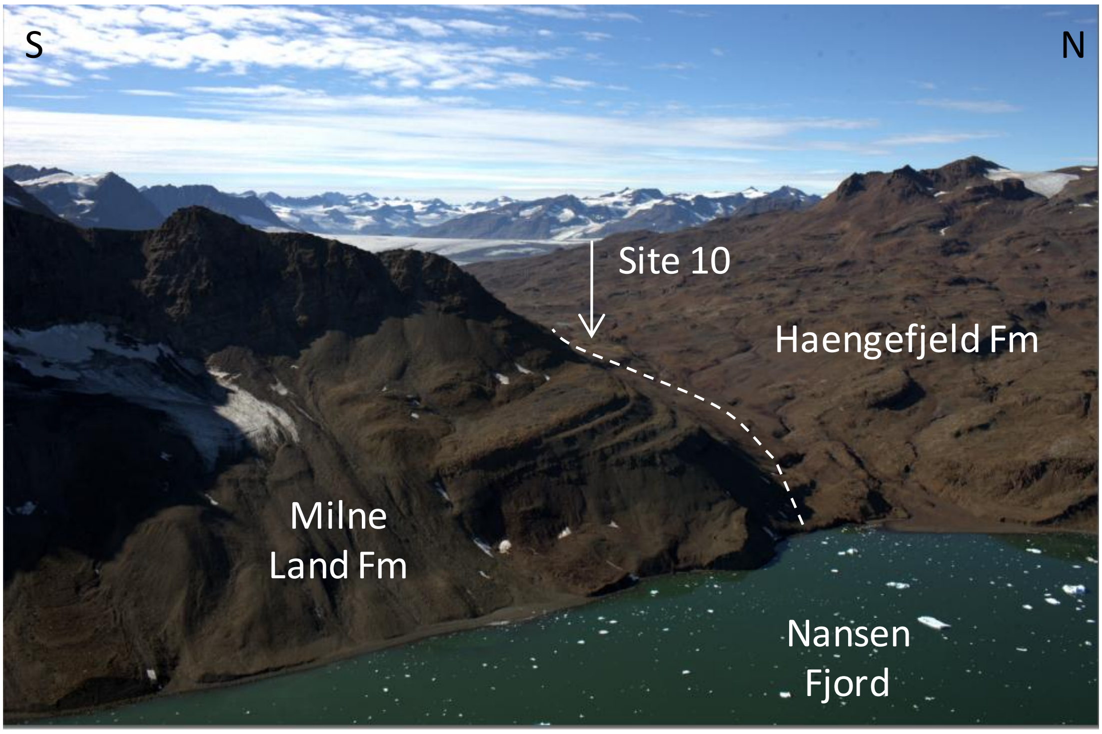

Fig. 3-35. *Panoramic view from Nansen Fjord of site 10 looking West.*

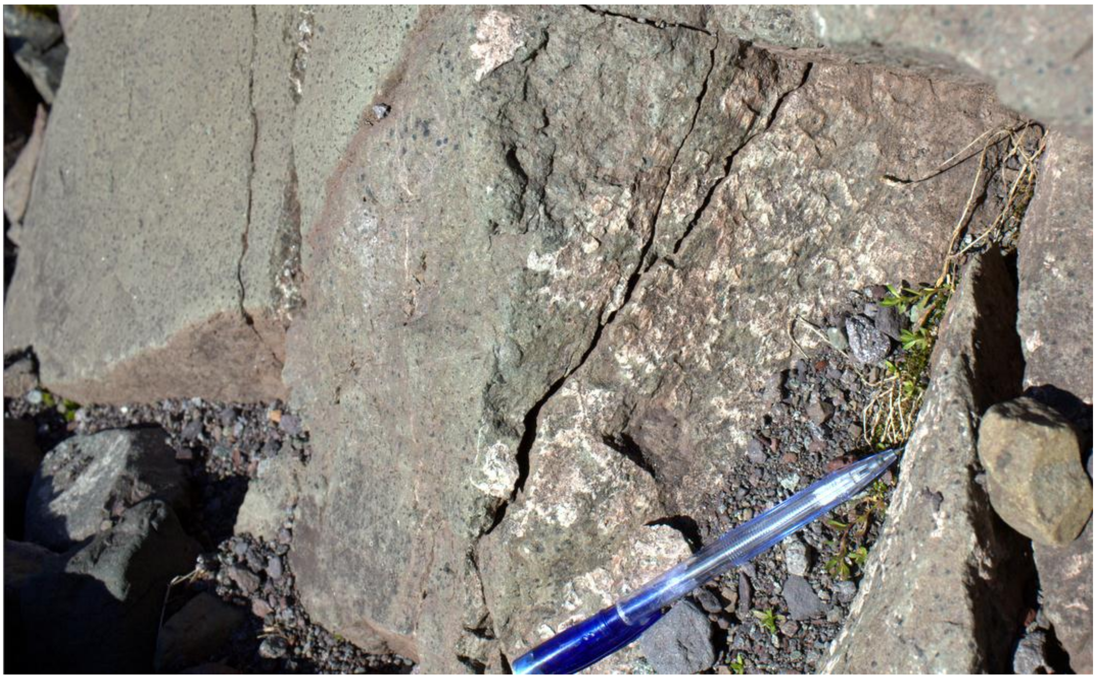
Fig. 3-36. *Dip oblique reverse fault at site 10.*

Fig. 3-37. *Strike-slip right lateral fault at site 10.*

Fig. 3-38. *Slickenside and calcite fibers along a normal fault plane at site 10.*

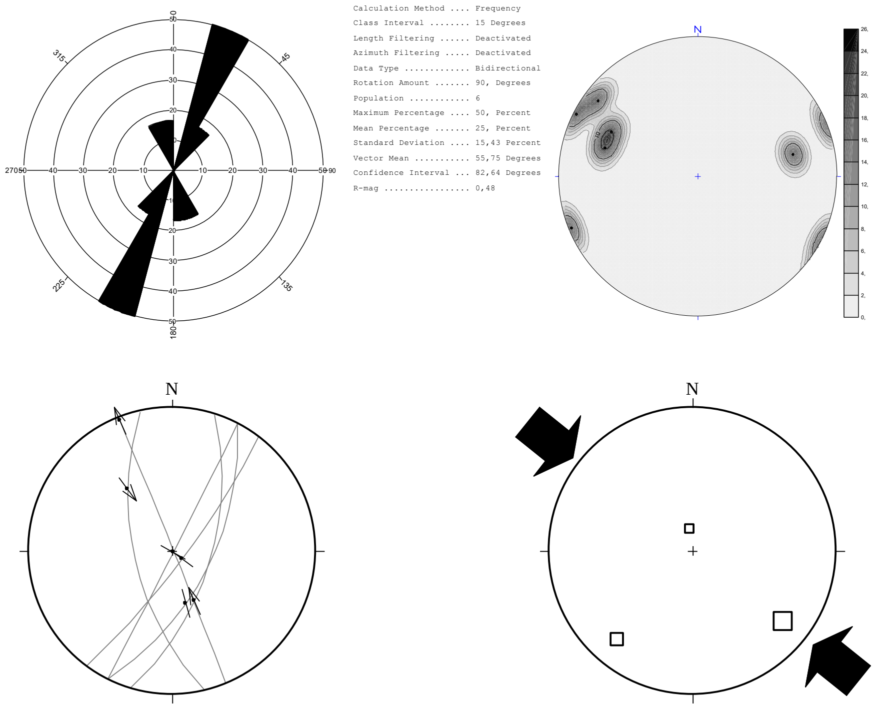

Fig. 3-39. *Structural data Site 10-103. Rose diagram, pole to plane, fault-slip vector and paleostress analysis (black arrows maximum horizontal stress;* □σ1>□σ2>□σ3).

3.4.8 Site 11

The site is located at Nunap Isuap (Fig. 3-6) where the gently sea-ward dipping plateau lavas of the Milne Land Fm are deeply intruded by the land-ward dipping coastal dyke swarm (Fig. 3-40). Oblique photos were collected to evaluate the presence of different generations of dykes. At site 11 was collected only one fault measurement showing a SSE-dipping normal fault parallel to the regional dyke swarm (Fig. 3-41).

Fig. 3-40. Oblique photo across Nunap Isuap. The E-W oriented dyke swarm cuts the SSE-dipping lava flows of the Milne Land Fm.

Fig. 3-41. Dip slip normal fault with slickenside and calcite fibers at site 11.

3.4.9 Site 12

This site is located on the eastern side of Kraemer Ø (Fig. 3-23). As for the previous site 4, the aim was to investigate the presence of faults along the contact of the

Skaergaard intrusion (Fig. 3-42). As described by Nielsen (2004) the intrusion is cut by a NE-SW right lateral fault with an estimated horizontal offset of 400 m. The well developed fault zone is intruded by a dyke bounded by strike-slip contacts (Fig. 3-43).

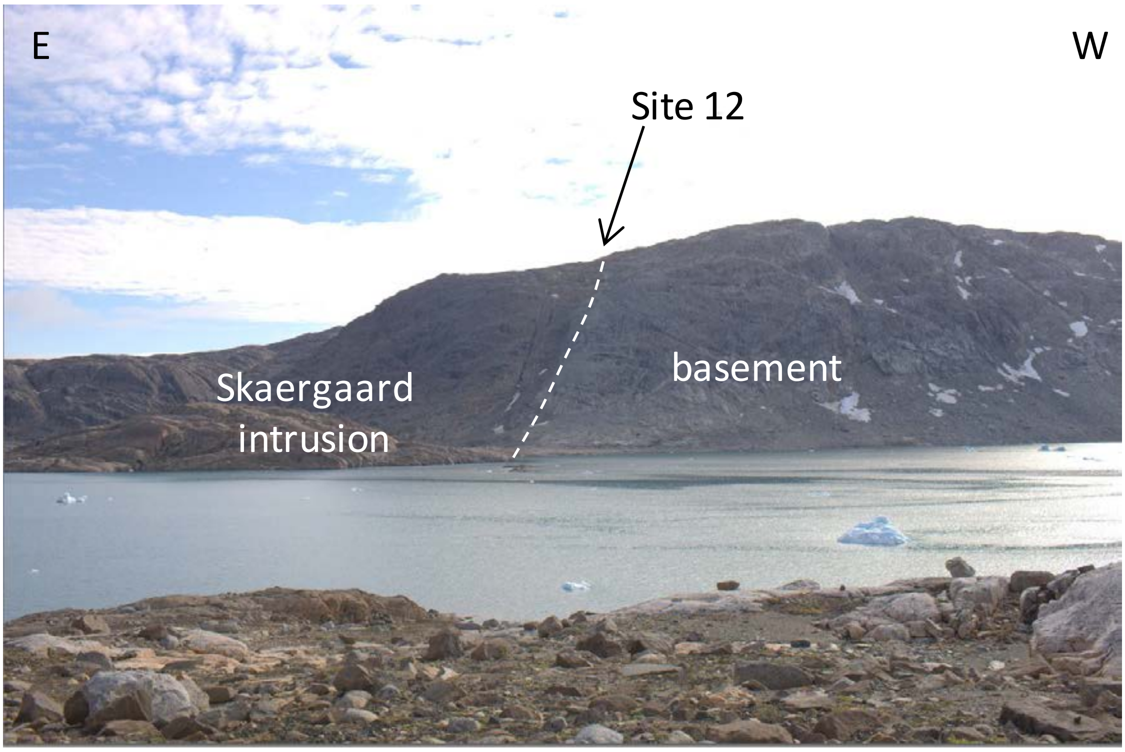

Fig. 3-42. Panoramic view of the western contact between the Skaergaard intrusion and basement rocks.

Fig. 3-43. NE-SW oriented right lateral fault at site 12. White arrows point to R riedel fault plane associate with the master fault (dotted line).

Fig. 3-44. Left lateral fault at site 12.

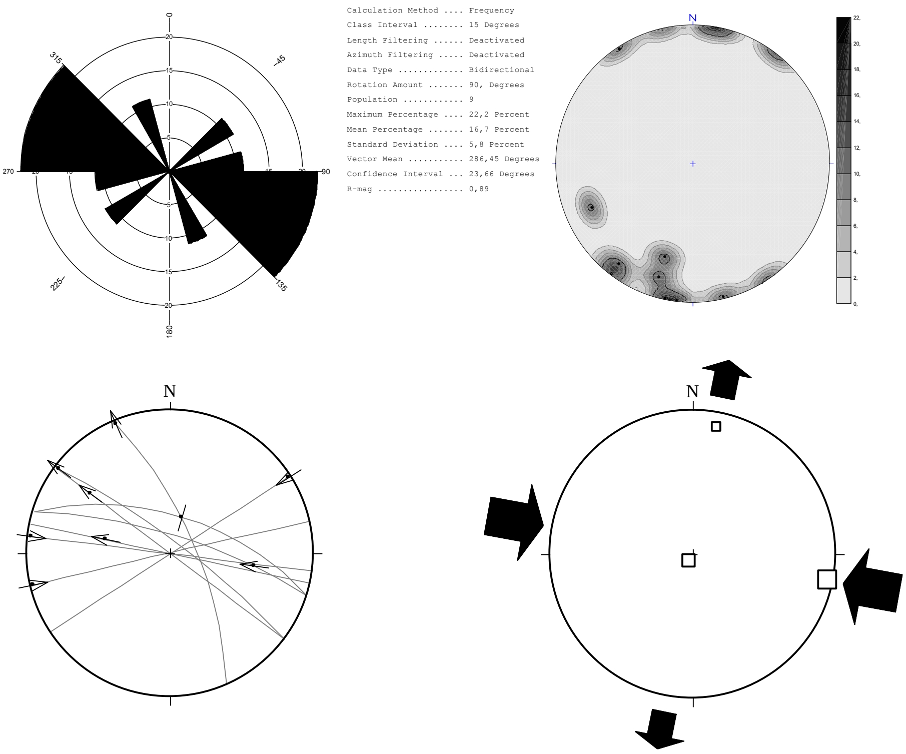

Fig. 3-45. *Structural data Site 12-98/121/122. Rose diagram, pole to plane, fault-slip vector and paleostress analysis (black arrows maximum horizontal stress; □σ1>□σ2>□σ3).*

3.4.10 Site 13

The site is located at the eastern corner of the Miki Fjord (Fig. 3-6). The area is represented by SSE-ward gently dipping volcaniclastic levels of the Haengefjeld Fm covered by the Milne Land plateau lavas (Fig. 3-46). The aim to visit this site was to investigate the presence and the kinematics of ESE-WNW oriented structure crossing the fjord.

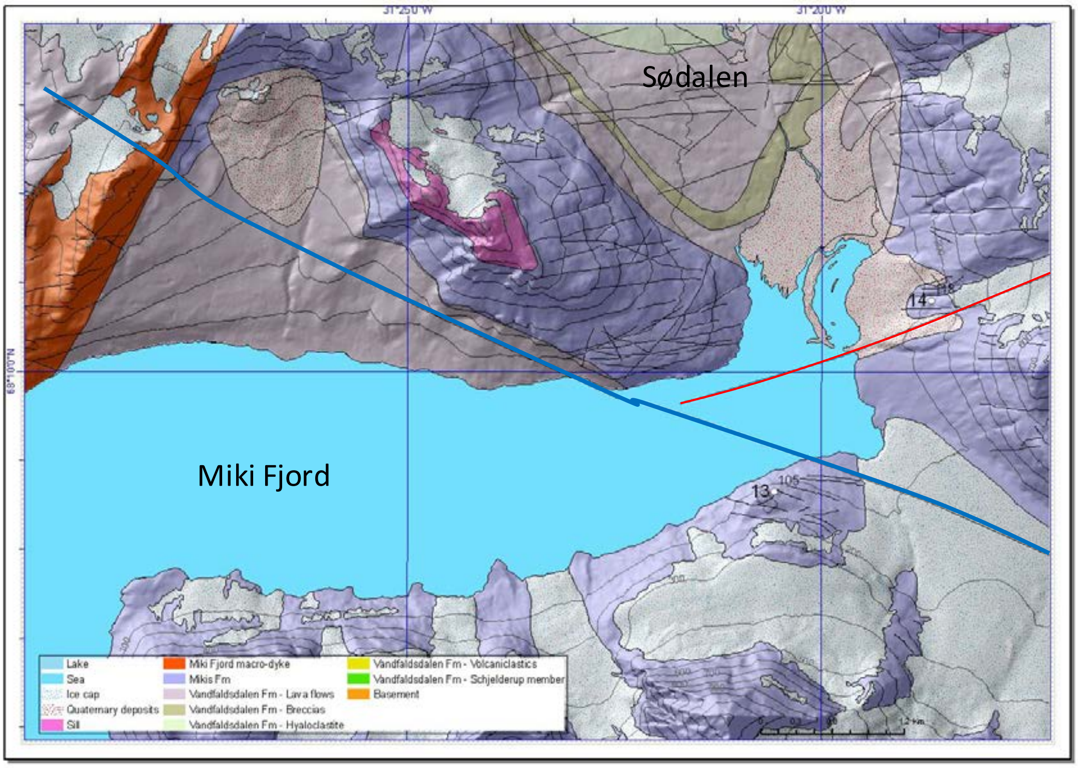

Fig. 3-46. Geological Map of the Miki Fjord area (after after Nielsen et al., 1981)

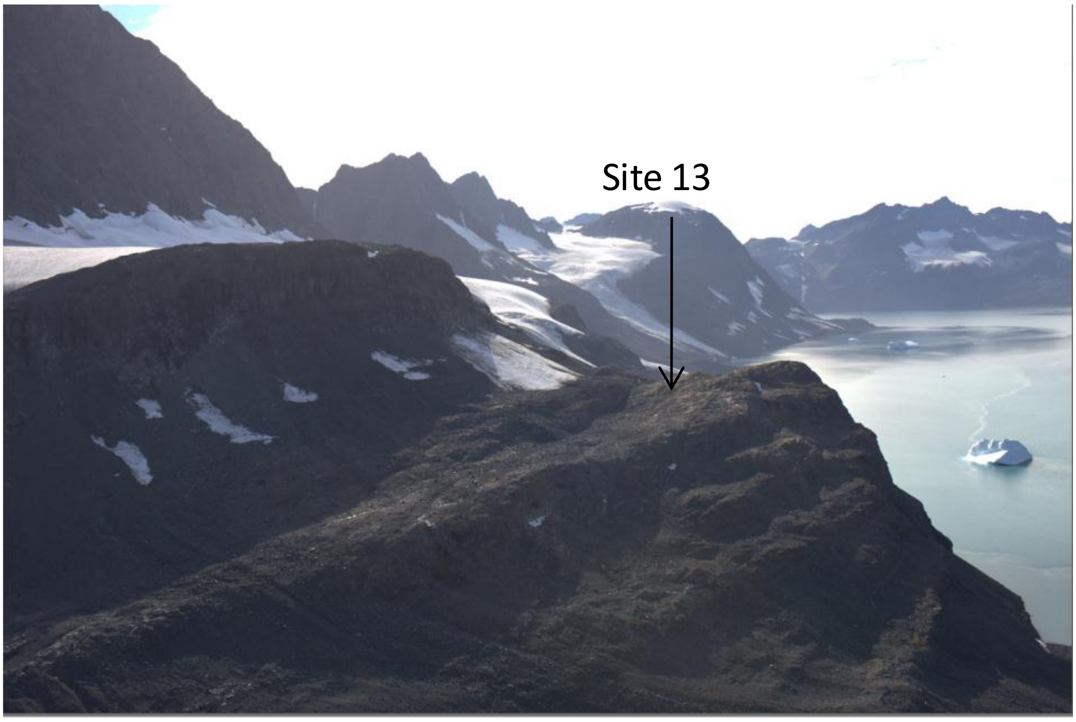

Fig. 3-47. Panoramic view of the Miki Fjord looking from the East.

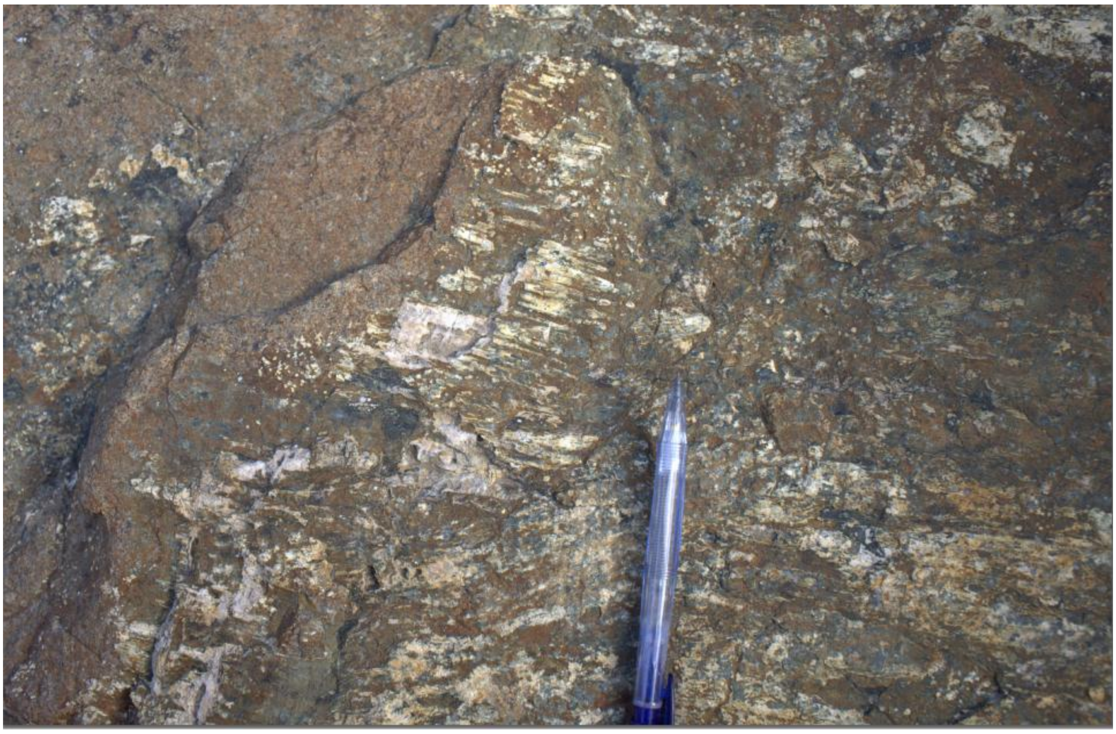

Fig. 3-48. Strike-slip movement along a fault plane at site 13.

Fig. 3-49. Dip oblique slickenside on a fault plane at site 13.

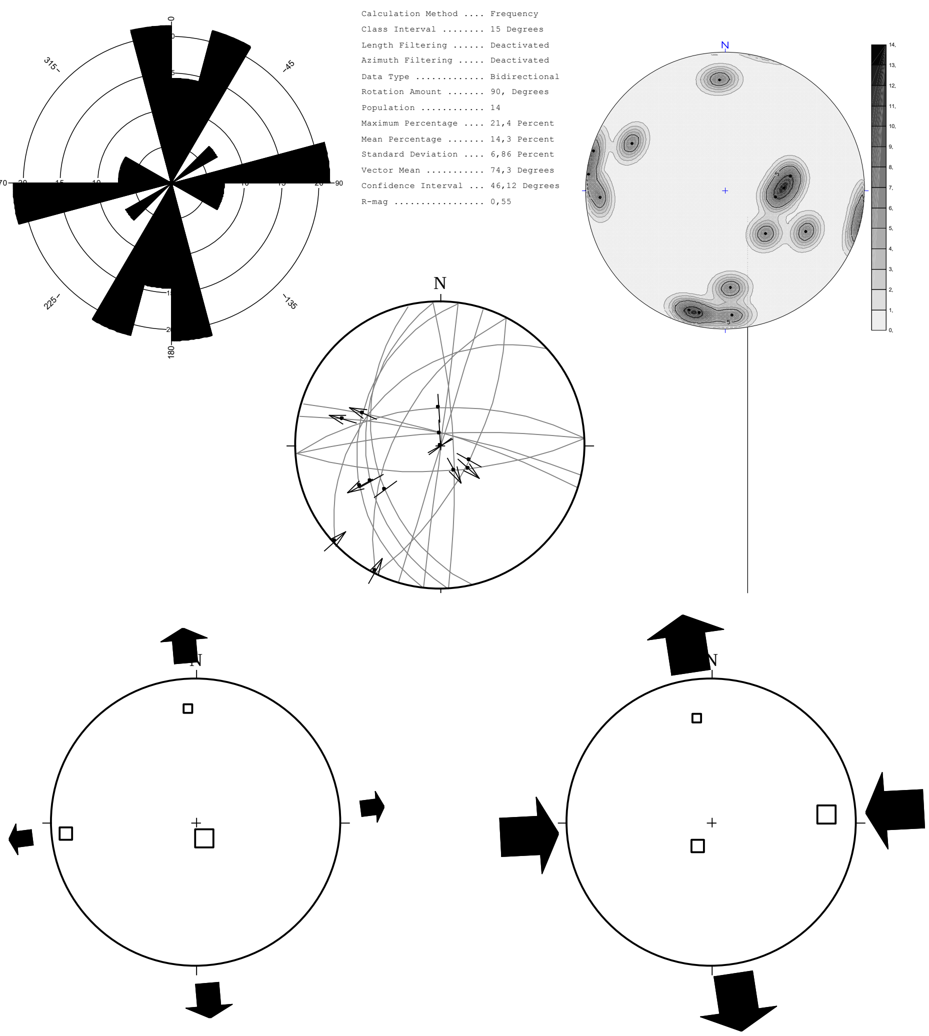

Fig. 3-50. *Structural data Site 13-105. Rose diagram, pole to plane, fault-slip vector and paleostress analysis (black arrows maximum horizontal stress;* □σ1>□σ2>□σ3).

3.4.11 Site 14

The site is located on the southernmost part of Sødalen (Fig. 3-46). This locality was visited to investigate the presence of a WSW-ENE oriented flexure-related normal fault (Fig. 3-51).

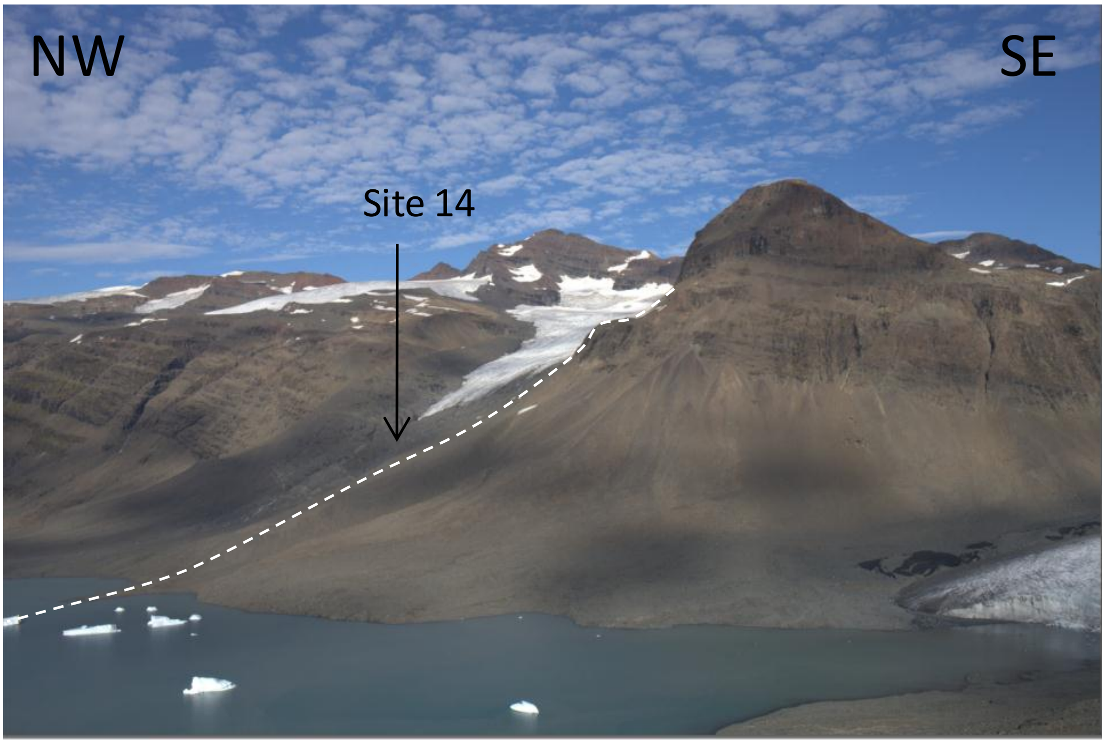

Fig. 3-51. Panoramic view of Site 14. Dotted line corresponds to a flexure-related normal fault.

Fig. 3-52. Dip slip slickenside and calcite fibers along the main fault trace at Site 14.

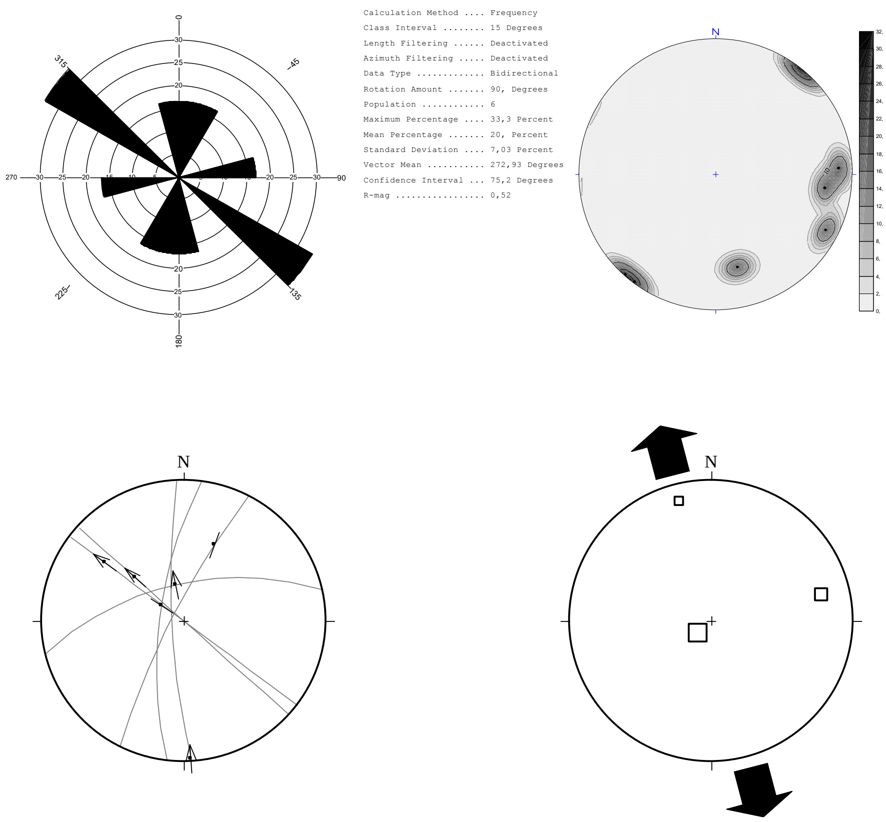

Fig. 3-53. *Structural data Site 14-118. Rose diagram, pole to plane, fault-slip vector and paleostress analysis (black arrows maximum horizontal stress;* □σ1>□σ2>□σ3).

3.4.12 Site 16

The site is located east of Sødalen (Fig. 3-6). In this area lava flows and volcaniclastis belonging to the Vandfaldsdalen Fm crop out (Figs 3-7 and 3-8). This locality was visited to investigate the kinematics and cross-cutting relationships between fault systems and dykes well visible from aerial photos (Fig. 3-54).

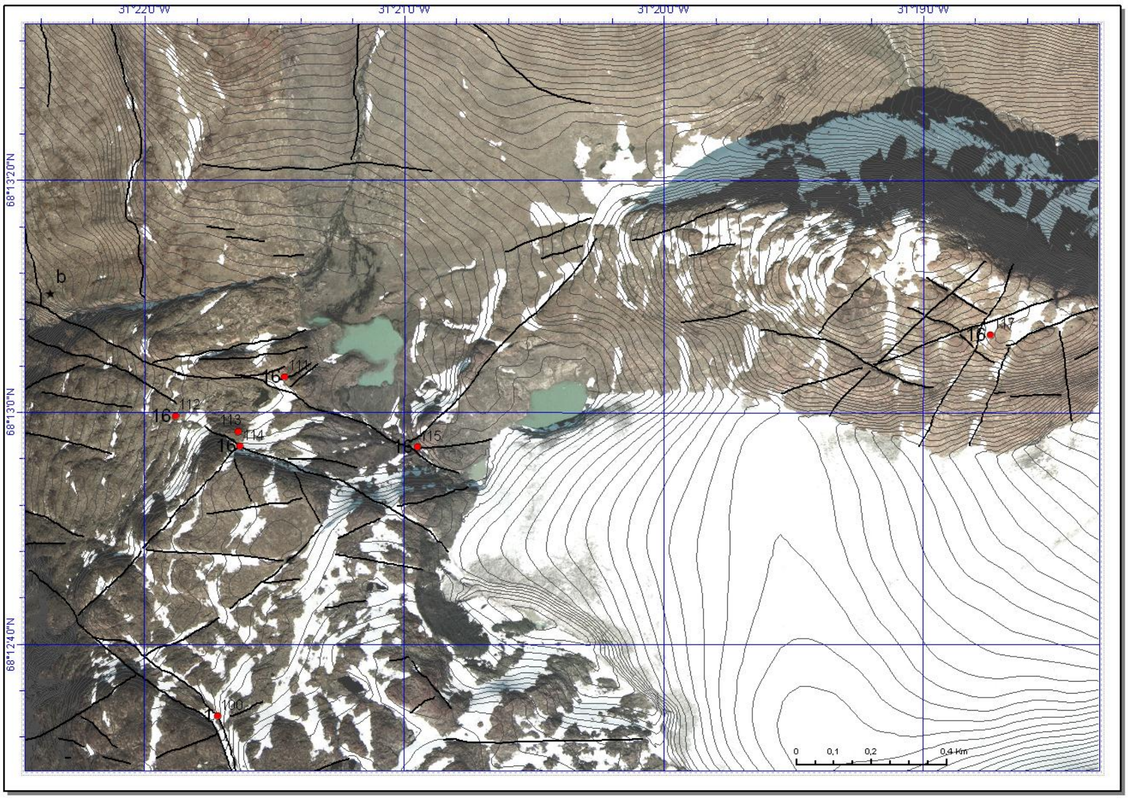

Fig. 3-54. Aerial photo (1:27 000 scale) with the distribution of waypoints visited at Site 16. Black lines are faults and dykes collected with the 3D-photogeology tool.

Fig. 3-55. Calcite infill along a fault zone at Site 16-111.

Fig. 3-56. ESE-WNW trending fault zone with calcite and probable epidote at Site 16-112.

Fig. 3-57. Well developed slickenside and calcite fibers along a crushed fault zone at Site 16-115.

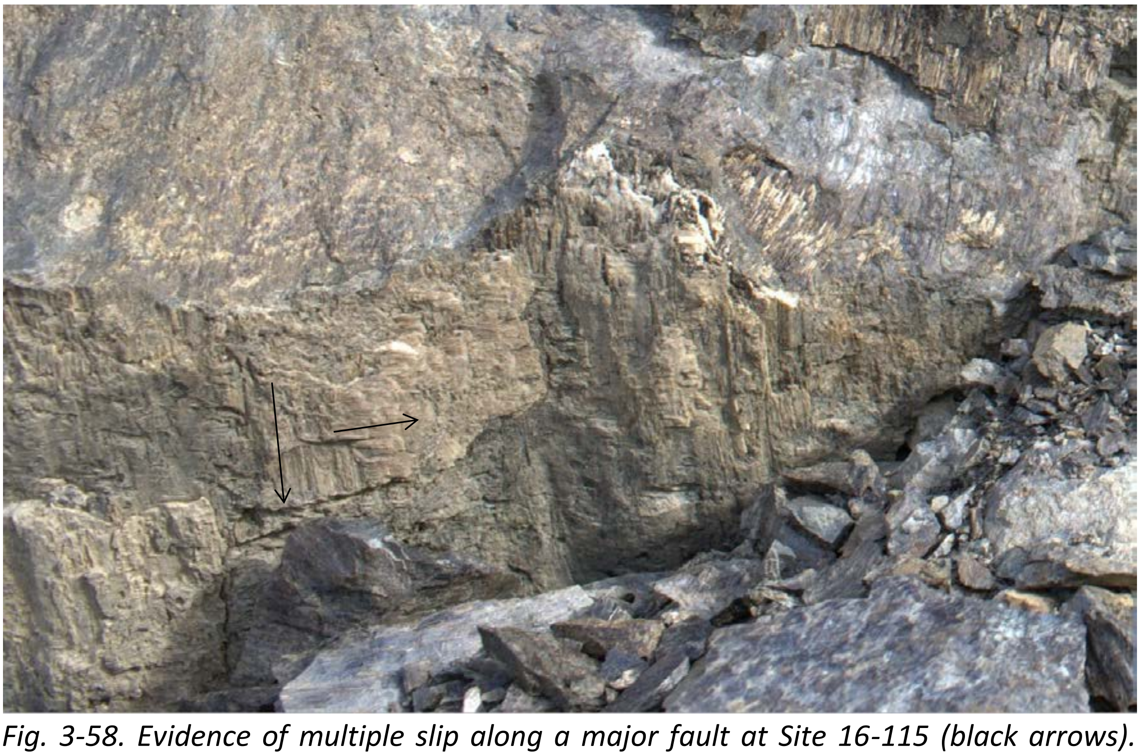

Fig. 3-58. Evidence of multiple slip along a major fault at Site 16-115 (black arrows). The strike-slip movement overprints the dip slip one.

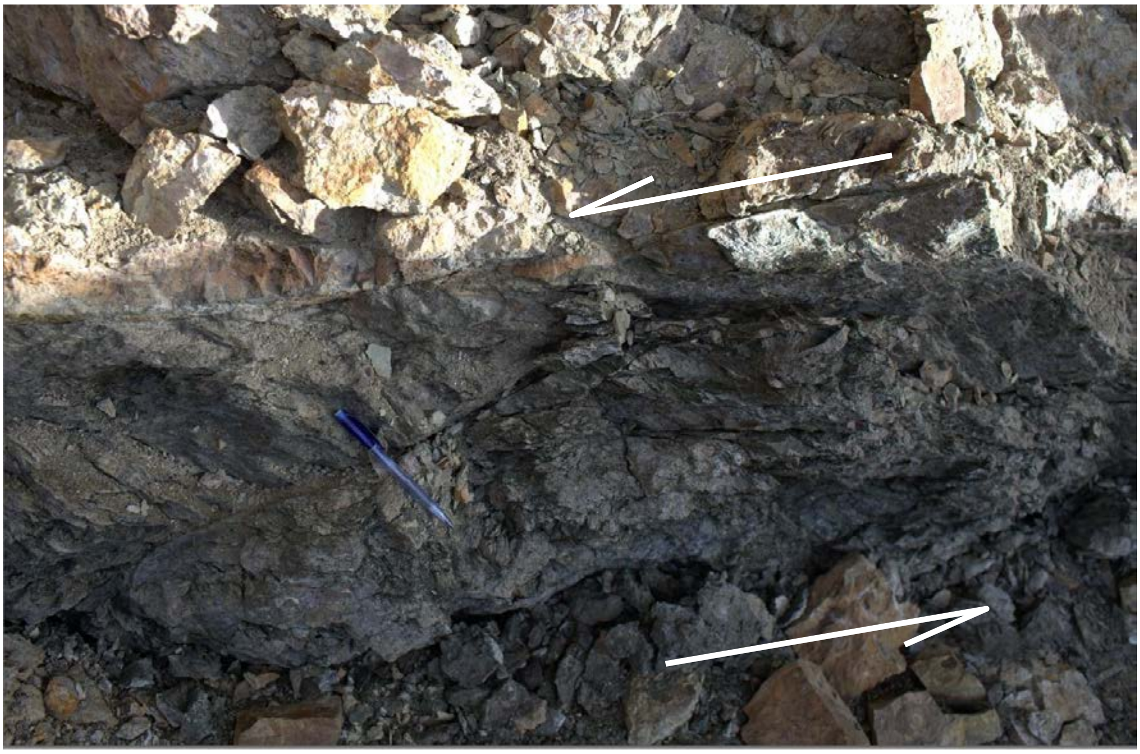

Fig. 3-59. Left-lateral fault zone at Site 16-115.

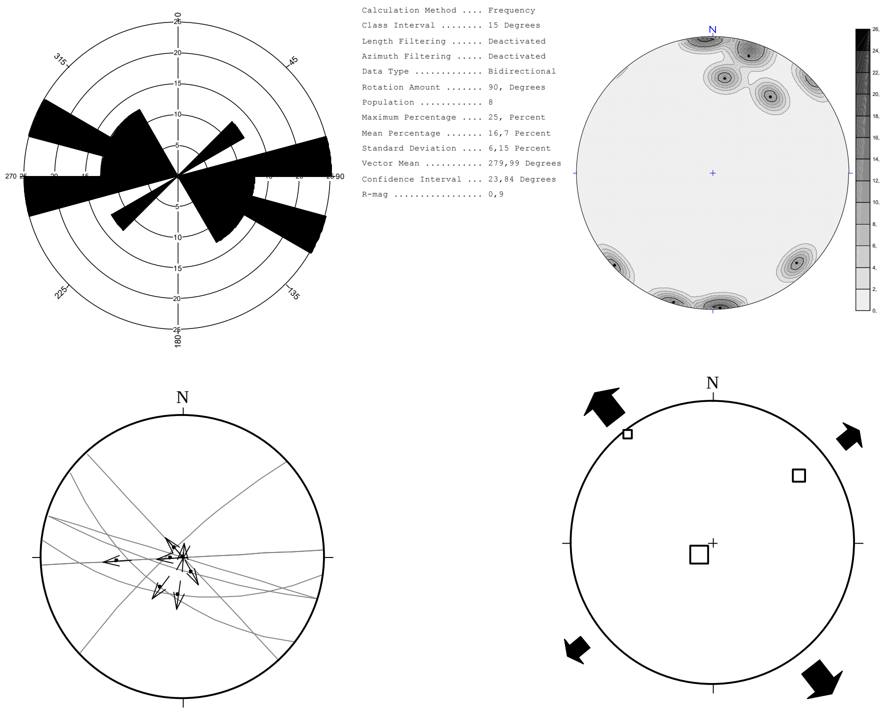

Fig. 3-60. *Structural data Site 16-111. Rose diagram, pole to plane, fault-slip vector and paleostress analysis (black arrows maximum horizontal stress; □σ1>□σ2>□σ3).*

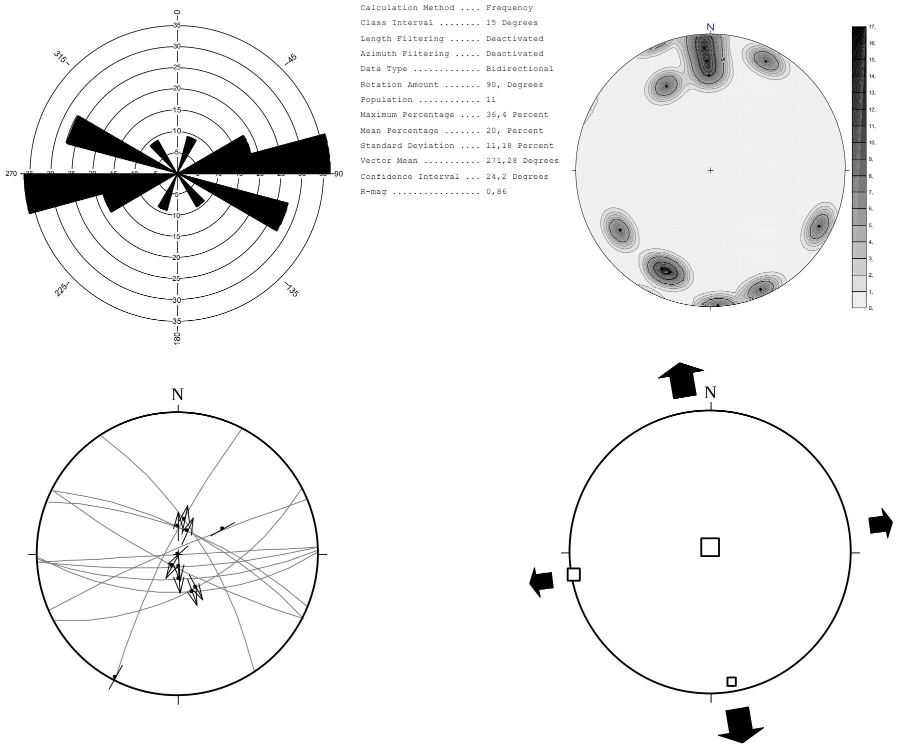

Fig. 3-61. *Structural data Site 16-112. Rose diagram, pole to plane, fault-slip vector and paleostress analysis (black arrows maximum horizontal stress; □σ1>□σ2>□σ3).*

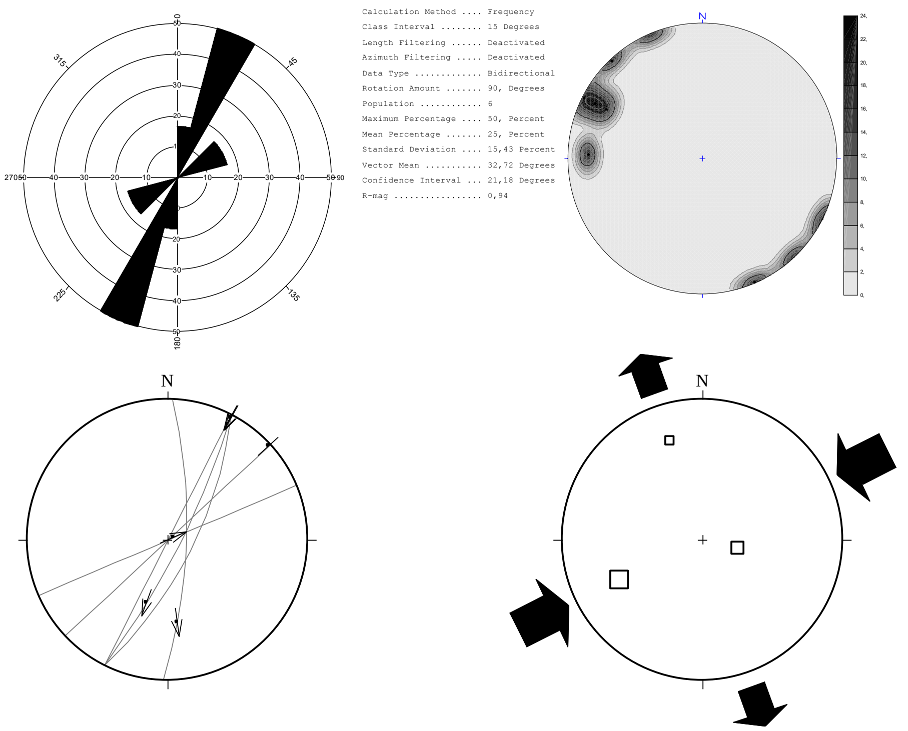

Fig. 3-62. *Structural data Site 16-113. Rose diagram, pole to plane, fault-slip vector and paleostress analysis (black arrows maximum horizontal stress; □σ1>□σ2>□σ3).*

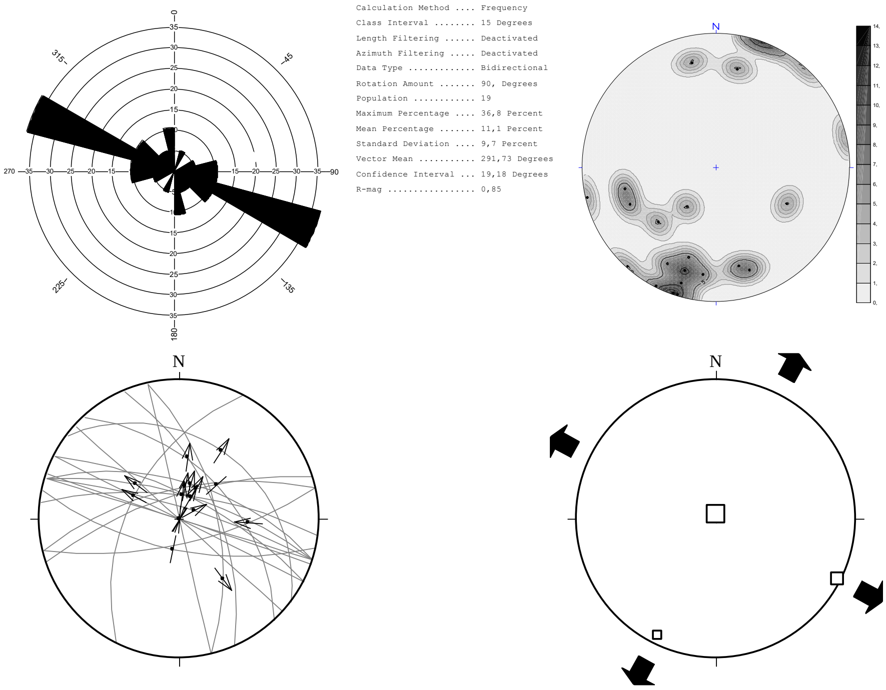

Fig. 3-63. *Structural data Site 16-114. Rose diagram, pole to plane, fault-slip vector and paleostress analysis (black arrows maximum horizontal stress;* □σ1>□σ2>□σ3).

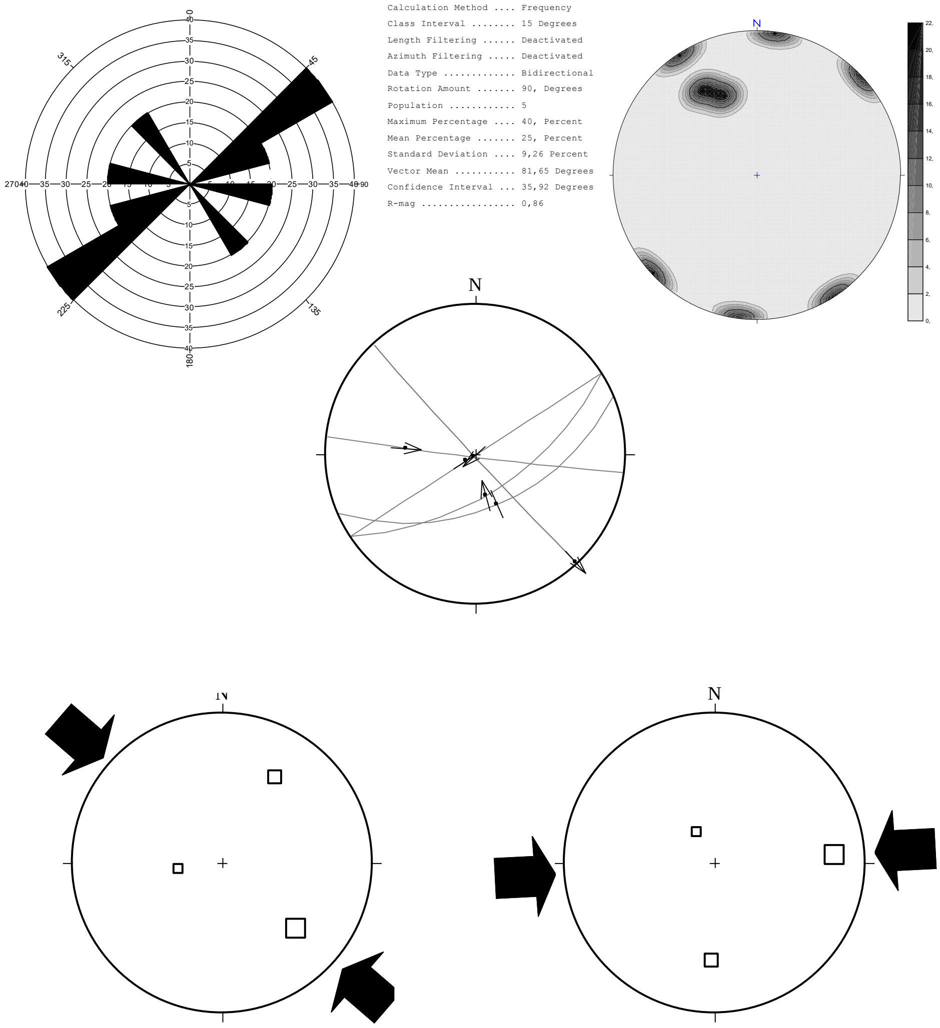

Fig. 3-64. *Structural data Site 16-115. Rose diagram, pole to plane, fault-slip vector and paleostress analysis (black arrows maximum horizontal stress; □σ1>□σ2>□σ3).*

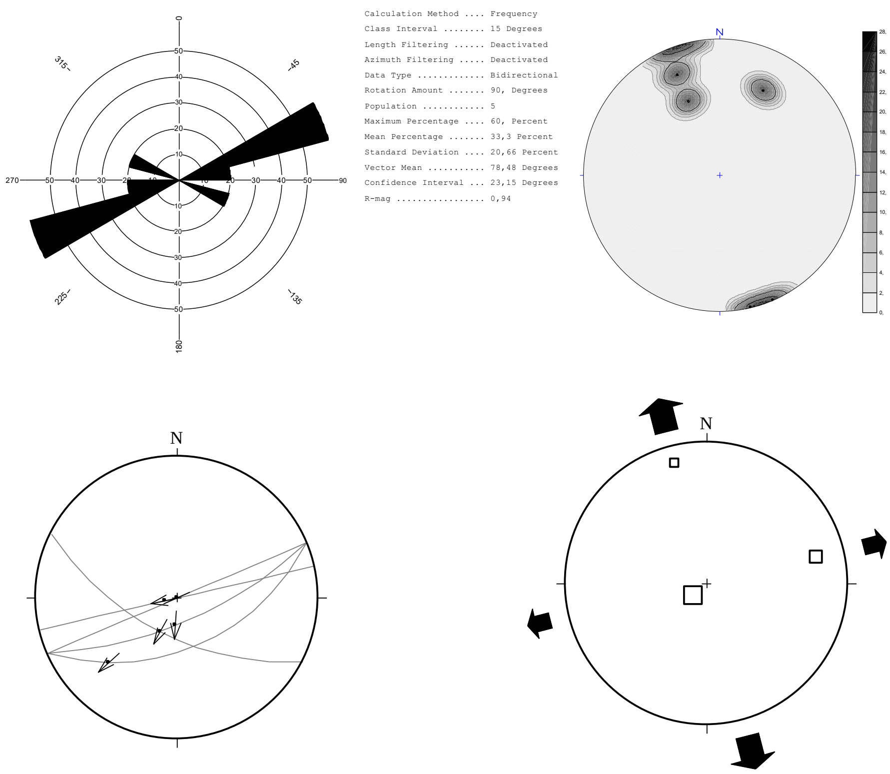

Fig. 3-65. *Structural data Site 16-117. Rose diagram, pole to plane, fault-slip vector and paleostress analysis (black arrows maximum horizontal stress;* □σ1>□σ2>□σ3).

4. Tectonic setting

4.1 Introduction

This paragraph represents a synthesis of the tectono-sedimentary evolution of the Kangerlussuaq Basin as it is well accepted and acknowledged.
The Cretaceous–Paleogene succession in the Kangerlussuaq Basin of southern East Greenland is an onshore analogue to the Faroes-Shetland region forming the conjugate margin (Larsen et al., 1999). The exposed 1 km thick sedimentary succession is dominated of mudstone and fine grained sandstone and records a Late Aptian–Albian transgression followed by Late Cretaceous highstand. The Cretaceous succession is unconformable overlain by Paleocene sandstones. During Paleocene time the Kangerlussuaq area experienced several episode of uplift leading to extensive erosion and deposition of coarse clastic sediments in the offshore areas to the south east. Outcrops illustrate a proximal–distal facies change from an inland bedload-dominated braidplain to stacked shallow marine and deltaic successions in the most distal areas to the southeast. The delta may have fed sand into a wide storm dominated shelf or directly into submarine channels/submarine fans in deeper basins towards the southeast, depending on the offshore basin physiography. The thick sedimentary succession allows recognition of repeated episodes of deltaic mouth-bar progradation most likely controlled by tectonic or magmatic uplift, shortly followed by the onset of volcanism. The sedimentary succession is overlain by Late Paleocene – Eocene volcaniclastics, pyroclastics and flood basalts reaching a thickness of 4–6 km.
The most prominent and probably the border fault of the basin is the NE-trending, SE-dipping, Sortekap Fault, a normal fault situated to the northwest of Pyramiden (Fig. 4-1). The fault has a minimum throw of 950m as shown by the displacement of the unconformity on top of the basement. Other faults with the same trend, but lesser throws are found to the southwest of Pyramiden and at the northeastern end of the Sortekap Fault, in the Sediment Bjerge (Larsen and Whitham 2005). Those to the southwest of Pyramiden have a NW dip and are antithetic to the Sortekap Fault as described in Nielsen (1975) and Nielsen & Brooks (1981). Faults in the Sediment Bjerge are probably splays at the end of the Sortekap Fault. These faults probably developed during a number of rift events. Antithetic faults southwest of Pyramiden show evidence for repeated periods of movement. In particular prior to the deposition of Paleocene is indicated by the fact that there is a progressive southeasterly thinning of Cretaceous strata across the faults due to post-Maastrichtian, pre-Palaeogene erosion (Larsen and Whitham 2005). The same faults appear inactive during Paleocene as no thinning across the faults occurs and sediment transport indicators southwest of Pyramiden less than one kilometre from a fault are directly towards it. Renewed fault movements after the deposition of Plaocene are indicated by displacement of the top of the unit.
Larsen and Whitham (2005) described a major Palaeogene depocentre existed to the east of the fjord Kangerlussuaq. This depocentre was controlled by a major NW–SE-oriented fault along the present Christian IV Gletscher. The Christian IV fault lineament was probably initiated in the Early Paleocene and its influence persisted into the earli-

est stages of flood basalt volcanism in the Late Paleocene–Early Eocene. Palaeogene depositional systems were focused at the tectonic lineament, which acted as a conduit for sediment being transported southeastwards towards the Faroe–Shetland Basin.
Two other structural features are prominent in the region: the coastal flexure and NE dipping basement surfaces. The coastal flexure affects strata in a zone 30 km inland and approximately parallel to the coast. In this zone, strata show a progressive increase in dip towards the southeast reaching more than 308 at the coast. The formation of the feature is constrained by a swarm of coast parallel dykes, which have a fan-like pattern, indicating that the formation of the flexure was contemporaneous with dyke intrusion (Nielsen & Brooks 1981). These dykes are normally magnetized, correlating with geomagnetic anomaly C24N indicating that the coastal flexure probably formed at this time (L. M. Larsen et al. 1989). Recent 40Ar/39Ar datings of the intrusions give ages of c. 55 Ma (Tegner et al. 1998; Karson & Brooks 1999). East of Kangerlussuaq, around Sortekap, the contact between crystalline basement and the Cretaceous and Palaeogene strata is a prominent NE-dipping peneplain. The surface is obvious and has been remarked upon by previous workers (Brooks 1979; Wager 1947). Brooks (1979) interpreted the feature as part of a large dome-like structure centered on Kangerlussuaq.

The following paragraphs will describe new insight achieved after the structural study and revise some old concept and interpretation in the light of the new data and ideas.

This study shows a four stages tectonic evolution of the Kangerlussuaq area:

1) Late Cretaceous-Early Paleocene rifting;
2) Middle-Late Paleocene oblique rifting;
3) Early Eocene coastal flexure and oceanic spreading;
4) Late Eocene-Early Oligocene basin inversion.

4.2 Late Cretaceous-Early Paleocene rifting

This event corresponds to the main phase in the formation of the Kangerlussuaq Basin and is characterized by NE-SW trending normal faults.

4.2.1 The Sortekap Fault

It is confirmed the importance of the NE-SW trending and SE-dipping Sortekap Fault as main rift-fault bounding the Kangerlussuaq Basin and probably responsible for accumulation of more than 800m of Cretaceous-Early Paleocene sediments.

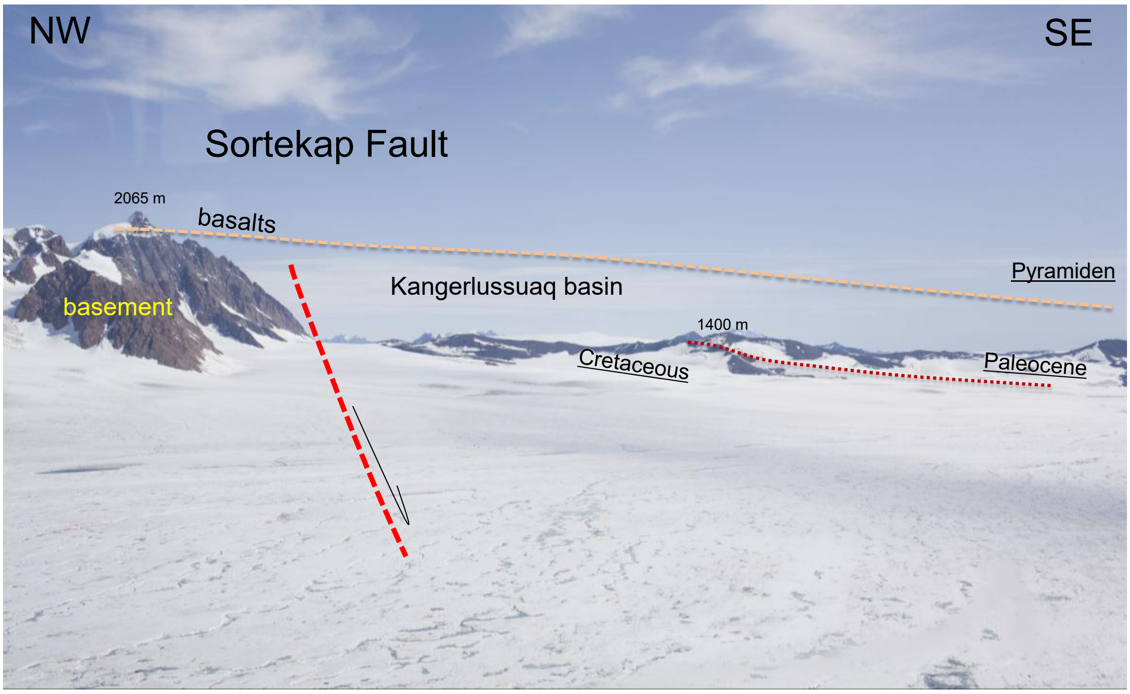

Fig. 4-1. Oblique photo across the Sortekap Fault. Basalts on top of Sortekap correspond most probably to Milne Land Fm as they are recognized inland not so far from this area.

Activity along this fault in Middle-Late Paleocene is not obvious since the basalts located on the footwall (Fig. 4-1) can be easily correlated across the hangingwall without any vertical offset. Moreover, there are two papers dating Palaeogene sediments from sections located both in the footwall and the hangingwall of the Sortekap Fault. The first paper by Jolley and Whitham (2004) dated sediments in Pyramiden and Fairy Tale Valley as post-LPTM (Late Paleocene Thermal Maximum), and the second paper, a new article published by Nøhr-Hansen (2012) concluded that the recorded fragments of *Palaeoperidinium pyrophorum* from the Rybjerg Fjord section suggest that the Klitterhorn Member (upper part of Sediment Bjerge Formation) and the lower part of Schjelderup Member (basal unit of Vandfaldsdalen Formation) are not younger than late Selandian and that the lower part of Willow Pass Member (middle part of Vandfaldsdalen Formation) may be of late Selandian age, and that the upper part of the Willow Pass Member may be of Thanetian age. Moreover, samples from Kulhøje Member (Vandfaldsdalen Formation), located in the hangingwall of Sortekap Fault, also include palynofloras typical of the T40 interval (Jolley and Whitham 2004). This result constrains the age of basalts that cover those sediments to the Eocene and for this reason should belong to the Milne Land Fm, the first of the volcanic sequences of the Plateau Basalts and not to the Vandfaldsdalen Fm that is the basal volcanic sequence of the Lower Basalts. As a consequence of this, the vertical movement along the Sortekap Fault is not obvious during Middle-Late Paleocene and the interpretation is that this fault is sealed by the lavas of the Milne Land Fm (Fig. 4-1).

4.2.2 The Nansen Fjord Fault

This fault was described first by Larsen and Whitham (2005) and called Christian IV Gletscher fault. The authors suggested a linear embayment preserving Cretaceous strata and controlling Palaeogene depositional systems controlled by a major NW-trending, SW-dipping normal fault in the lower Christian IV Gletscher, the Christian IV Fault. The fault had two main periods of movement, prior to the formation of a major sequence boundary in the Late Paleocene–Early Eocene and afterwards during the extrusion of the initial volcanic succession (Fig. 4-2).

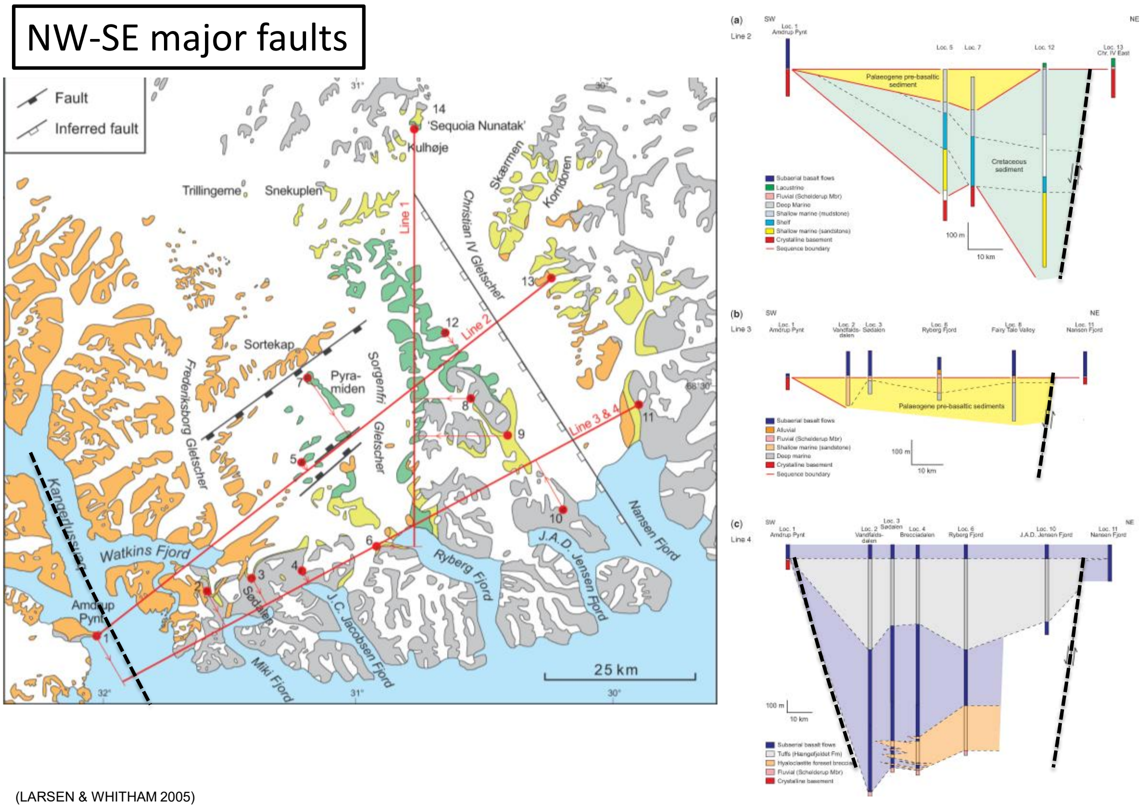

(LARSEN & WHITHAM 2005)

Fig. 4-2. Stratigraphic evidence for a major NW-SE trending fault in the Christian IV Gletscher (modified after Larsen and Whitham 2005)

This study refers to this fault as the Nansen Fjord Fault. The only difference in the interpretation is the age of what they called Vandfaldsdalen Fm. The footwall is represented by basement rocks unconformably covered by Paleocene sediments that, in turn, are topped by the Nansen Fjord Fm (Larsen et al., 1999) belonging to the Lower Basalts and pre-breakup. The footwall is made by Cretaceous-Paleocene sediments covered by the Lower Basalts (Haengefjeld Fm, Mikis Fm and the Vandfaldsdalen Fm) that in this side of the fault seem to be very different but coeval with the Nansen Fjord Fm. For this reason the Nansen Fjord Fault was a very important tectonic feature during the entire Paleocene.

4.2.3 The Kangerlussuaq Fjord Fault

For the same reasons described previously (Fig. 4-2) we infer the presence of a major NW-SE trending fault along the Kangerlussuaq Fjord with a down-faulted NE side. This fault is also inferred by other geologic constraints as the Skaergard intrusion cropping out at the east side of the fjord. The Skaergaard layered gabbro was intruded at 55,4 Ma (Hirschman et al. 1997) in upper crustal levels at an estimated depth of 2-3 km (Larsen and Tegner 2006) just after the emplacement of Milne Land Fm and followed by a strong subsidence to accommodate more than 4km of Plateau Basalts in a relatively short time. This entire story is not represented in the west side of the fjord (Amdrup Pynt) where the Milne Land Fm is sitting on top of sediments and basement (Fig. 4-2).

4.3 Middle-Late Paleocene oblique rifting

This stage corresponds to the volcanic rift with the emplacement of the Lower Basalts along a rift that is more restricted than the previous one and mainly localized in the SE sector of the NE-SW trending Sødalen Fault.

4.3.1 The Sødalen Fault

The Sødalen Fault is a NE-SW trending rift fault re-activated as left-lateral dip oblique in Mid-Late Paleocene. The footwall is characterized by a basement high (Gabbrofjeld High) covered by no more than 50m of sandstones belonging to the Klitterhorn member of the Ryberg Fm. Unconformably on top the shoreface sandstones the Schjelderup member of the Vandfaldsdalen Fm starts followed by Mid-Late Paleocene lavas (Figs 4-3 and 4-4). Along the hangingwall, fluvial sandstones of the Schjelderup member lie on top of sandstone and mudstones of the Sediment Bjerge Fm. In Vandfaldsdalen the minimum offset across the fault is 250m that correspond to thickness of Paleocene sediments but is seems to be more vertical separation moving NE-ward where it accommodates the entire thickness of the Lower Basalts (1000-1500m).

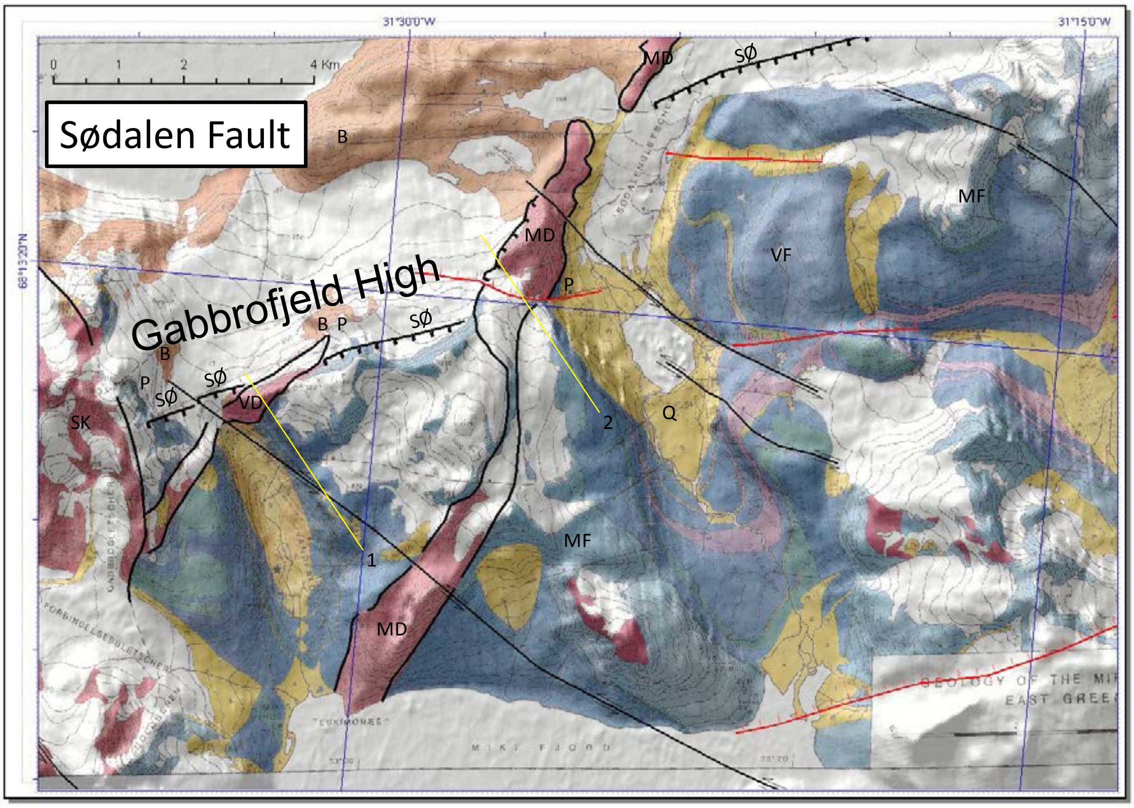

Fig. 4-3. Geological Map of the Miki Fjord area (modified after Nielsen et al. 1981)

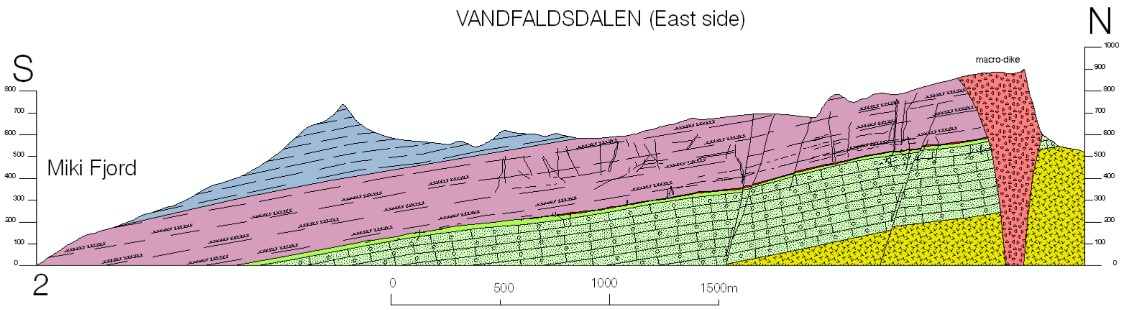

Fig. 4-4. Geologic cross-section of Vandfaldsdalen across the Sødalen Fault.

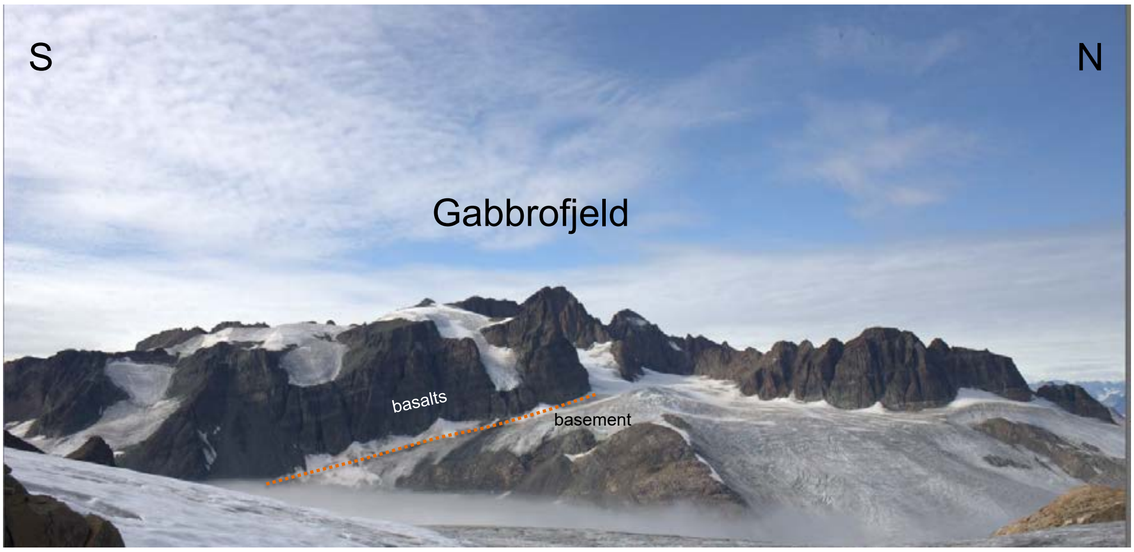

Fig. 4-5. Oblique photo of the Gabbrofjeld High. It represents the footwall of the Sødalen fault where the Klitterhorn member of the Sediment Bjerge Fm lies unconformably on basement rocks.

4.3.2 The Watkins Fjord Lineament

The Geological Map of Greenland at 1:500.000 scale sheet 13 Kangerdludssuaq, the authors describe a Precambrian basement consisting mainly of Archaean granodioritic to tonalitic orthogneisses interlayered with supracrustal rocks of sedimentary and volcanic derivation, and cut by later mafic dikes (Wager 1934; Wager & Deer 1939; Bridgwater et al. 1978; Meyers 1985). In particular it is emphasized a mineralized shear zones with mafic dikes of presumed Proterozoic age that define a pronounced structural trend separating tonalitic, granodioritic to granitic gneiss in granulite facies from similar gneiss that shows an Archaean retrogression from granulite to amphibolite facies (Fig. 4-6). The ENE-WSW trending contact between the two different basement gneisses is called here the Watkins Fjord Lineament. This old discontinuity is parallel and very close to the Sødalen Fault suggests that the pre-Tertiary structures may in part control the architecture of the rift basin and the clear deflection of the coastline at 68°N together with other aspects of the Tertiary structural and intrusive development, as also evidenced by Dennis et al. (1985).

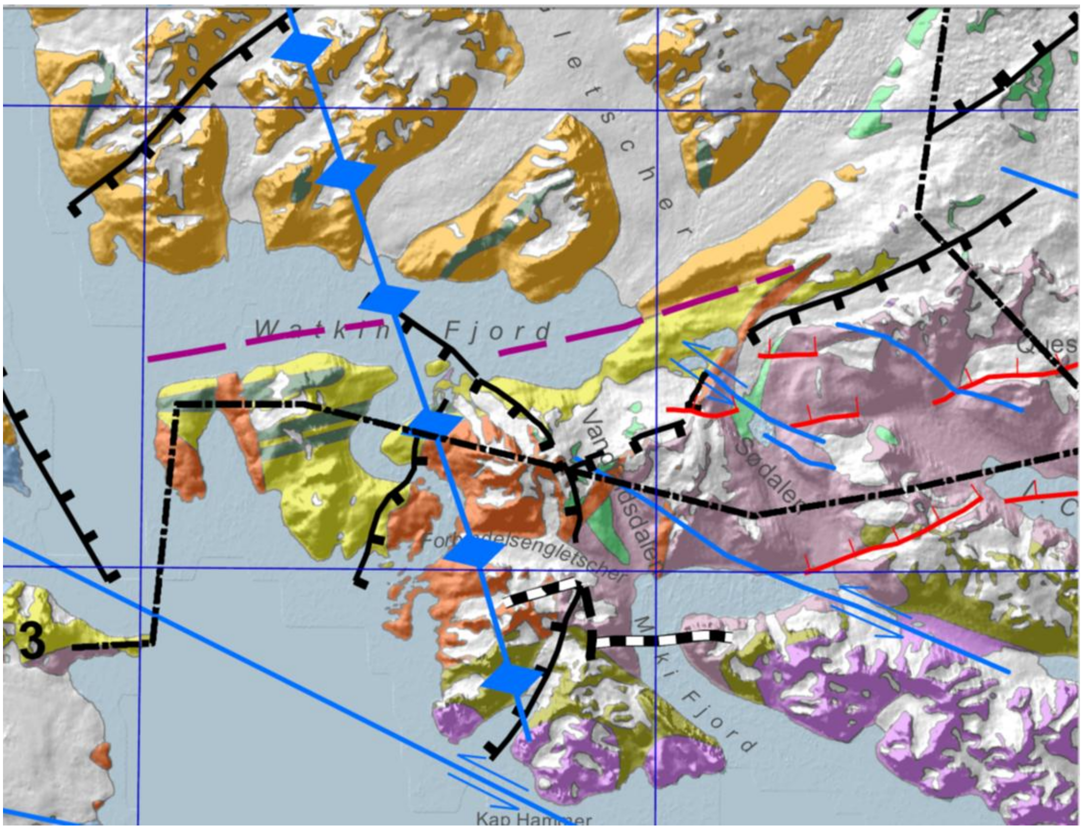

Fig. 4-6. The Watkins Fjord Lineament (purple dashed line) is a ENE-WSW trending contact between two different type of Archaean basement (modified after Geological Map of Greenland sheet 12).

4.3.3 The Gabbrofjeld High

The Gabbrofjeld High is a very pronounced NE-SW trending structure extending toward the Fairytale Valley where it is masked and seems to disappear probably due to the NE-tilting of the entire Kangerlussuaq basin caused by the downthrown along the Nansen Fjord Fault. The structural high developed probably in Early Paleocene and separates the Kangerlussuaq Basin into two areas: Sediment Bjerge-Kulhøje sector to the NW and the Sødalen-Willow Pass sector to the SE. The two areas show a strong difference in the Mid-Late Paleocene tectono-magmatic and sedimentary evolution.

The Gabbrofjeld High is also marked by:

1) distribution of Early Paleocene shallow marine sandstones of the Klitterhorn member of Sediment Bjerge Fm respect to the deep marine Fairy Tale member. The shallow marine seems to be more concentrates above the structural high in a NE-SW trend from Kangerlussuaq Fjord toward Christian IV Gletscher (cf. Annexes 3 and 4)
2) the Lower Basalts emplaced in Middle-Late Paleocene (Vandfaldsdalen Fm, Mikis Fm and Haengefjeld Fm) are distributed along the SE sector of the Sødalen Fault while the coeval Kulhøje lacustrine member of the Vandfaldsdalen Fm is mainly recognized in the NW sector. The thickness of the lacustrine sequence is little more than 100m at Kulhøje while the Lower Basalts can reach more

than 1500m. The difference in thickness is interpreted here as an evidence of tectonic activity along the Sødalen Fault;

3) between 56 Ma and 55.5 Ma a series of tholeiitic sills and layered gabbros (Sill Complex 56 Ma; Mikis Fjord Macrodyke 55.8 K. Thrane pers. comm.; Skaergaard Gabbro 55.4 Ma) are emplaced very close to the Sødalen Fault and mainly on the SE side of the fault.

The three geological evidences described above highlight the importance of the Sødalen Fault as main rift fault during Middle-Late Paleocene (Figs 4-7 and 4-8).

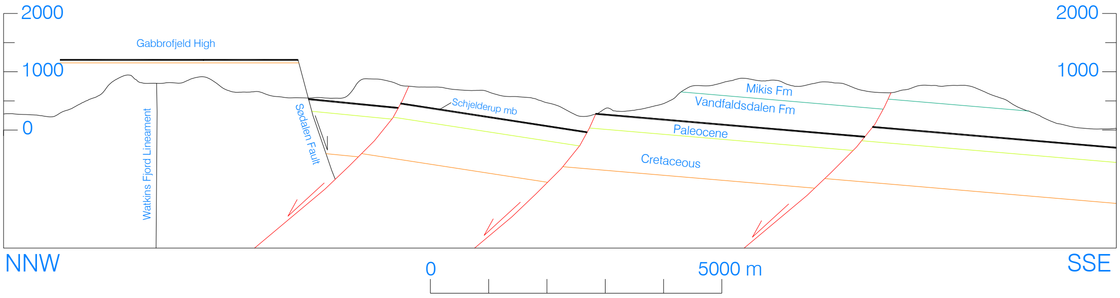

Fig. 4-7. NNW-SSE geologic cross-section showing the vertical throw along the Sødalen Fault. Thick black line represents the Schjelderup fluvial sandstone; red faults are flexure-related faults. Dip angles were measured using the 3D-mapping tool.

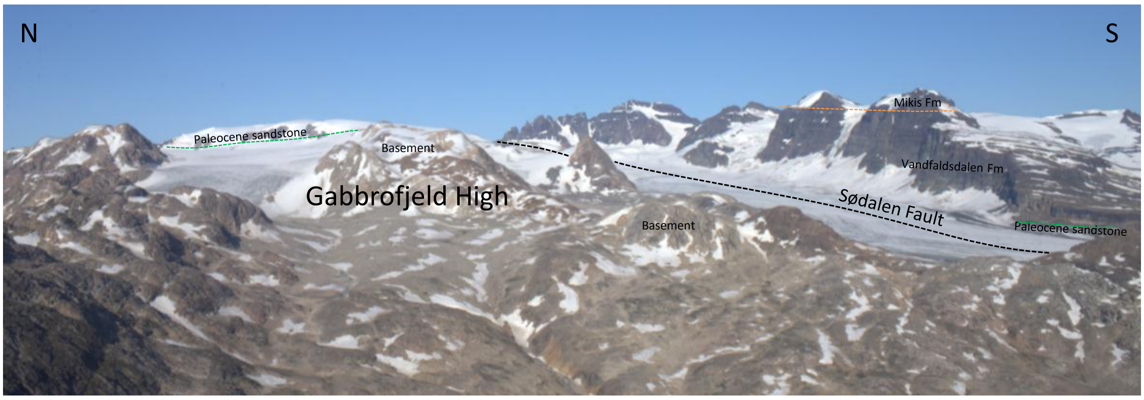

Fig. 4-8. Oblique photo across the Gabbrofjeld High and the Sødalen Fault along the Sødalengletscher. The estimated vertical offset is more than 500m in this part of the fault. Paleocene sandstones on the footwall unconformably lie on top of basement rocks while the same sediments on the hangingwall lie on top of Paleocene mudstones.

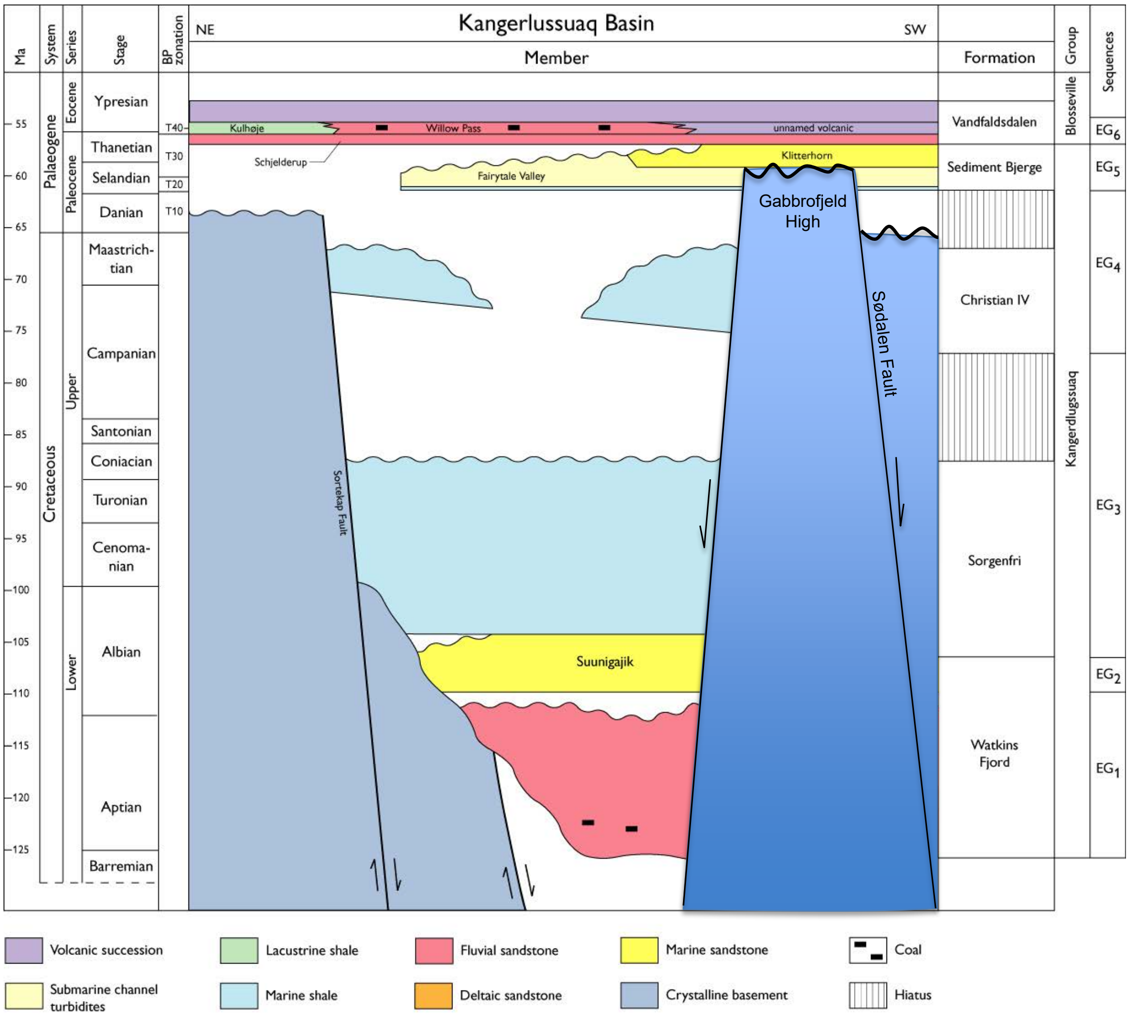

Fig. 4-9. Stratigraphic chart of the Kangerlussuaq Basin showing the position of the Sødalen Fault and the Gabbrofjeld High (modified after Larsen et al. 1999).

4.3.4 Some remarks on the Vandfaldsdalen Formation

The Lower Basalts of the Kangerlussuaq region were established as a separate part of the volcanic province by L.R. Wager and coworkers (e.g. Wager 1947). Complex stratigraphy and a wide geochemical range (Brooks & Nielsen 1982a) have made it difficult to correlate the Lower Basalts with the prevalent and more uniform tholeiitic plateau basalts to the north and east. Over the years, several correlation schemes have been proposed (e.g. Nielsen et al. 1981; Larsen et al. 1989), but without the necessary stratigraphic control. The general stratigraphy and structure of the Lower Basalts have been described by Nielsen et al. (1981), Hansen & Nielsen (1999) and Ukstins (2000), but the correlation with the regional plateau basalt formations originally identified in the Scoresby Sund region (Larsen et al. 1989) has remained unresolved. The identification of a suite of orthopyroxene-bearing marker flows in the Milne Land Formation on the eastern shores of Nansen Fjord (Fig. 4-10), and correlation with similar flows on the peninsula between J.A.D. Jensen Fjord and Nansen Fjord, suggests the possibility of a lithological correlation to the type area of the Lower Basalts in the Miki Fjord area. The orthopyroxene- bearing lavas have now also been sampled in the lower part of the plateau basalts (the Irminger Formation of Nielsen et al. 1981) overlying the Lower Basalts on the south shore of inner Miki Fjord and these studies show that the Irminger Formation is identical with the Milne Land Formation (see also Larsen, L.M. et al. 1999). The eastward correlation of the formations of the Lower Basalts in the Miki Fjord area (Fig. 4-10) suggests that the Lower Vandfaldsdalen Formation and Mikis Formation are only locally developed shield volcanoes (Peate et al. 2003). No equivalents to the wide variety of the Lower Vandfaldsdalen Formation volcanics have been observed towards the east in the Ryberg Fjord and J.A.D. Jensen Fjord area, whereas the Upper Vandfaldsdalen Formation can be followed eastwards to the shores of Nansen Fjord. The Mikis Formation seems to represent a volcanic structure, probably a shield volcano (Peate 2000), between the Upper Vandfaldsdalen Formation and the overlying tuffs and volcanoclastic sediments of the Hængefjeldet Formation. The variably sorted tephra deposits between the Milne Land Formation and the informal 'Nansen Fjord Formation' on the east shores of Nansen Fjord (Larsen, L.M. et al. 1999), like the equivalent deposits in J.A.D. Jensen Fjord, show no signs of reworking and provide a correlation across the fjord, and there is no compelling evidence at this location for a major hiatus between the eruption of the Lower Basalts and the overlying plateau basalts. Correlation of the tephra deposits indicates that lavas assigned to the 'Nansen Fjord Formation' on the east side of Nansen Fjord (Larsen, L.M. et al. 1999) are equivalent to lavas of the Vandfaldsdalen Formation on the west side of Nansen Fjord.

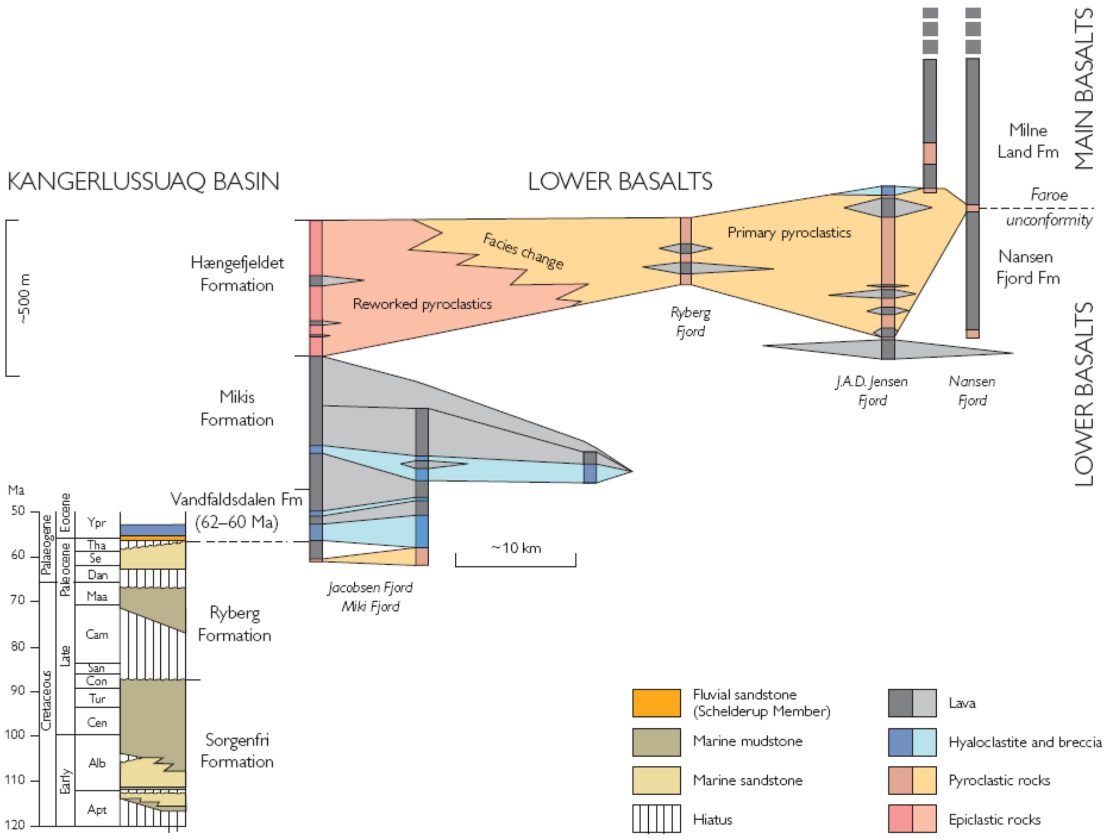

Fig. 4-10. The pre-basaltic sedimentary succession (Larsen et al. 2006), and the Lower Basalts (Peate et al. 2003) (after Brooks 2011).

The Vandfaldsdalen Formation was recognized by Wager (1947), described by Soper et al. (1976) and formalized by Nielsen et al. (1981). The stratigraphic sequence belonging to the Vandfaldsdalen Formation starts with few meters of fluvial sandstones called the Schjelderup Member, followed by almost 550m of lava flows, volcaniclastic layers, pillow breccias and hyaloclastites. The formation is conformably covered by the Mikis Fm that in turn passes laterally and upward to the Haengefjeld Fm. The total thickness of the three formations, at their maximum observed development, lies between 1.8 and 2.5 km (Nielsen et al. 1981). Larsen et al. (2005) described a sedimentary sequence above the Schjelderup mb and formalized two new members of the Vandfaldsdalen Formation: the Kulhøje and the Willow Pass members and, recently, Nøhr-Hansen (2012) dated new specimens from Kangerlussuaq presenting a new generalised history of the stratigraphic nomenclature for the pre-basaltic sedimentary succession in Kangerlussuaq modified after Larsen et al. (2005) (Fig 4-11). The author concluded: the palynological data indicate as only the lower part of the Vandfaldsdalen Formation (the Schjelderup Member and maybe the Willow Pass Member) may be time equivalent with the Urbjerget Formation, whereas the upper part of the Vandfaldsdalen Formation (the Kulhøje Member volcanics) may be younger than the Nansen Fjord Formation and older or time equivalent with the lower part of the Milne Land Formation.

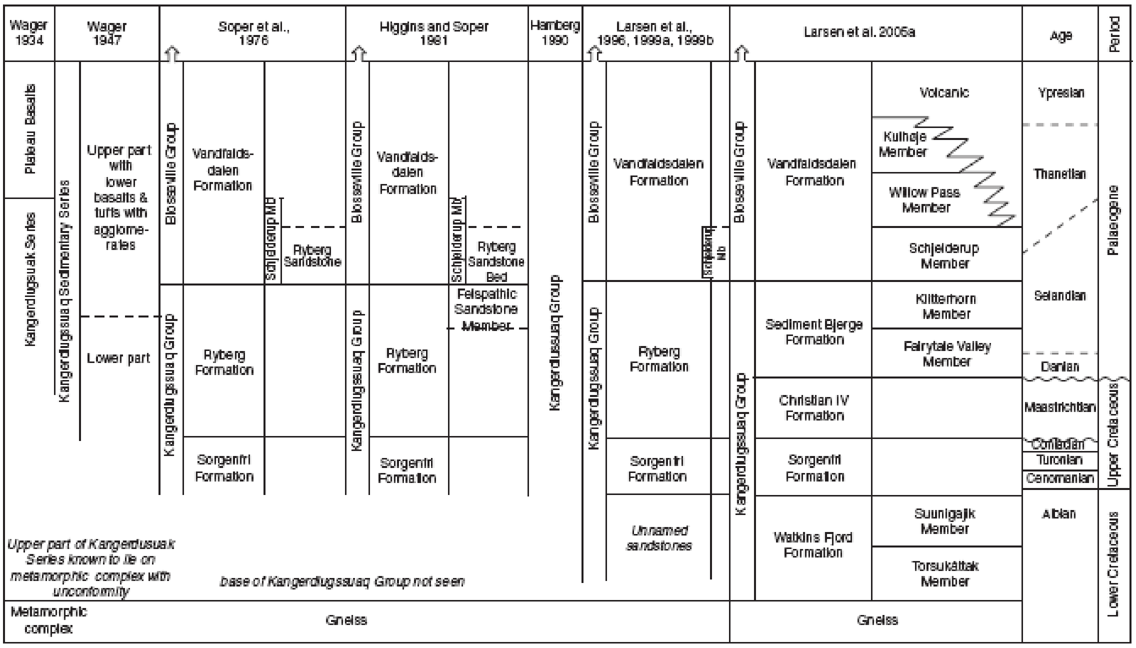

Fig. 4-11. Nomenclature of pre-basaltic sequence in Kangerlussuaq (from Nøhr-Hansen 2012).

It should be mentioned here that Jolley and Whitham (2004) due to a partial and wrong evaluation of the geological data available in the Kangerlussuaq area, concluded that "*the onset of basaltic volcanism in the east Greenland area is attributable to late sequence T40, significantly later than the onset of volcanism in the Faroe Islands or in the Faroe–Shetland Basin*". The latter sentence is inconsistent with absolute age dating and it comes from a misinterpretation of stratigraphic relationships between Selandian-Thanetian sediments and coeval volcanics.

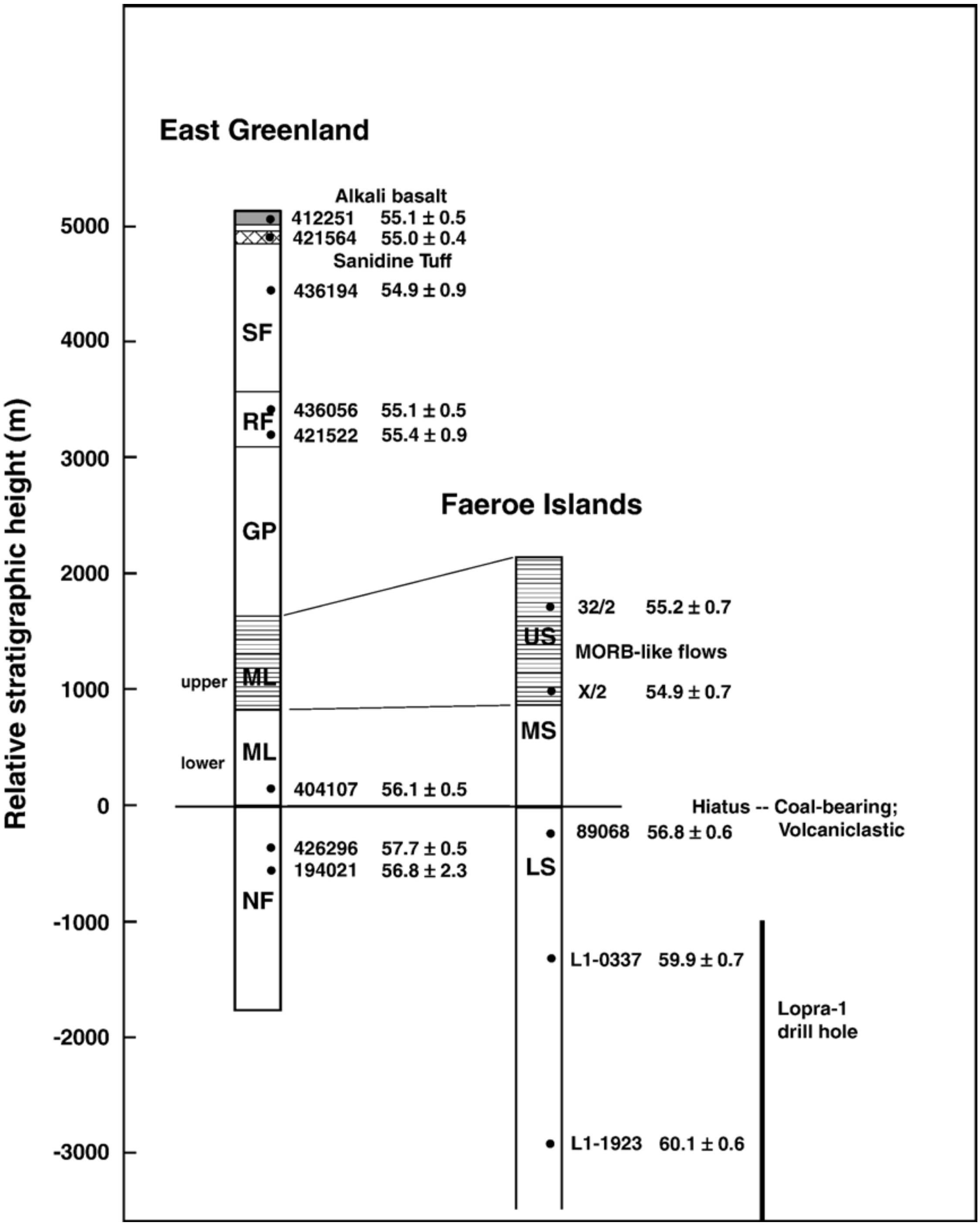

Fig. 4-12. Stratigraphic divisions of the lava formations and ages from Storey et al. (2007).

Combining the results from (1) volcanic stratigraphy and (2) absolute age dating (Fig. 4-12), (3) sediment stratigraphy and (4) biostratigraphy a modified scheme for the Middle-Late Paleocene is proposed here to avoid misfitting in the volcano-sedimentary evolution. In order to better understand the tectonic evolution of this area it is useful to consider two widespread and well recognized events in Kangerlussuaq: the fluvial sandstones of Schjelderup mb and the Milne Land Fm (Fig. 4-13).

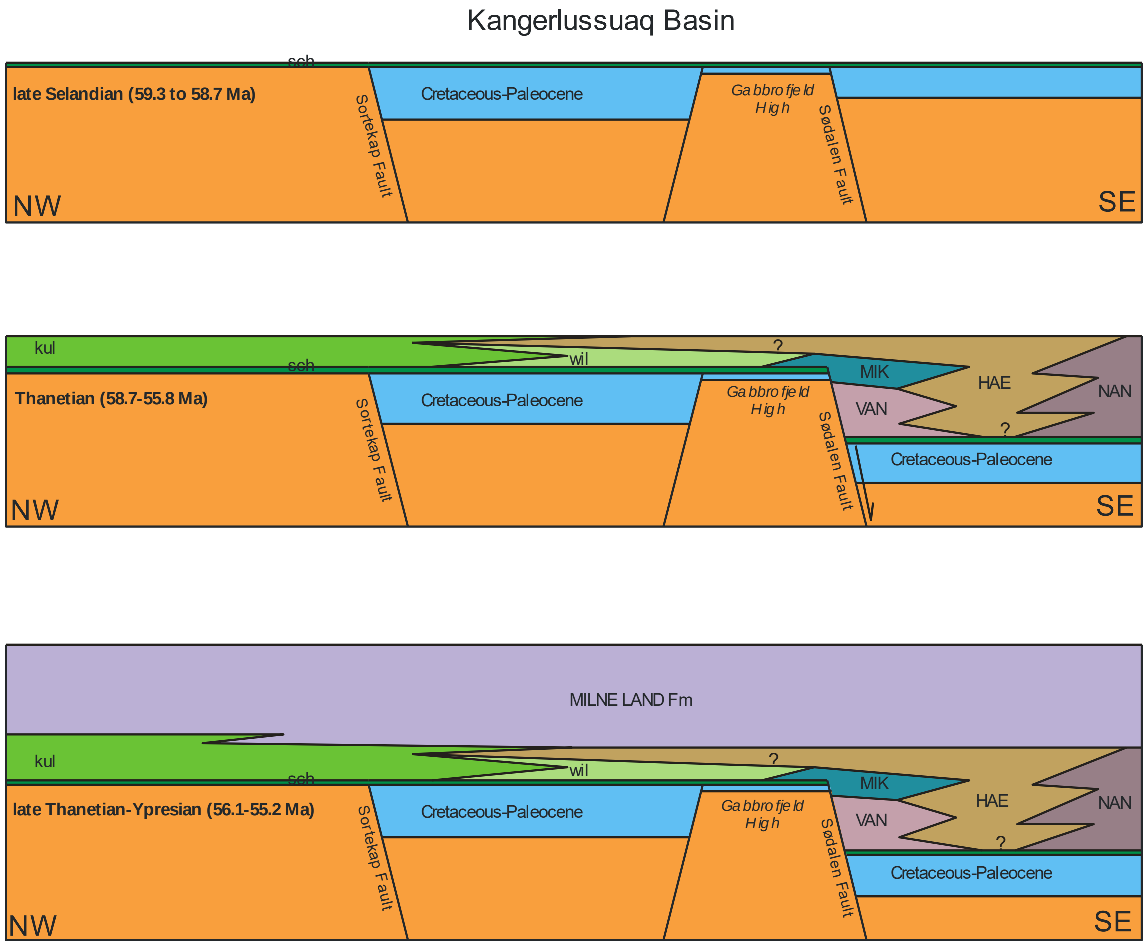

VAN: Vandfaldsdalen Fm (volcanics), sch: Schjelderup mb, wil: Willow Pass mb, kul: Kulhøje mb; MIK:Mikis Fm (volcanics); HAE: Haengefjeld Fm (volcaniclastics); NAN: Nansen Fjord Fm (volcanics). Ages from Nøhr-Hansen (2012) and Storey et al. (2007).

Fig. 4-13. Stratigraphic relationships of Middle-Late Paleocene volcano-sedimentary sequences in the Kangerlussuaq Basin.

After the sedimentation of the fluvial sandstones (sch) (Selandian) unconformably upon basement rocks, Cretaceous and Early Paleocene sediments, the Gabbrofjeld High and the Sødalen Fault separate the initial volcanic rift (to the SE from a sector to the NW characterized by lacustrine environment (kul) (Thanetian/early Ypresian). This latter is covered by latest Thanetian/early Ypresian volcanics of the Milne Land Fm (56.1±0.5 Ma).

4.3.5 The macrodykes complex and the oblique rifting evidence

Large dykes up to 1000 m thick and 10 to 15 km long occur in the Miki Fjord area. They are termed macrodykes and have been described by Bird et al. (1985), White et al. (1989), Blichert-Toft et al. (1992), Geist & White (1994) and Momme & Wilson (2002). They are thought to be co-magmatic with the Skaergaard intrusion and show layering, abundant xenoliths and autoliths, rheomorphic effects (e.g. Naslund 1986) and development of granophyres and pegmatites. The Kræmer Ø macrodyke was interpreted by Momme & Wilson (2002) as a feeder to the overlying basalts. The Miki Fjord and

Vandfaldsdalen macrodykes has been the subject of studies of reaction and hybridisation with the country rocks (Rosing et al. 1989; Blichert-Toft et al. 1992; Waight & Lesher 2010), which have implications on the mechanism of contamination seen in some of the lavas, particularly the Lower Basalts.
During fieldwork in 2010 three samples from the layered Vandfaldsdalen and Miki Fjord Macrodykes and from a later dyke were collected for age dating using Baddeleyite analysis.

Sample #523101 (Fig 4-14) belongs to the Miki Fjord Macrodyke (Fig. 4-15) while sample #523102 belongs to the Vandfaldsdalen Macrodyke (Fig. 4-16). The two layered dykes up to 500-m wide, are NNE-SSW oriented and related to the breakup of the continental crust with composition and age similar to the Skaergaard Layered Gabbro.

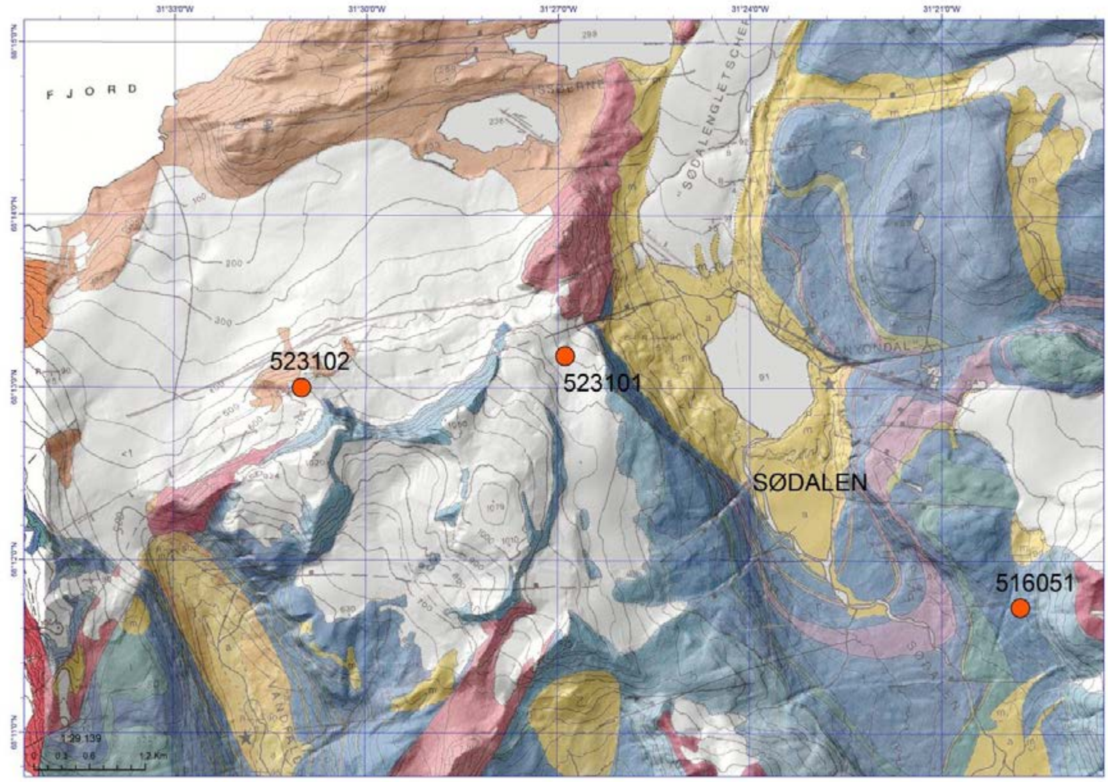

Fig. 4-14. Geological Map of the Miki Fjord area (Nielsen et al. 1981).

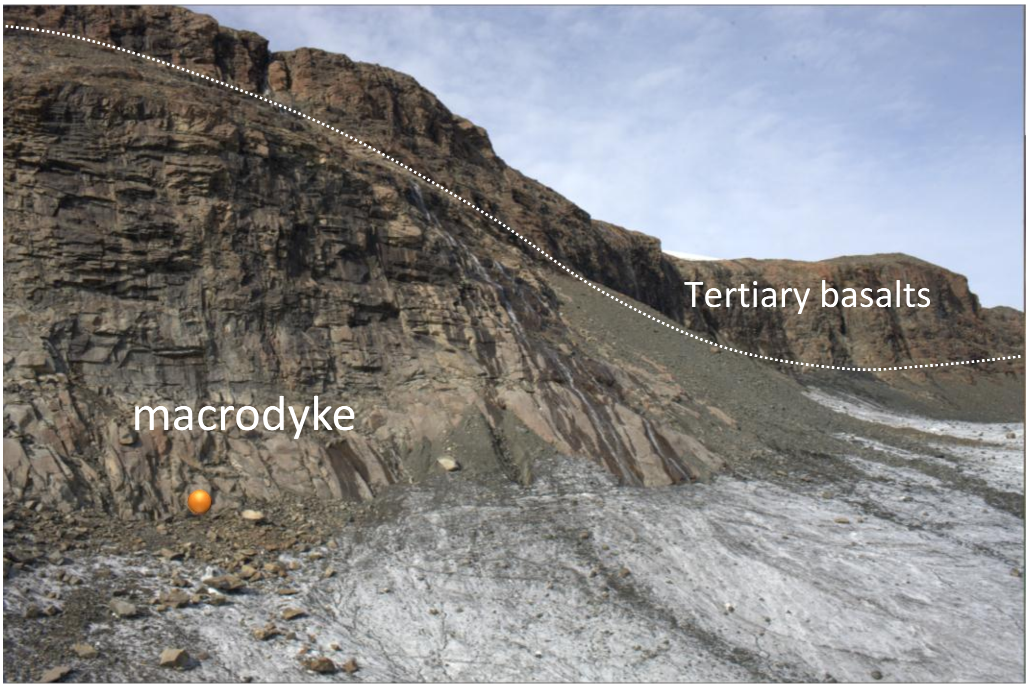

Fig. 4-15. Location of sample #523101.

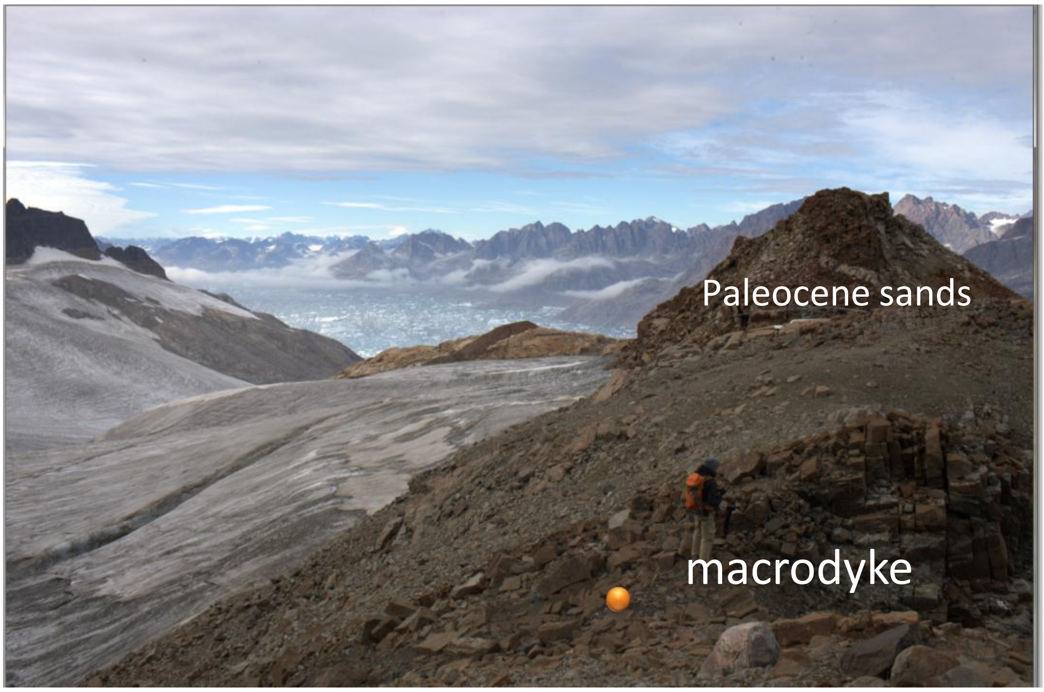

Fig. 4-16. Location of sample # 523102

Sample #516051 (Fig. 4-14) belongs to an E-W oriented dyke system cross-cutting old structures and dykes. This late dyke swarm could be considered post-breakup since it cuts through the flexure-related structures that are coeval with the breakup.

Fig. 4-16. Location of sample #516051

Dating these intrusive events was important to define the relationship between the Macrodyke complex and the Skaergaard intrusion, both related to the breakup history at 55Ma and the initiation of the post-breakup tectonics that is supposed to be younger (Late Eocene) and responsible for uplift and inversion of the Kangerlussuaq basin. Unfortunately only sample 523101 from the Miki Fjord Macrodyke was suitable for age dating (Fig. 4-17)

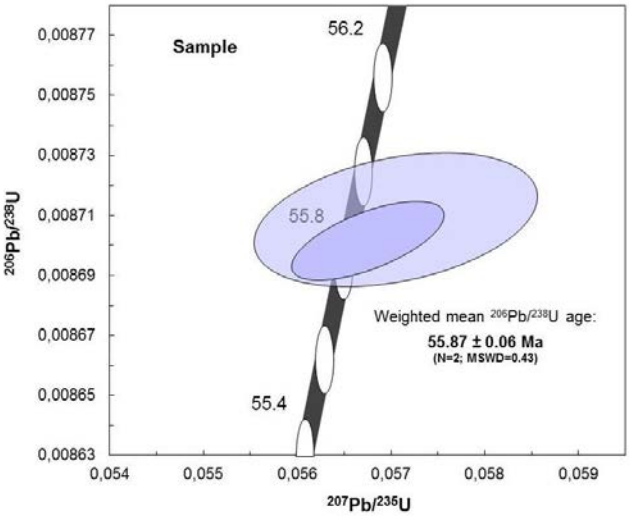

Fig. 4-17. Age plot (Baddeleyite analysis) for the Miki Fjord macrodyke sample (Thrane K. pers. Comm.)

This is a very important result that establishes chronological relationship between the gabbro intrusions close to or related to the continental breakup: Macrodykes at 55.8 Ma followed by the Skaergaard Gabbro at 55.4 Ma that in turn, is thought to be expression of the breakup.

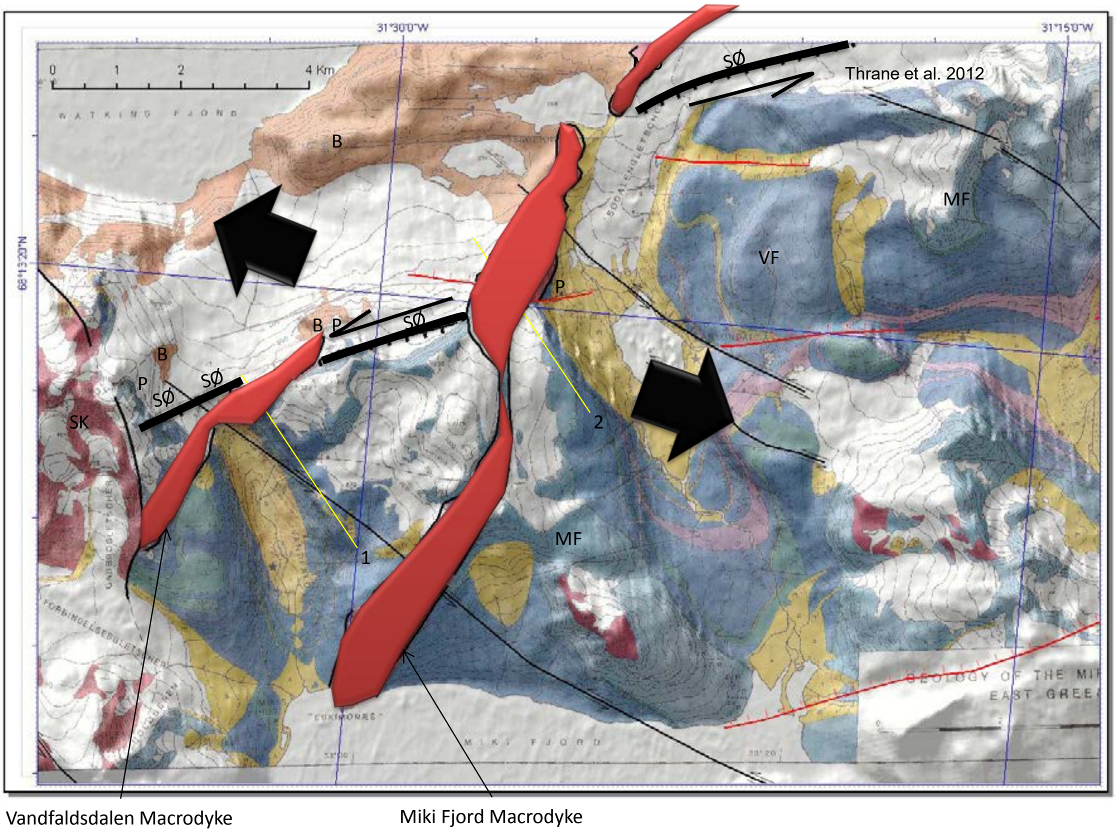

Fig. 4-18. Structural relationships between macrodykes and Sødalen Fault.

The macrodykes cut through the Sødalen Fault, previously documented, and show en-echelon geometry. This structural relationship and the direction of extension (Fig. 4-18) combined with strike-slip evidences documented along the fault, (cf. Chap. 3) suggest a mechanism of oblique rifting in Selandian-Thanetian, until the intrusion of the macrodykes at 55.8 Ma that correspond to the Paleocene/Eocene boundary. This mechanism is coherent with the paleostress reconstructed from analysis of fault-slip data (cf. Chap. 3).

Oblique rifting arises when the bulk extension direction is not perpendicular to the boundaries of a deforming zone. In extensional environments, the geometry and kinematics of fault patterns often suggest that extension is not perpendicular to the boundaries of the deforming domain (Tron and Brun 1991; McClay and White 1995; Corti 2008) (Figs 4-19 and 4-20).

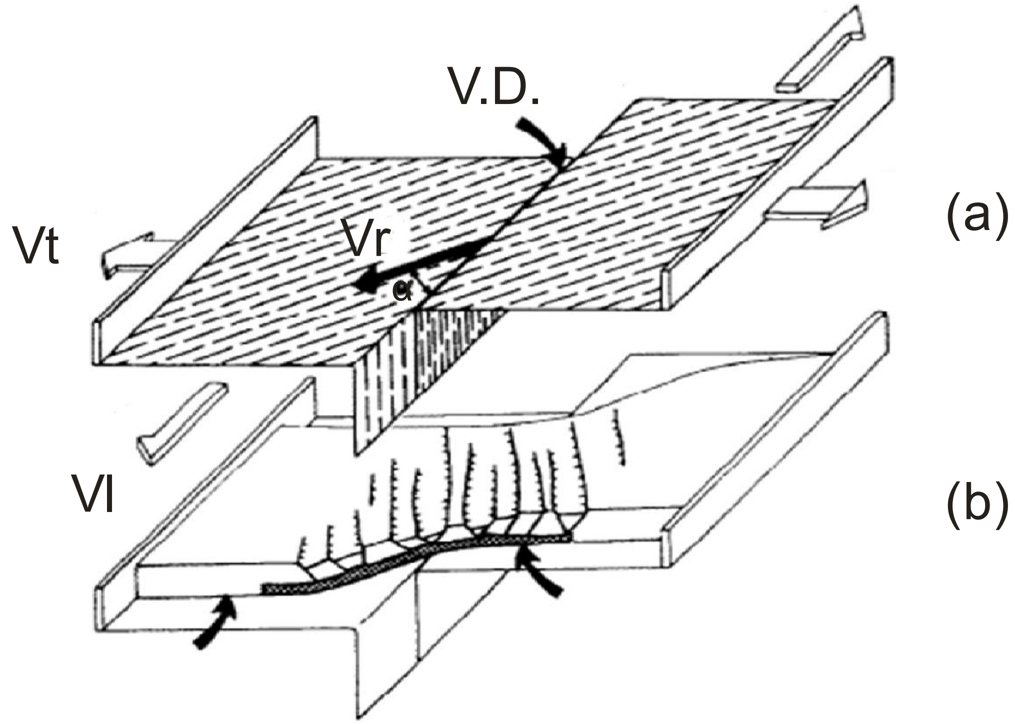

Fig. 4-19. Oblique view of the deformation box used by Tron and Brun (1995). (a) The shaded areas are the plastic sheets on the rigid basal plates; the longitudinal velocity is (Vl), the transverse velocity (Vt), the angle between the velocity discontinuity (V.D.) (α), and the stretching vector Vr. (b) Sketch showing a deforming model in situ (modified after Tron and Brun 1995)

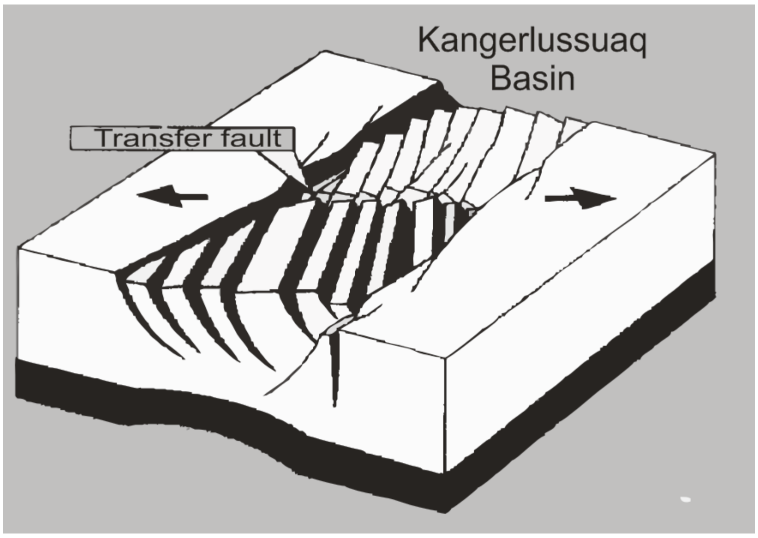

Fig. 4-20. Tectonic configuration of the Kangerlussuaq basin. The former border fault (Sortekap Fault) is abandoned and rift is mainly concentrated along re-activated faults in a narrow area. Examples of transfer fault are the Nansen Fjord and Kangerlussuaq Fjord Faults.

4.4 Early Eocene coastal flexure and oceanic spreading

In a classic paper Wager and Deer (1938) described the coastal dyke swarm as following the coast for over 800 km from near Scoresby Sund to Tasiilaq. Larsen, H.C. (1978) discussed the offshore extensions of this swarm. Wager & Deer (1938) noted a constant relationship between the dip of the lavas, the density of the swarm and the dip of the dykes.

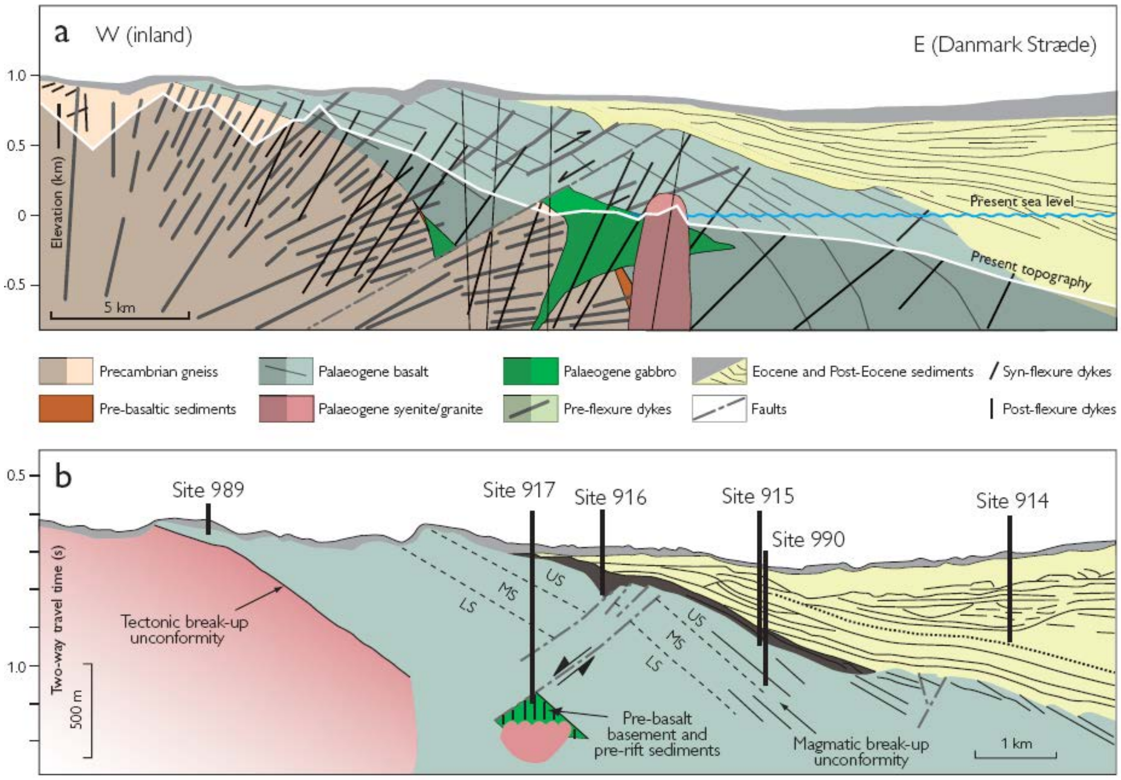

Fig. 4-21. The coastal flexure of the East Greenland continental margin. ***a****: Diagrammatic cross-section of the East Greenland margin, showing flexured basalts and gabbros, numerous dyke generations and late felsic intrusions.* ***b****: Interpreted seismic section across the margin showing some of the sites drilled on Legs 152 and 163 of the Ocean Drilling Program.* ***LS****,* ***MS*** *and* ***US*** *refer to Lower, Middle and Upper Series basalts. After Brooks (2011), redrawn from Larsen, H.C. & Duncan (1996).*

Thus, the densest part of the dyke swarm occurs where the lavas have the steepest dip, i.e. close to the coast. The dykes are nearly perpendicular to the lavas over the entire width of the swarm, suggesting that they have been tilted along with their hosts. Wager & Deer (1938) also noted that the coastal dyke swarm cuts the gabbros but not the syenites at Kangerlussuaq. In a detailed study of the dyke swarms of the Skaergaard intrusion area, Nielsen (1978) recognised at least four generations, the first two being tholeiitic, the third alkaline and the final one containing both transitional and alkaline members. Figure 4-21 shows an example of the complexity. Nielsen (1978) was able to tie their intrusion ages to the plutonic events and set up an igneous stratigraphy spanning from *c.* 58 to *c.* 36 Ma. On the basis of chemical similarities Gill *et al.* (1988) claimed that Nielsen’s earliest dykes were contemporaneous with the Lower

Basalts. A more detailed study of the elemental and isotopic compositions of the dykes was made by Hanghøj *et al.* (2003). Dykes therefore play a key role in documenting the tectonic and magmatic evolution.
Along the coast from Kangerlussuaq Fjord up to Nansen Fjord, ENE-WSW trending coast-parallel dyke swarm intensively cuts through the Milne Land Fm (equivalent to Irminger Fm) that, in turn dips 30-35º SSE. Moving inland from the coast the intensity of dykes is reduced and the extension is accounted by ENE-WSW trending flexure-related land-ward dipping normal faults. This change of mechanism from magmatic extension to normal faulting is also associated to marked reduction in dips of the lavas around 7-12º SSE and less than 5º inland (Pedersen et al. 1997).

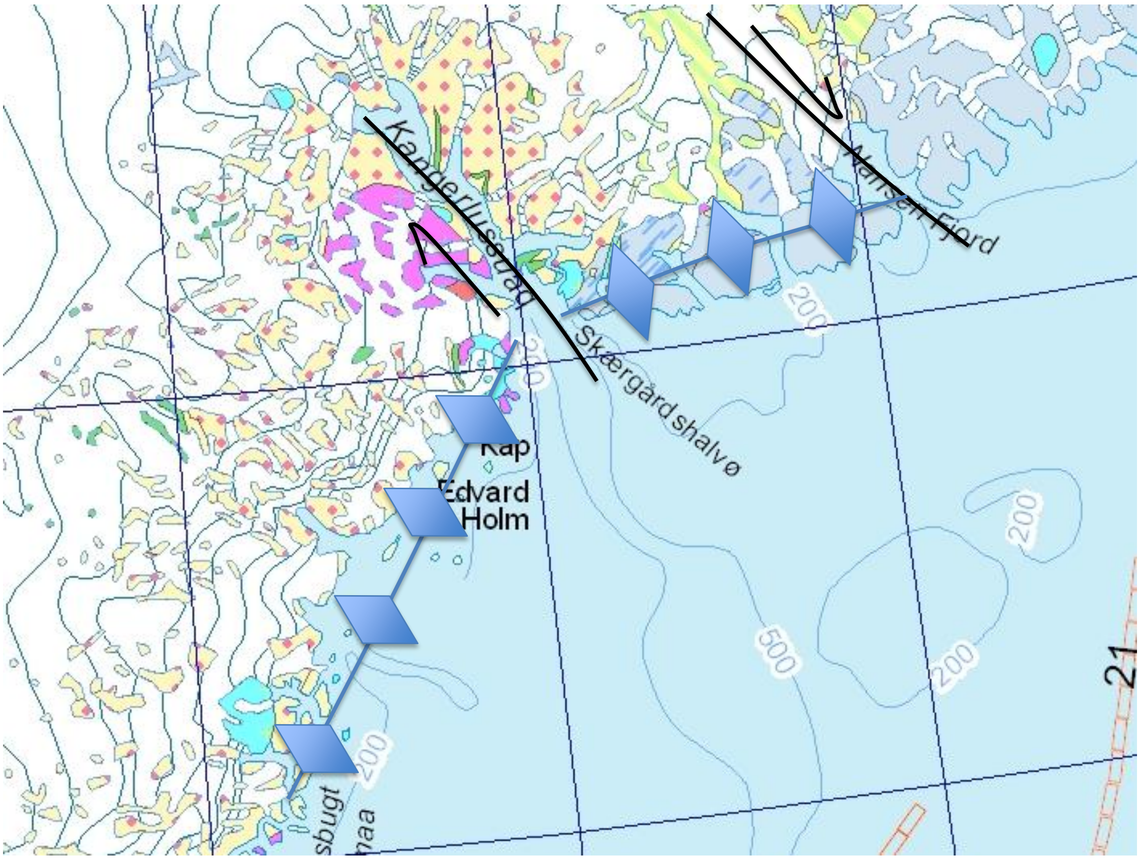

Fig. 4-22. Map showing the hinge trend of the coastal flexure and the relationship with Kangerlussuaq and Nansen Fjord Faults.

The hinge of the coastal flexure represents a structural feature that can be used for tectonic analysis. In fact, the flexure described south of Kangerlussuaq Fjord is more or less coast-parallel with a NNE-SSW trend. The same hinge, between Kangerlussuaq Fjord and Nansen Fiord is ENE-WSW trending and it disappears moving northward toward the east side of Nansen Fjord (Fig. 4-22). All these geological evidences: (1) the abrupt change of the flexure trend from NNE-SSW to ENE-WSW across the Kangerlussuaq Fjord and (2) the absence of flexure on the east side of Nansen Fjord, are used here to confirm the presence of the two major faults: the Kangerlussuaq and the Nansen Fjord faults. Moreover, on the east side of Nansen Fjord the Plateau Basalts show a progressive dip from 5-7º to 10-12º from inland toward the coast (Pedersen et al. 1997) suggesting that the hinge of the flexure should be offshore due to a right-lateral movement along the Nansen Fjord Fault. The same kinematics is assumed for the Kangerlussuaq Fjord Fault.

4.4.1 Analogues for the coastal flexure

Models to explain the coastal flexure (Larsen and Saunders 1998) imply active loading due to the Seaward Dipping Reflectors onto the continental/stretched crust that for this reason subsides to accommodate the emplacement of basalt flows (Fig. 4-23).

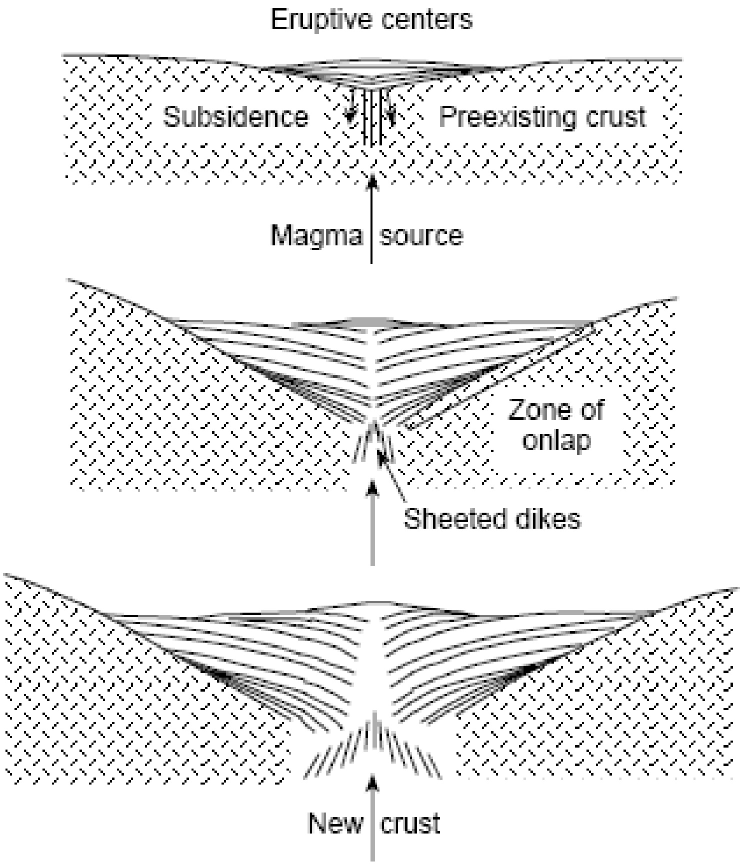

Fig. 4-23. The principle of seaward-dipping reflector sequence (SDRS) formation (see also Fig. 11). The interpretation builds on the model for crustal accretion in Iceland (Pálmason, 1986). A. Initiation of SDRS formation during breakup and formation of the featheredge of the SDRS onlapping onto continental crust (Larsen and Saunders 1998).

A possible analogue for the coastal flexure can be the Moresby Rift and Moresby Seamount in the Woodlark Basin (Papua New Guinea) where subsidence to accommodate the infilling of the rift basin is accounted by a low-angle normal faults (Fig. 4-24). The parallelism with Kangerlussuaq is straightforward if we consider the Plateau Basalts instead of sediments that in turn can enhance the subsidence needed to accommodate at list 6 km of Plateau Basalts during breakup. Moreover this analogue can also explain post-breakup uplift in the Faroes sector as depicted in Figure 4-24.

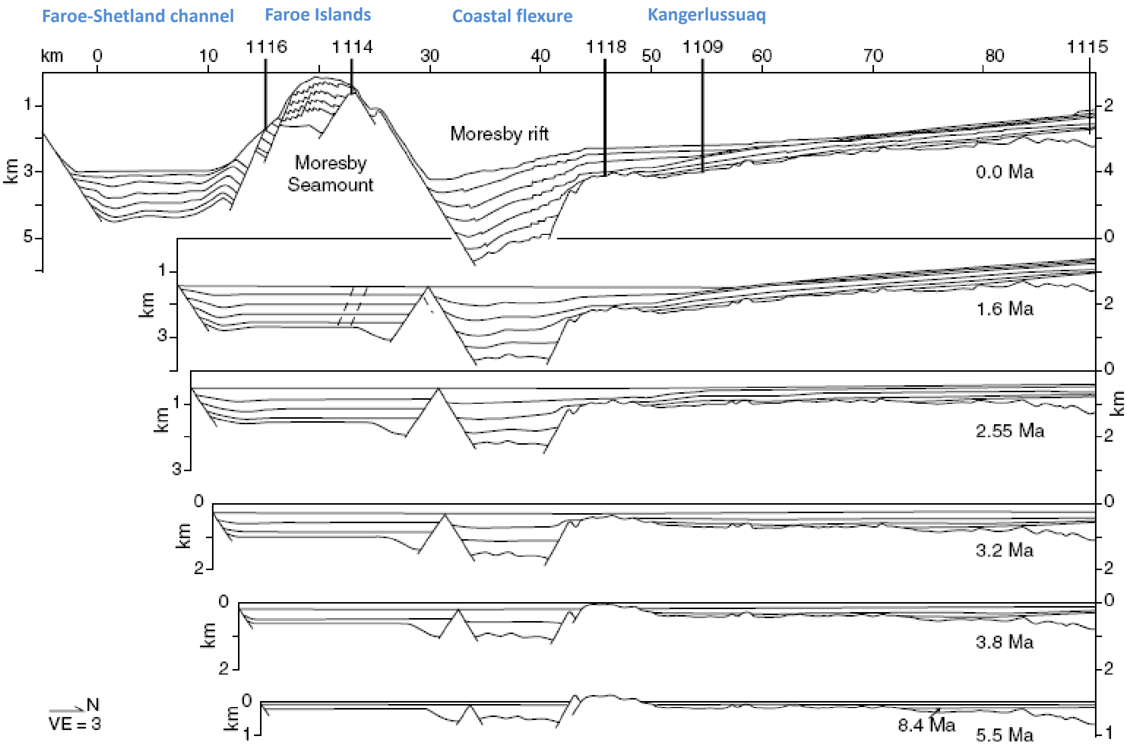

Fig. 4-24. Interpreted line drawing of MCS profile 1366 in the Woodlark Basin, reconstructed at 1.6, 2.55, 3.2, 3.8, and 5.5 Ma (lower panels) using constraints from seismic stratigraphy after Taylor and Huchon (2002).

Another mechanism to explain the coastal flexure is the crustal-scale bending that produces gentle up-warping and down-warping. Examples are arching of cover rocks above an intruding pluton, drape folds and forced folds. Forced folds are formed when sediments, which cover a more rigid basement, flex and drape the deep fault scarps in response to components of vertical movement along basement faults (Fig. 4-25).

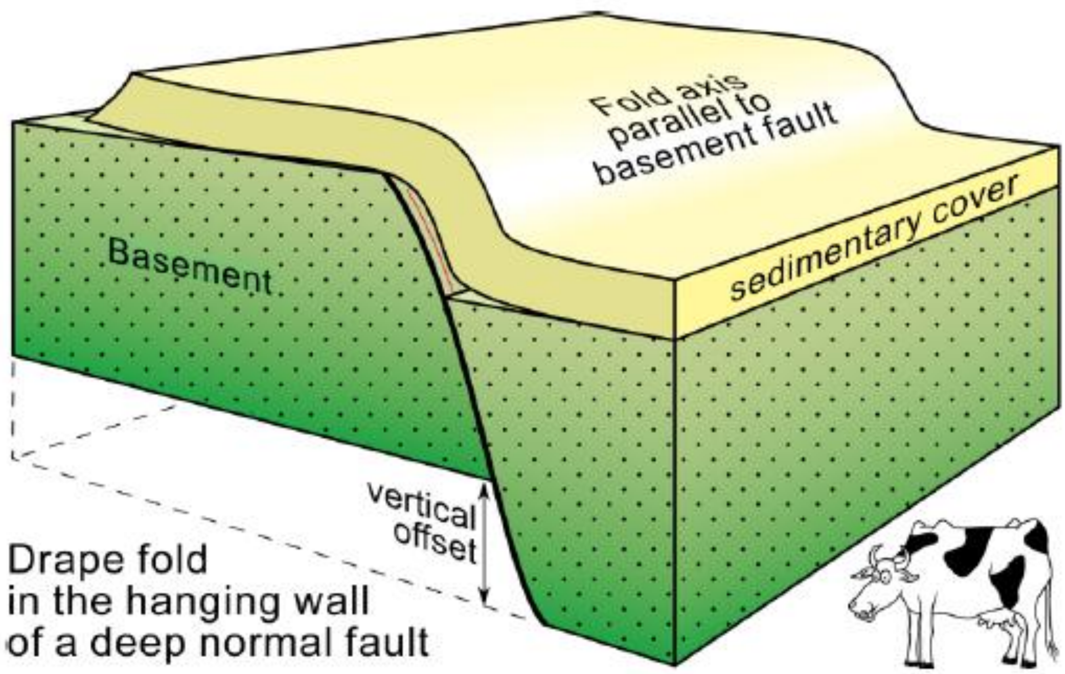

Fig. 4-25. Example of drape fold (flexure) formed in the hanging wall of a deep normal fault. Fold axis represents the hinge of the flexure in South East Greenland.

4.5 Late Eocene-Early Oligocene basin inversion

Structural data collected during fieldwork end presented in Chapter 3, highlight a tectonic event characterized by strike-slip faults that cut the Miki Fjord Macrodyke and the flexure related faults (Guarnieri 2011). Moreover, the reconstructed paleotress shows ESE-WNW oriented maximum horizontal stress in a strike-slip tectonic setting (cf. Chap. 3). A sample from a dyke swarm related to this fault system was collected in 2010, for age dating using Baddeleyite analysis without success. That means the age of this late deformation event should be infer from other geological information.
Seismic line offshore East Greenland, described in Chapter 5, show a prograding wedge that is believed to be of Late Eocene-Oligocene age (T. Nielsen personal communication) that can be related to the uplift of the coastal area.

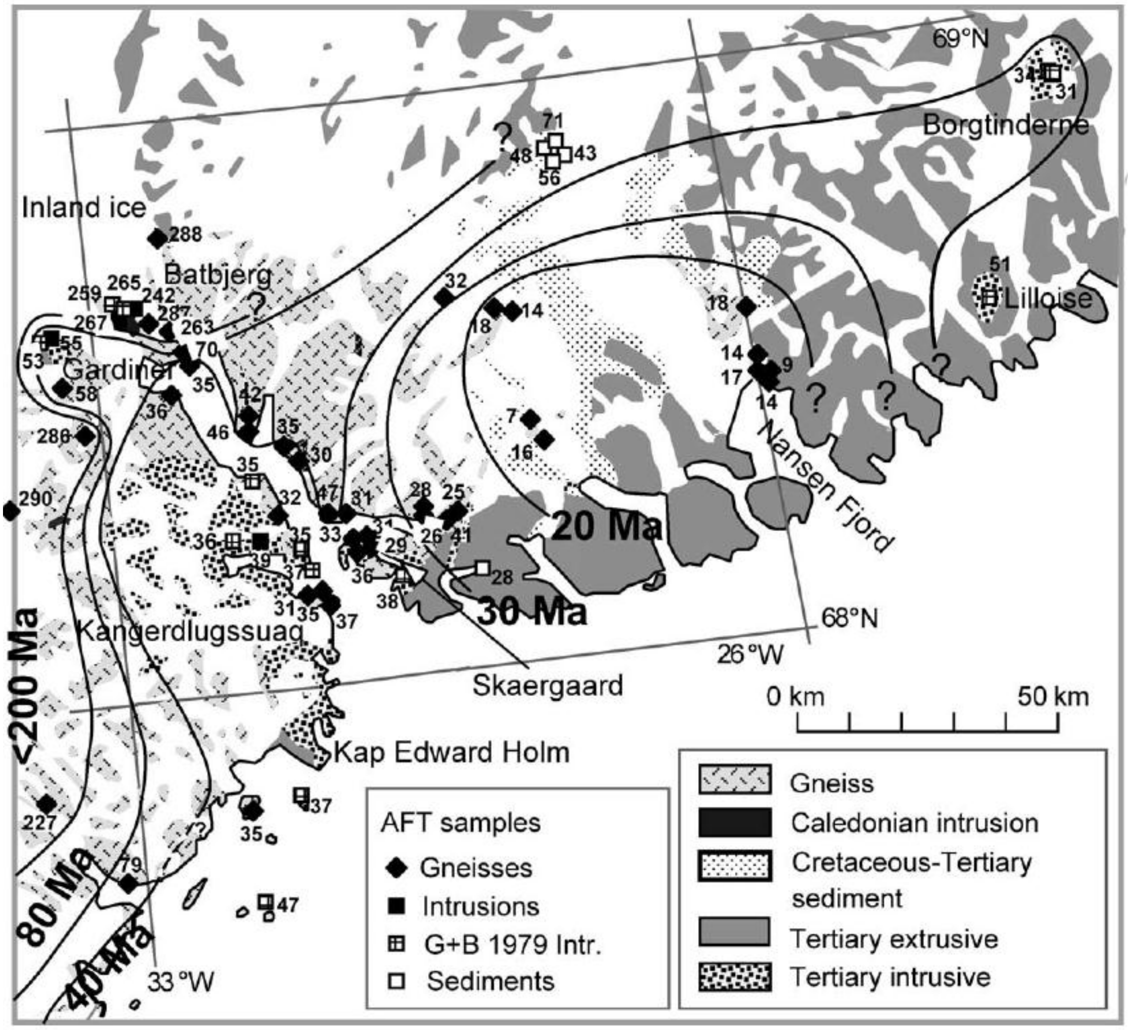

Fig. 4-26. Apatite FT age distribution in the Kangerlussuaq area. Sample locations and apatite FT ages are shown for present and earlier published analyses (Gleadow and Brooks, 1979 (G + B); Hansen, 1996). The geological map is based on Escher and Pulvertaft (1995). (after Hansen and Brooks 2002)

Geomorphological studies (Brooks 1979) have shown that the East Greenland margin was subjected to two main uplift events: the formation of a domal structure rising to c. 6 km above present sea level and centred on the Kangerlussuaq area, and a regional uplift of c. 2 km giving the high East Greenland coastline. These two topographic features could well have different causes. Fission-track studies (Gleadow & Brooks 1979; Hansen 1992, 1996, 2000; Hansen & Brooks 2002; Hansen & Reiners 2006) show that uplift and erosion took place c. 20 Ma after the continental breakup and continued into the Neogene (Fig. 4-26), but precise mechanisms for these events remain obscure, the delay probably being inconsistent with the idea of underplating as suggested by Brooks (1985), Cox (1993) and White et al. (2008).
Other information concerning regional tectonic events affecting the area can be achieved from Plate Tectonics. It is well known that in Late Eocene-Early Oligocene major plate re-organization took place in the North East Atlantic (Fig. 4-27).

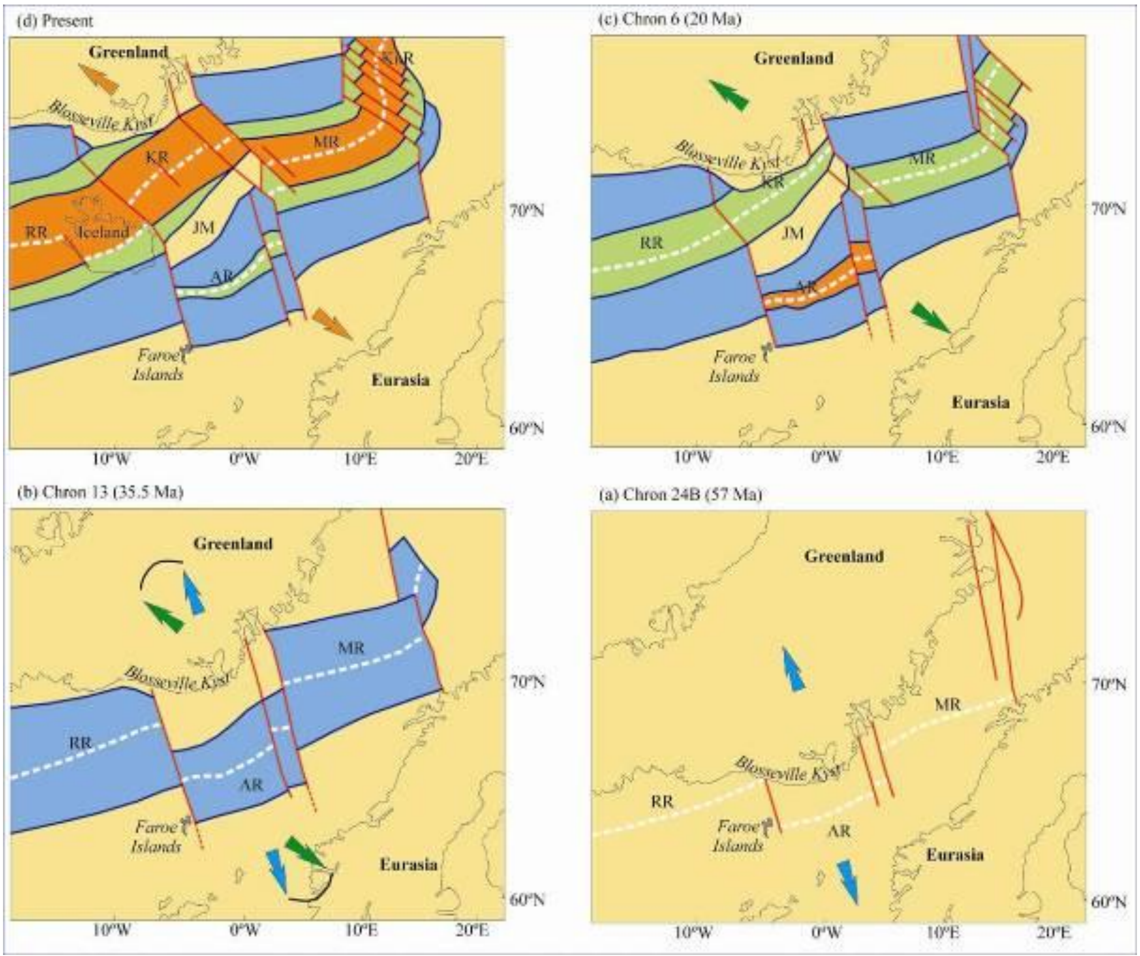

*Fig. 3. Plate tectonic evolution of North Atlantic Ocean. (**a**) Initiation of seafloor spreading. The relative plate motion vector (blue arrows) is given by the trend of East Jan Mayen Fracture Zone and Senja Fracture Zone—Hornsund Fault Zone (blue lines). (**b**) Major plate reorganization and change in direction of relative plate separation (from blue to green arrows). Rifting and associated magmatism occurred in East Greenland, along the SW Barents Sea margin, and possibly along the mid-Norwegian margin South to the northern Vøring Basin. (**c**) The Kolbeinsey Ridge (KR) propagated northward in East Greenland (between Chron 13 and 6C) and eventually separated the Jan Mayen microcontinent from East Greenland. Linkage between the Kolbeinsey and Mohns Ridges (MR) was achieved by development of the West Jan Mayen Fracture Zone. The Aegir Ridge (AR) was abandoned. (**d**) The plate configuration established following linkage of the Kolbeinsey and Mohns Ridges has been maintained to the Present (After Lundin and Doré, 2002).*

When spreading in the Labrador Sea ceased in the earliest Oligocene, (Chron 13, 35 Ma) (Lavwer et al., 1990), Greenland became part of the North American plate. At this time, a significant counter-clockwise rotation of the opening direction took place in the Norwegian Sea, changing from NNW–SSE to NW–SE (Fig. 4-27). The ca. 30° rotation can be defined from the difference in trend of the East and West Jan Mayen Fracture Zones. The onset of the changes in plate motions at Chron 13 times can be deduced from the eastward termination of the West Jan Mayen Fracture Zone (Olesen, et al., 1997). From Oligocene to Present, the North Atlantic spreading continued in a NW–SE direction (Fig. 4-27).

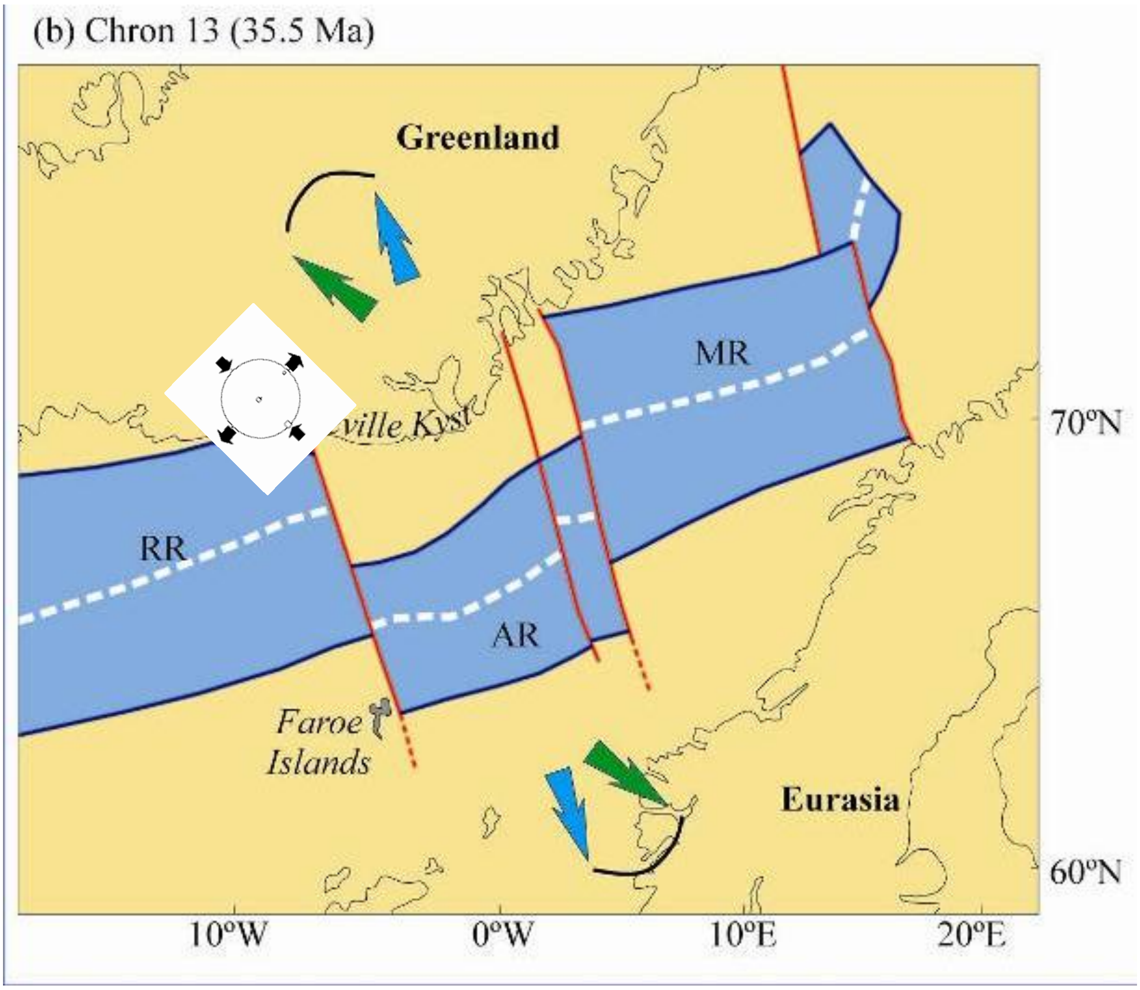

Fig. 4-28. Plate reconstruction in Late Eocene-Early Oligocene showing change in Plate motion and paleostress from fault-slip data in Kangerlussuaq.

Figure 4-28 shows plate configuration that pre-dates the separation of the Jan Mayen Microcontinent. It should be noticed the correspondence between the direction of motion of Greenland (green arrow) and the maximum horizontal stress reconstructed from fault-slip data (cf. Chap. 3). This is considered the initial stage and the cause of uplift in the Kangerlussuaq area and coincide with cooling, uplift and erosion documented by Apatite fission track data described above.

Faults related to this tectonic event are characterized by strike-slip movements as described in Chapter 3 and Guarnieri (2011). Along N120ºE trending structures the movements are left-lateral with associated extensional features and dykes ESE-WNW oriented. These structures are well described in Sødalen where they cut through older structures (Fig. 4-29).

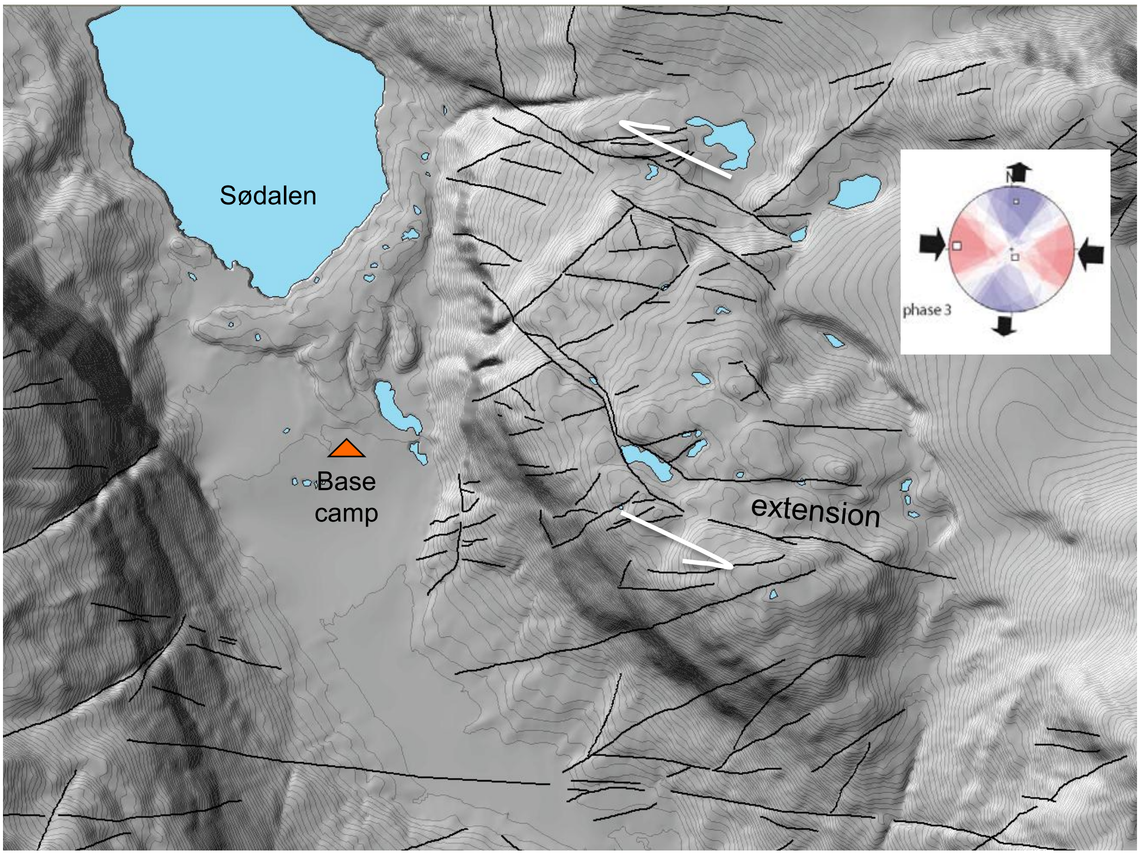

Fig. 4-29. DEM with major lineament (faults and dykes) around Sødalen. White arrows shows left-lateral kinematics along N120ºE trending faults together with the reconstructed paleostress.

Other structures cutting through the basalt and sill sequence are documented in the Fairy Tale Valley (Fig. 4-30).

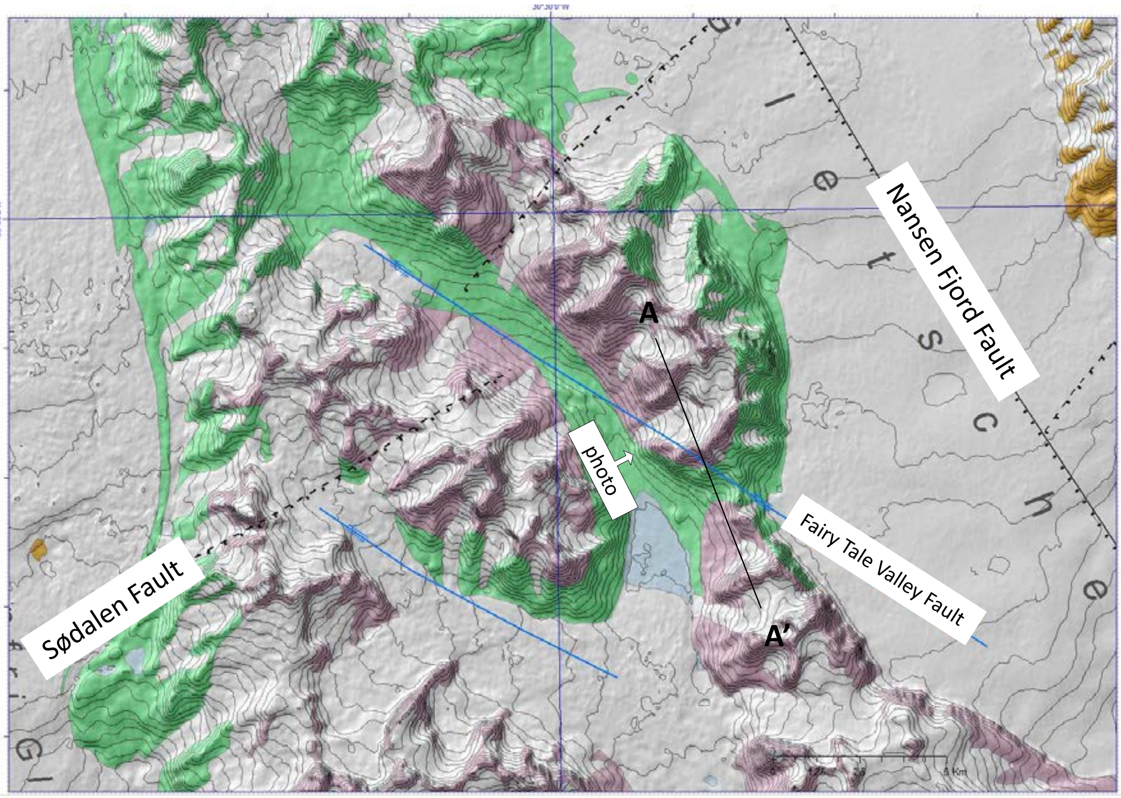

Fig. 4-30. Geological map of the Fairy Tale Valley (from Geological Map of Greenland 1:500 000 scale).

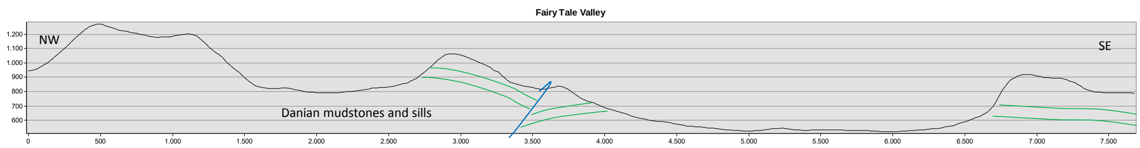

Fig. 4-31. Cross-section A-A' showing the reverse component of the Fairy Tale Valley Fault associated to the Late Eocene Early Oligocene inversion of the basin. Location in Figure 4-30.

Fig. 4-32. Oblique photo across the Fairy Tale Valley Fault showing the reverse character of the fault. Location in Figure 4-30.

5. Seismic lines offshore East Greenland

5.1 Description of offshore seismic reflection data

Over the last 30 years, a number of seismic reflection and seismic refraction experiments have been carried out offshore East Greenland. The NAD project in the early 80's resulted in the first deep seismic re-flection profiles in the area with acquisition taking place during the summers of 1980, 1981, and 1982.

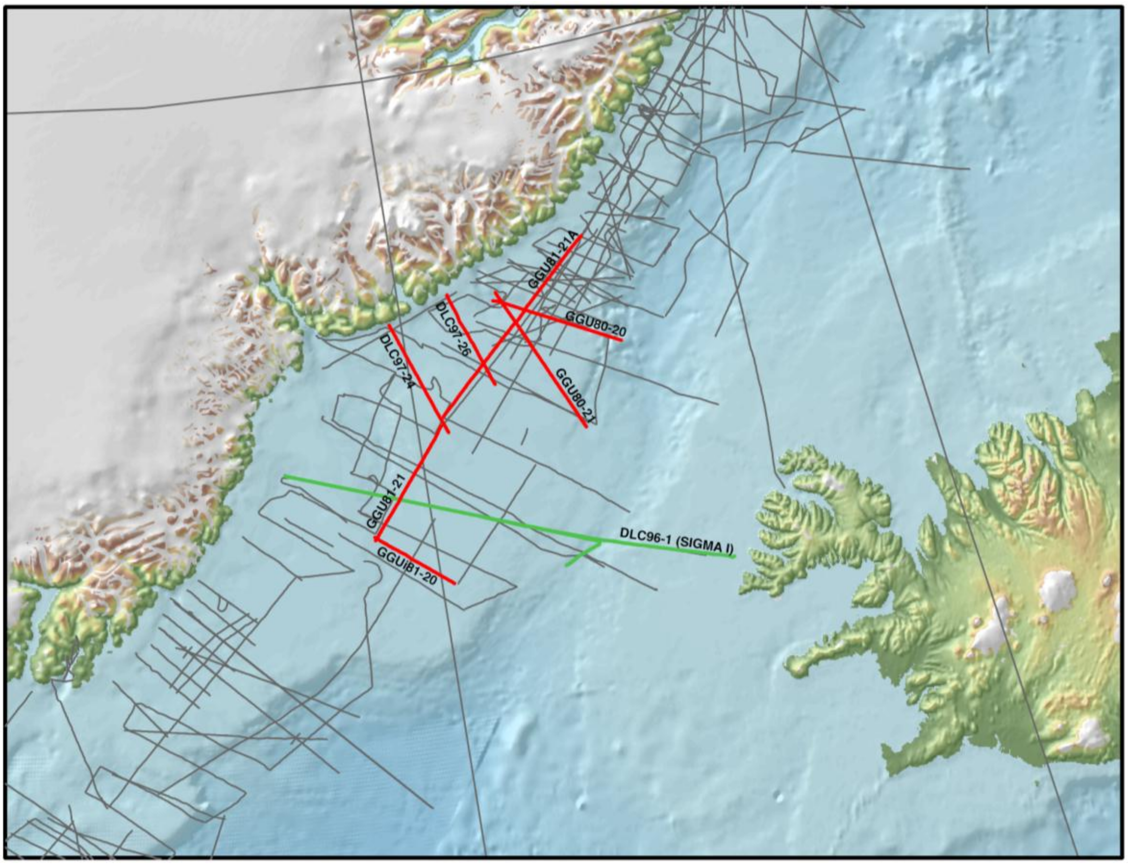

Fig. 5-1. Location Map Offshore East Greenland between Kangerlussuaq Fjord/Blosseville Coast and Iceland. Seismic profiles collected over the last 30 years include a combination of high resolution shallow reflection, deep reflection, and deep refraction profiles. Profiles highlighted in red are shown here. The GGU80 and GGU81 profiles are deep reflection data and were collected as part of the NAD project in the early 1980's (Larsen, 1985). The DLC97 profiles are shallow seismic reflection profiles and were collected in 1997 to support drilling and sampling of the flood basalts offshore that are exposed at the seabed or buried beneath only thin sediments (Hopper et al., 1998). The green profile is a deep refraction profile shot in 1996 to determine the nature and structure of the deep crust along the Greenland-Iceland Ridge (Holbrook et al., 2001).

A summary report of the key results is found in Larsen (1985). In 1996, a deep reflection seismic experiment with coincident seismic refraction profiles was carried out along the SE Greenland margin. The northern-most refraction profile was collected along the Greenland Iceland Ridge to elucidate the nature and deep structure of the crust (Holbrook et al., 2001). Finally, a number of shallow seismic reflection experiments were carried out in the 1990's to support offshore scientific drilling (Fig 5-1). Of particular relevance for the study area here was a high resolution shallow survey in 1997 (Hopper et al., 1998).

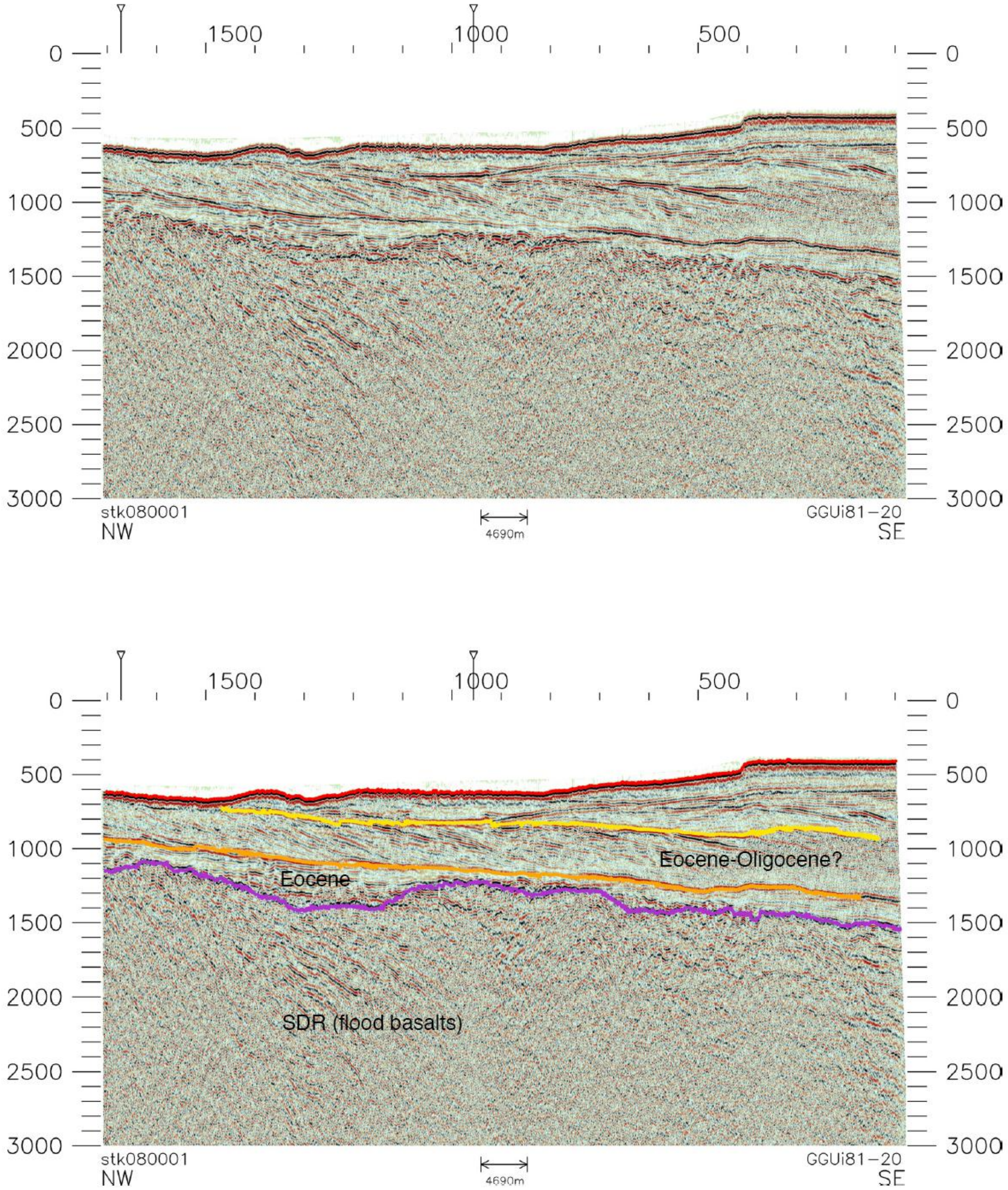

Fig. 5-2. Profile GGU81-20: Uninterpreted and interpreted seismic sections. Vertical scale is two way travel time in msec. Top horizontal scale is shotpoint number (nominal spacing of 50 m). Vertical exag-geration of the seafloor is approximately 20:1. Red horizon is the seafloor. Purple horizon is the top bas-alt. Below top basalt, a wedge of seaward dipping reflectors characteristic of flood basalts along volcanic rifted margins is observed. The basalt is capped by a thin cover of Eocene sediments, above which is a

prograding wedge of sediments that is capped by two sequence boundaries marked by the yellow and orange horizons. The prograding wedge is believed to be late Eocene to Oligocene in age (Tove Nielsen, personal communication).

A key problem with seismic acquisition in the area is the presence of thick basaltic sequences. These typically form prominent seaward dipping reflectors that are characteristic of volcanic rifted margins (e.g. Larsen and Jakobsdottir, 1988; Eldholm and Grue, 1994). Profile GGU81-20 shows a particularly well developed example of this. These dipping reflectors are the offshore equivalent of the thick pile of lava's exposed onshore along the Blosseville Coast (Fig. 5-2). The offshore lava sequences were sampling during Ocean Drilling Program legs 152, 163, and 163x (Saunders et al., 1998; Larsen et al., 1999; Thy et al., 2007).

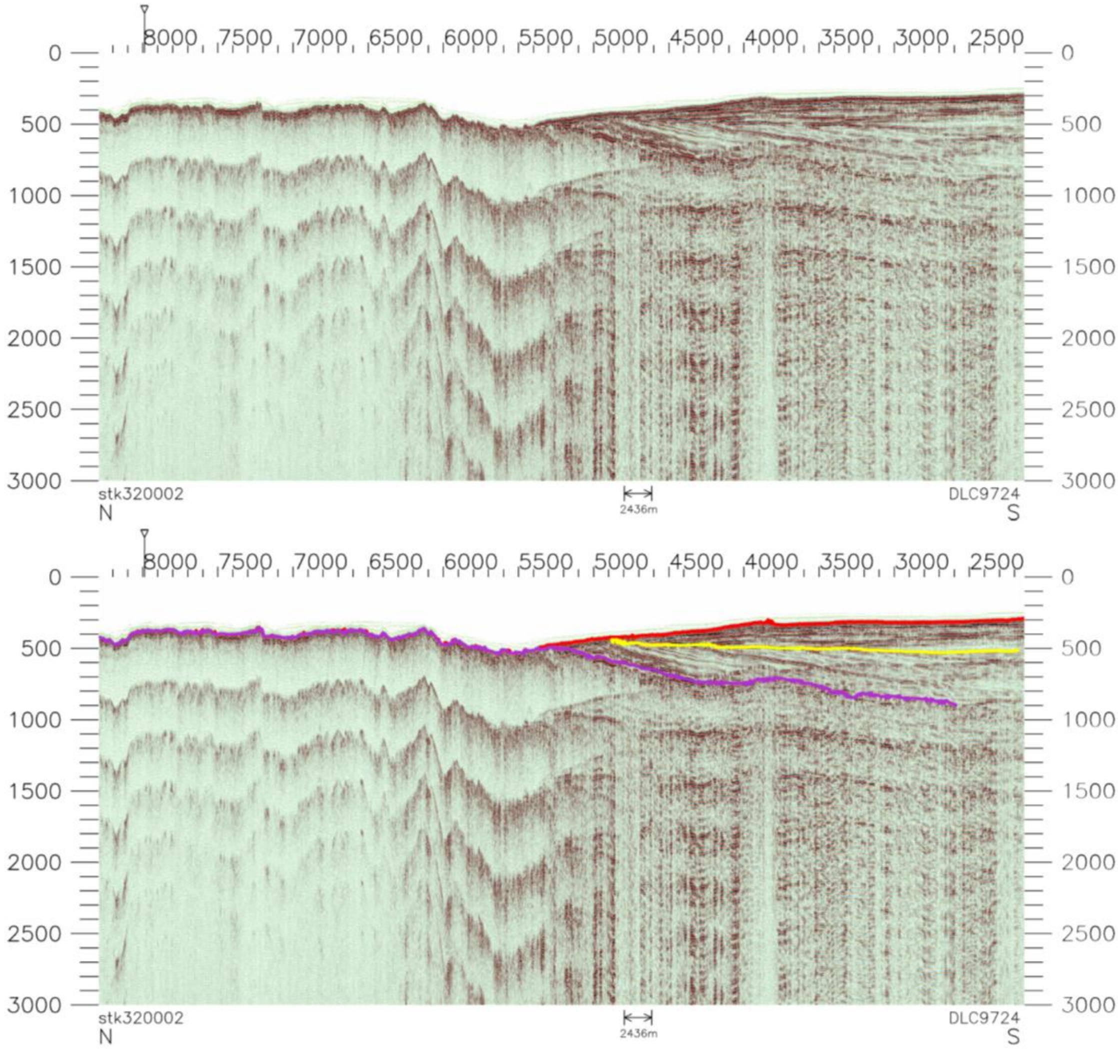

Fig. 5-3. Profile DLC97-24. Uninterpreted and interpreted seismic sections. Vertical scale is two way trav-el time in msec. Top horizontal scale is shotpoint number (nominal spacing of 12.5 m). Vertical exaggeration of the seafloor is approximately 20:1. This profile is located closer to shore and may overlie transitional or continental crust, although basalt is exposed at the seafloor beginning around shotpoint 5300. A prominent angular unconformity (yellow horizon) separate recent sediments from Eocene sediments that directly overlie the basalt.The age of the unconformity is unknown, but is

likely Miocene or younger. Evidence for the Late Eocene-Oligocene prograding wedge of sediment observed in the other seismic profiles is lacking.

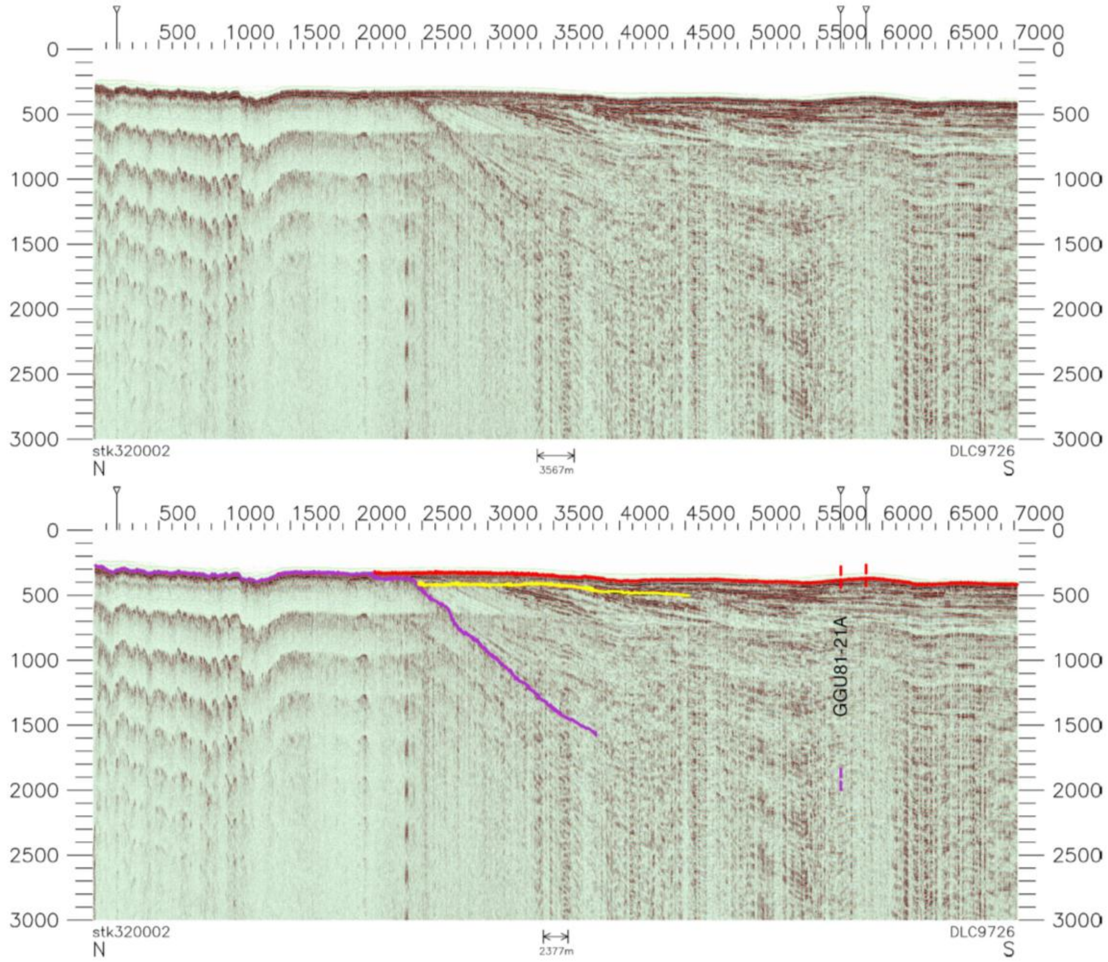

Fig. 5-4. Profile DLC97-26. Uninterpreted and interpreted seismic sections. Vertical scale is two way trav-el time in msec. Top horizontal scale is shotpoint number (nominal spacing of 12.5 m). Vertical exaggera-tion of the seafloor is approximately 20:1. This profile is located just north of Nansen Fjord. Color coding of horizons is same as previous. Note that the top basalt and Eocene sediments show much steeper seaward dip. As in DLC97-24, a prominent angular unconformity separates the very sediments from older sediments. Beneath this unconformity, there are hints of prograding sediments that could correspond to those observed in the other profiles. However, the high resolution system is insufficient for good imaging below the first seabed multiple and the deeper sedimentary sequences cannot be confidently interpreted.

The lava piles are up to 5 km thick onshore (Larsen et al., 1999) and at least 4 km thick offshore (Hopper et al., 2003). Along East Greenland, the feather edge of the basaltic sequences are underlain by continental crust, but farther seaward, a transition to overthickened oceanic crust is observed (Korenaga et al., 2000; Holbrook et al., 2001; Hopper et al., 2003).

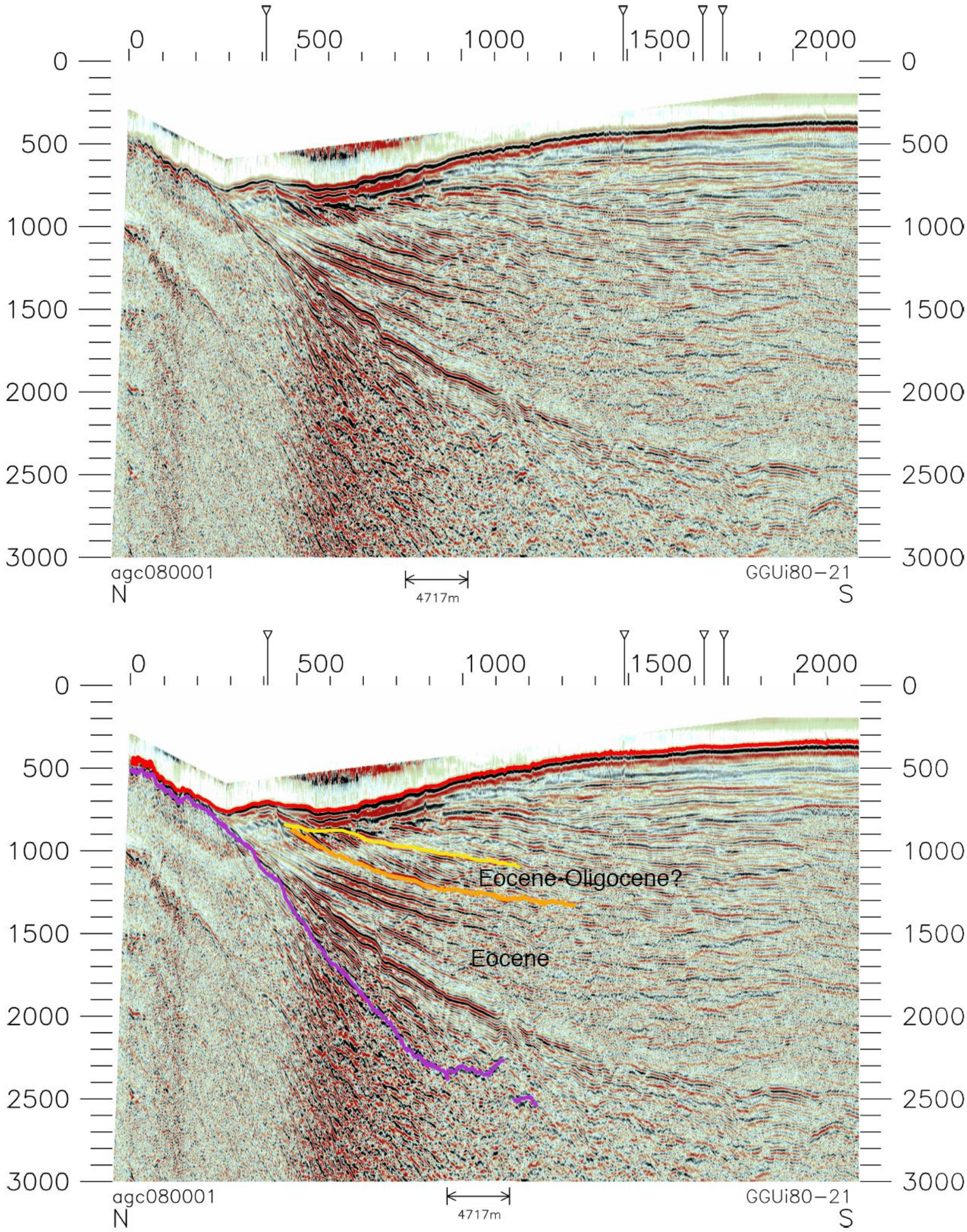

Fig. 5-5. Profile GGU80-21: Uninterpreted and interpreted seismic sections. Vertical scale is two way travel time in msec. Top horizontal scale is shotpoint number (nominal spacing of 50 m). Vertical exag-geration of the seafloor is approximately 20:1. Red horizon is the seafloor. Purple horizon is the top bas-alt. The basalt is capped by a thin cover of Eocene sediments, above which is a prograding wedge of sediments that is capped by two sequence boundaries marked by the yellow and orange horizons, similar to that observed farther south on Profile GGU81-20. Note the steeply dipping top bas-alt, similar to Profile DLC97-26. Basalt crops out at the seabed around shotpoint 250.

Along the Greenland-Iceland ridge, the location of the continent-ocean transition is highly uncertain, so it is difficult to determine the crustal type of the offshore region near the study area of this report. SIGMA profile 1 (green line in location map) shows a velocity structure indistinguishable from present day Ice-land, and has an oceanic character along its entire length. Like Iceland, however, the oceanic thickness is extreme, between 30-40 km thick, compared to the global average of 7-9 km thick oceanic crust. Profile GGU81-20, which shows the classic SDRs is very close to the SIGMA 1 profile, and thus is likely underlain by over-thickened oceanic crust. To the north where seismic profiles extend very close to shore, the top basalt reflection is observed to crop out at the seabed, and there is no imaging below this hard surface. Based on the offshore seismic data, the seaward extent of continental crust cannot be determined.

The top basalt reflection is clear in all the seismic profiles, and there appears to be a dramatic change to north, beginning at approximately Nansen Fjord. In the two southern-most profiles, GGU81-20 and DLC97-24, the top basalt reflection remains very shallow, and shows very little seaward dip (Figs 5-3 and 5-4). Only a thin Eocene sedimentary cover is observed. In contrast, the three northernmost profiles show a pronounced seaward deeping of the top basalt reflection.

A key observation in the seismic profiles is a prograding wedge of sediments bounded by prominent sequence boundaries (Fig. 5-5). This prograding wedge is commonly observed along much of the East Greenland coast is believed to be late Eocene to Oligocene in age (T. Nielsen, personal communication). To the south where the basalt is shallow, this wedge is underlain by only a thin veneer of sediment that covers the basalt, whereas to the north, it covers a wedge of sediment that thickens rapidly seaward (Fig. 5-6).

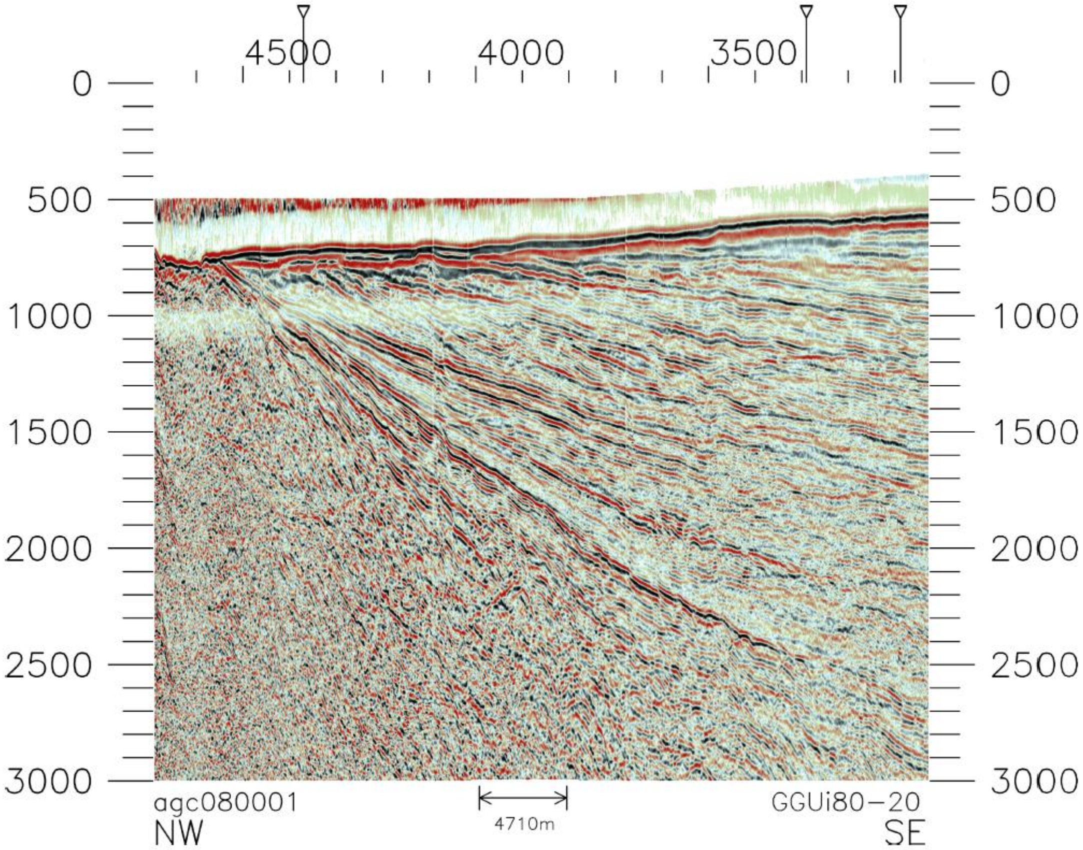

4500
4000
3500
0
500
1000
1500
2000
2500
3000
agc080001
NW
4710m
GGUi80-20
SE

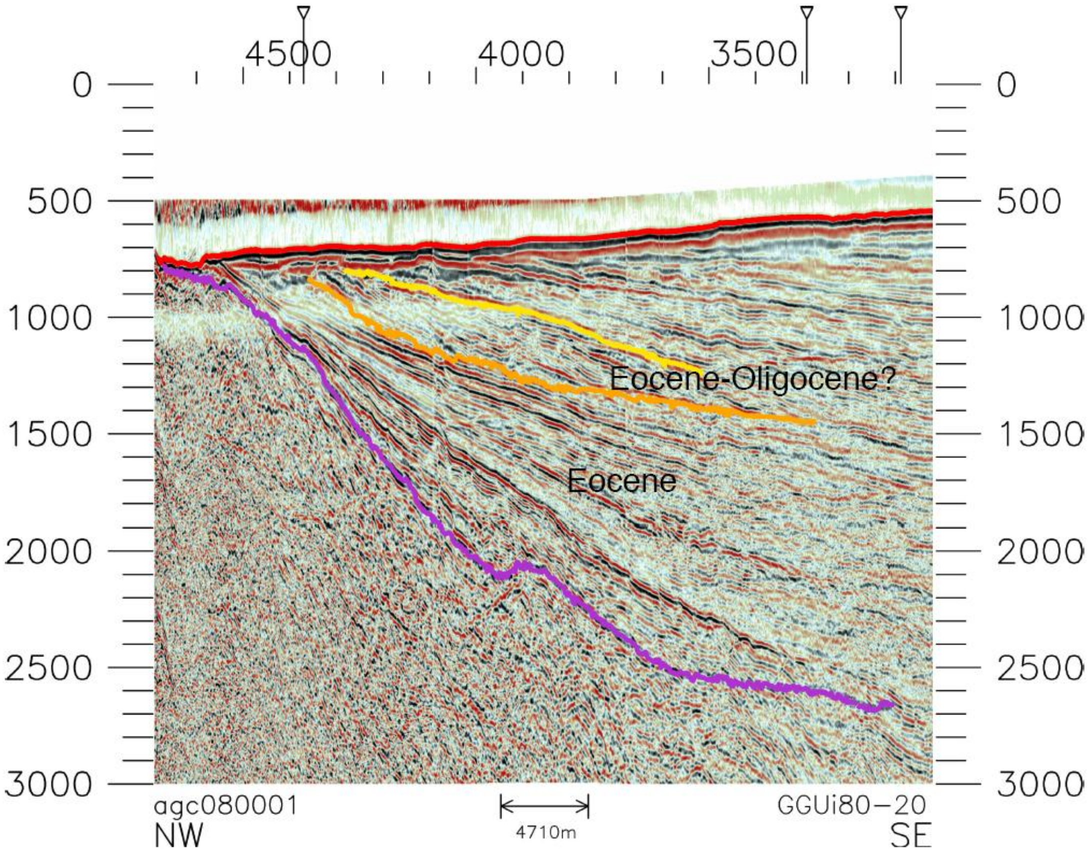

4500
4000
3500
0
500
1000
1500
2000
2500
3000
Eocene-Oligocene?
Eocene
agc080001
NW
4710m
GGUi80-20
SE

Fig. 5-6. Profile GGU80-20: Uninterpreted and interpreted seismic sections. Vertical scale is two way travel time in msec. Vertical exaggeration of the seafloor is approximately 20:1. Red horizon is the sea-floor. Purple horizon is the top basalt. The basalt is capped by a thin cover of Eocene sediments, above which is a prograding wedge of sediments that is capped by two sequence boundaries marked by the yellow and orange horizons, similar to that observed farther south on Profile GGU81-20. Note the steeply dipping top basalt, similar to Profiles DLC97-26 and GGU80-21. Basalt crops out at the seabed around shotpoint 4600.

Unfortunately, convincing seismic ties between the profiles cannot be established with the current data sets. Profiles GGU81-21 and GGU81-21A (Fig. 5-7) are parallel to the coast and provide the only possibility to tie the data together. Unfortunately, there is a data gap to north, and the cross with the DLC97 profiles occurs over thick sediments and the high resolution system cannot image deep enough. The tie line confirms, however, the rapid deepening of the top basalt reflection described above. To the south, a maxi-mum sediment thickness of <500 msec is observed, whereas to the north, more than 2000 msec of sediment covers the basalt.

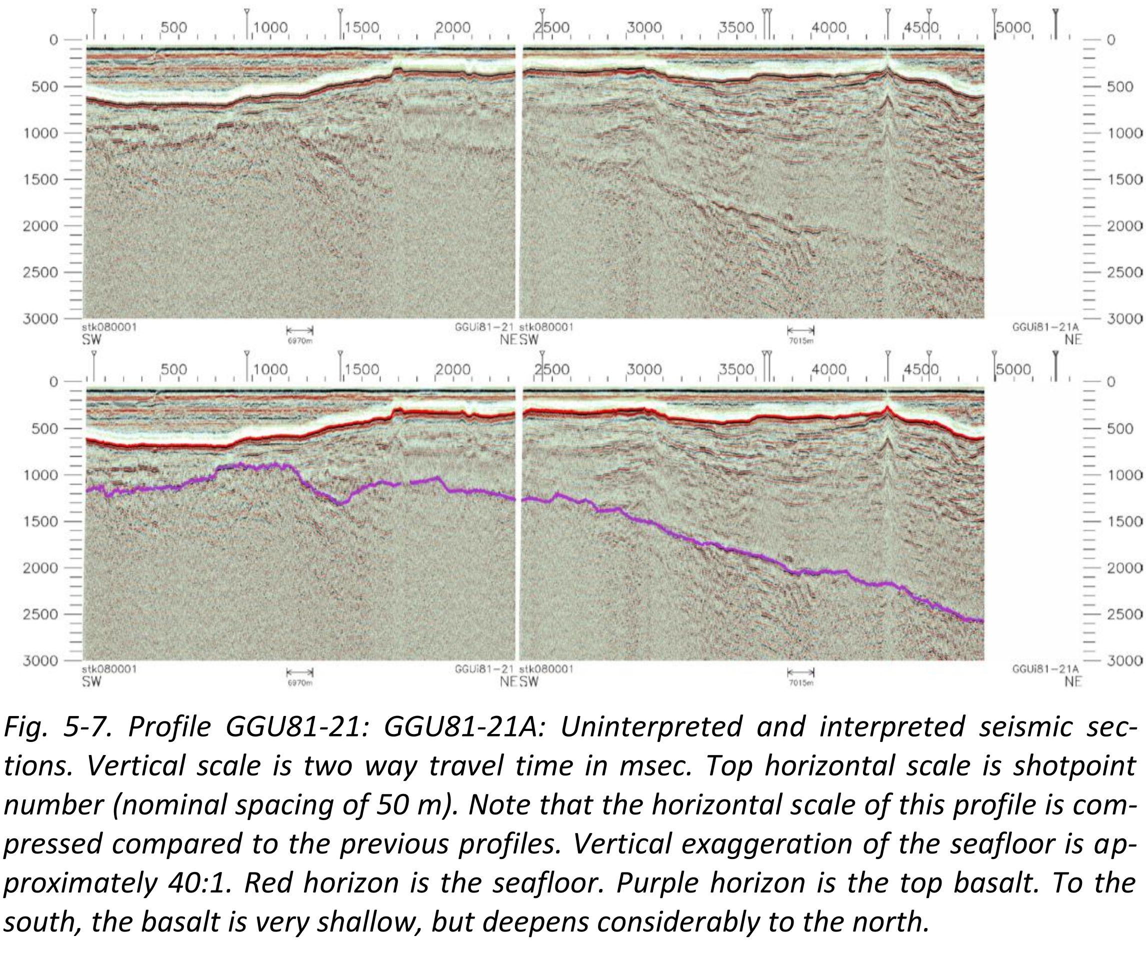

Fig. 5-7. Profile GGU81-21: GGU81-21A: Uninterpreted and interpreted seismic sections. Vertical scale is two way travel time in msec. Top horizontal scale is shotpoint number (nominal spacing of 50 m). Note that the horizontal scale of this profile is compressed compared to the previous profiles. Vertical exaggeration of the seafloor is approximately 40:1. Red horizon is the seafloor. Purple horizon is the top basalt. To the south, the basalt is very shallow, but deepens considerably to the north.

6. Correlation with the Faroe-Shetland area

6.1 Tectono-Stratigraphic framework of the Faroe-Shetland Basin

The Faroe-Shetland Basin comprises a series of NE–SW-trending sub-basins (Fig. 6-1) that formed during a sequence of Late Paleozoic, Mesozoic and Paleocene rift events following the end of the Caledonian orogeny (c. 390 Ma; Coward 1990). The sub-basins are separated by horst blocks (locally referred to as 'highs' or 'ridges') that are cored by metamorphic basement rocks. Where sampled by drilling this thisbasement can be correlated with Precambrian gneisses of the Lewisian Complex exposed onshore in NW Scotland (Ritchie & Darbyshire 1984; Hitchen & Ritchie 1987).

The Clair Basin is a continental basin of Devonian-Carboniferous age that encompasses the area around the Rona High and may extend westwards to the Westray and Corona highs (Fig. 6-2)(Smith and Ziska, 2010). The maximum observed thickness of sedimentary rocks in the Clair Basin is ca. 1 km (e.g. Smith and Ziska, 2010). Devonian-Carboniferous sedimentary rocks reach a thickness of more than than 4 km in the Orcadian Basin that extends from Shetland over Orkney and Caithness to the Moray Firth. As the Devonian-Carboniferous basins of Northwest Europe and East Greenland are located within the Caledonides, it has been proposed that these basins may be the result of extension due to gravitational collapse of orogenic thickened crust (McClay et al. 1986) .Post-orogenic gravitational collapse. However, transtensional deformation may have been important during the evolution of the Orcadian Basin (see Dewey and Strachan, 2003) .

Permo-Triassic sedimentary rocks are penetrated by a few wells in the western part of Faroe-Shetland Basin (6-3)(e.g. Quinn and Ziska, 2010), and further to the southeast throughout most of the West Orkney, Papa, Solan and West-Shetland basins (e.g. Stoker et al., 1993). Overall, Triassic faulting along NNE-SSW trending faults controlled the distribution of known Permo-Triassic sedimentary rocks in the Faroe-Shetland Basin and neigbouring areas (Coward et al. 2003).

Jurassic extension in NW Europe (Doré et al. 1999) was characterized by the formation of mainly north–south-trending rifts, including the North Sea and Porcupine Basins and parts of the Halten Terrace. However, the lack of north–south-trending structures within the Faroe–Shetland Basin implies that late Jurassic rifting probably did not occur here. Early Cretaceous rifting has been inferred from the observation that packages of coarse-grained, Early Cretaceous clastic sediments thicken towards the hanging walls of mainly NE–SW trending normal faults within the Faroe–Shetland Basin (Booth et al. 1993).

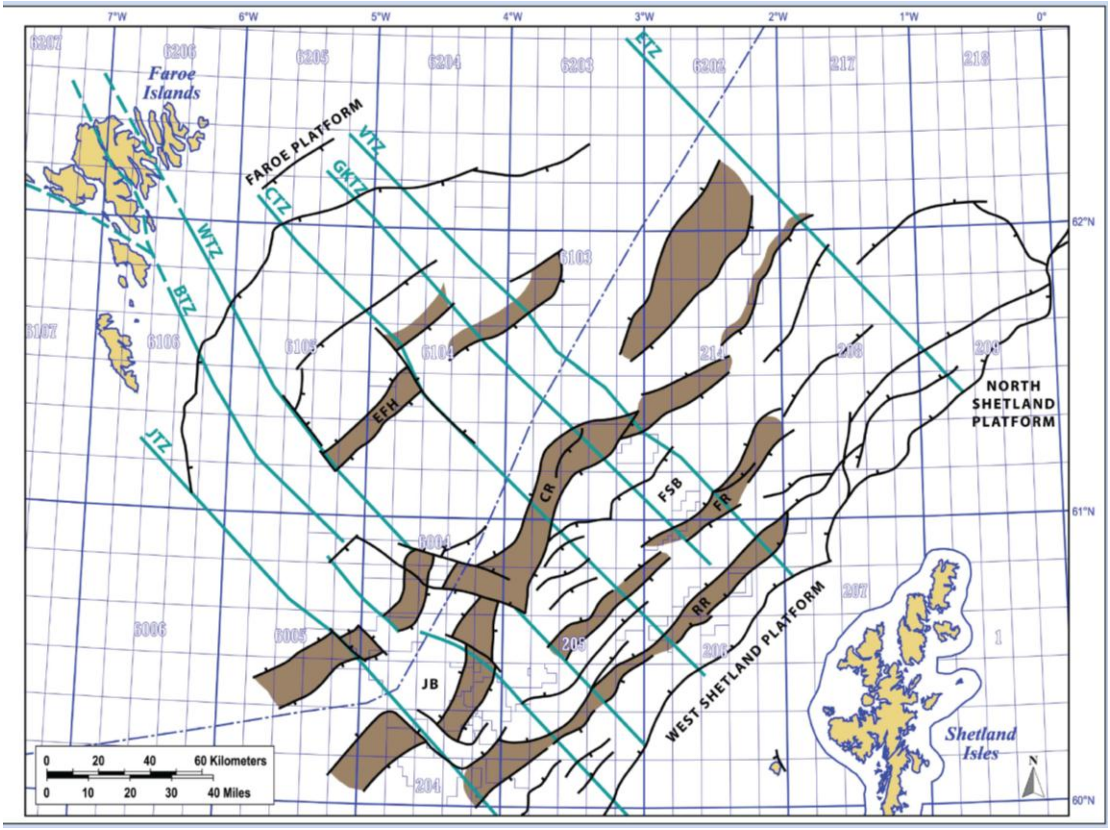

Fig. 6-1. Structural elements of the Faroe–Shetland Basin (after Ellis et al. 2009).

Minor rifting in the Middle Cretaceous (Dean et al. 1999) continued into the Late Cretaceous against a backdrop of rising eustatic sea levels, leading to dominantly marine conditions and the deposition of a regressive, highly mud-prone sequence (Mudge & Rashid 1987; Turner & Scrutton 1993). The dominant NE–SW trend of the Faroe–Shetland Basin had been established by the end of the Cretaceous, by which time rifting had ceased and basin flank uplift gave rise to deposition of a regressive Paleocene succession (Smallwood & Gill 2002). Paleocene rifting in the SW part of the Faroe–Shetland Basin has been inferred by Dean et al. (1999) on the basis that some Cretaceous normal faults appear to have been reactivated during the Paleocene. Nevertheless, Dean et al. (1999) acknowledged that these 'rift' faults could be attributed to minor deformation during post-rift thermal subsidence (Duindam & van Hoorn 1987). Alternatively, fault initiation and/or reactivation at this time may have been associated with differential compaction of sediments over structural highs (e.g. Færseth & Lien 2002).

Current models for the development of the NE Atlantic margin imply a progressive northwestward migration in the locus of active rifting, towards the eventual zone of continental break-up (Lundin & Doré 1997). Thus, evidence for a Paleocene rift event may exist beneath, and be largely obscured by, the thick Palaeogene lava pile in the NW part of the present-day Faroe– Shetland Basin (Fig. 6-1). Continental break-up (Eldholm & Grue 1994) was associated with widespread basin uplift and magmatism across the NE Atlantic region, in the form of continental flood basalts, sill and dyke complexes, igneous centres, magmatic underplating and the deposition of regional tuff horizons (White & McKenzie 1989; Naylor et al. 1999; Lundin & Doré 2005). Following continental break-up in the early Eocene (c. 54 Ma) the tectonic evolution of the Faroe–Shetland Basin has been dominated by thermal subsidence and the growth of large-scale Cenozoic anticlines (Davies et al. 2004; Stoker et al. 2005; Ritchie et al. 2008). These folds have been attributed to a variety of mechanisms including ridge push, sedimentary draping and reactivation of basement structures (Doré et al. 2008).

6.2 Transfer Zones within the Faroe-Shetland Basin

Rift-oblique lineaments were initially recognized within the Faroe–Shetland Basin by Duindam & van Hoorn (1987) and further discussed by Rumph et al. (1993), who inferred several lineaments from interpretations of regional gravity and magnetic datasets, and suggested tentatively that these lineaments were transfer zones. Some of the lineaments identified by Rumph et al. (1993) appear to form a key component of the tectonic architecture of the Faroe–Shetland Basin (Fig 6-1) (Jolley & Morton 2007; Ellis et al. 2009). Various workers have argued that the distribution of Paleocene sediments in the southeastern part of the basin was strongly influenced by the above mentioned and similar rift-oblique lineaments (Mitchell et al. 1993; Grant et al. 1999; Lamers & Carmichael 1999; Naylor et al. 1999), implying that the lineaments had significant structural and geomorphological expressions during and after rifting (see Gawthorpe & Leeder 2000). More recently, with hydrocarbon exploration interest turning towards the Faroese sector in the NW part of the basin, it has been proposed that rift-oblique lineaments played an important role in the transport of sediments sourced in the Kangerlussuaq region of Greenland (Larsen et al. 1999; Larsen & Whitham 2005), through the Faroe Islands (Passey & Bell 2007; Ellis et al. 2009), and into the Faroe–Shetland Basin (Whitham et al. 2004; Frei et al. 2005; Jolley & Morton 2007). They are believed to have exerted a control upon the Paleocene sediment distribution within this part of the basin, as well as on the distribution and thickness of subaerial basalt flows, shallow marine hyaloclastites (White et al. 2003; Ellis et al. 2009), the locations of dyke swarms (Naylor et al. 1999) and igneous centres (Rumph et al. 1993; Ritchie et al. 1999).

Several previous workers have inferred large-scale (basinwide) strike-slip or transpressional deformation along NW-SE-trending lineaments within the Faroe–Shetland Basin and elsewhere on the NE Atlantic margin (e.g. Dean et al. 1999; Ellis et al. 2009). These interpretations were based primarily on the lateral offsets in the continental margin, the presence of en echelon Cenozoic anticlines within strata that overlie the inferred position of these lineaments, and on the apparent offsets of structural highs within the Atlantic margin basins (Fig. 6-1) (Dean et al. 1999; Brekke 2000; Ritchie et al. 2003). The hypothesis that these lineaments accommodated regional strike-slip movements implies they are likely to be associated with the classic indications of strike-slip faulting, such as the presence of positive and negative flower structures within the Cenozoic overburden (e.g. Harding 1990). These features should be clearly visible and capable of being mapped along strike using up-to-date high-resolution 3D seismic datasets. However, case studies by Moy and Imber (2009) involving detailed seismic interpretation of the Cenozoic section around parts of three of the lineaments identified by Rumph et al. (1993) did not present indications of typical strike-slip features. Moy and Imber (2009) found:

- that the investigated (c. 20 km long) part of the Victory Liniament appears to have originated as the result of of local igneous and/or hydrothermat activity
- that the structural expression related to the c.20 km long investigated part of of the Clair Lineament possibly is related uplift above igneous intrusions.
- that the investigated part of the Judd Lineament has the character of a typical transfer fault being active during the Late Cretaceous and Paleocene times (Fig. 6-4 and 6-5).

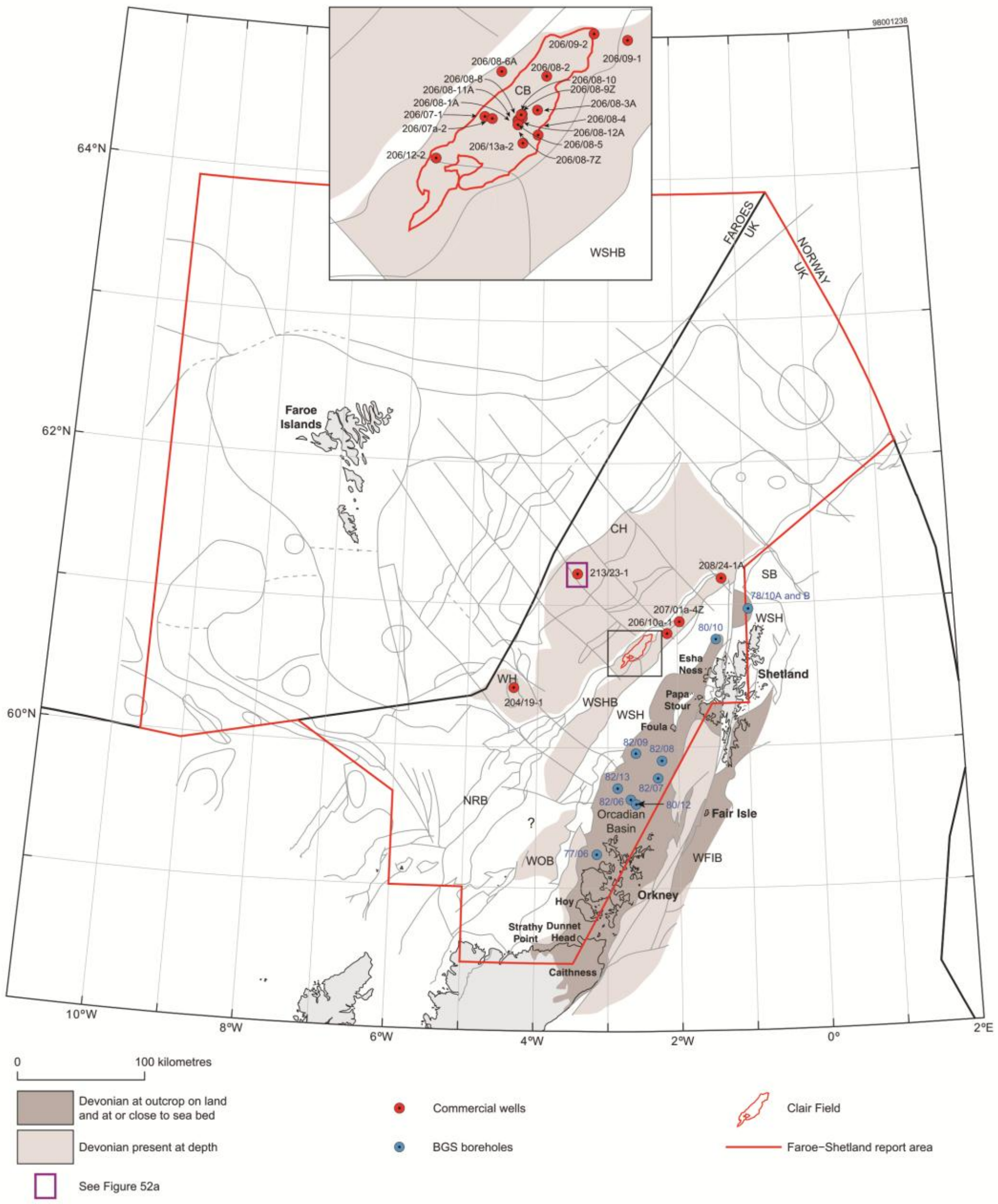

Fig. 6-2. Distribution of Devonian Strata in the Faroe-Shetland region. CH=Corona High, NRB=North Rona Basin, SB=Sandwick Basin, WFIB=West Fair Isle Basin, WH=WestrayHigh, WSH=West Shetland High, WSHB= West Shetland Basin, WOB=West Orkney Basin. Outline of present day structural elements outlined in grey. From Smith and Ziska (2010).

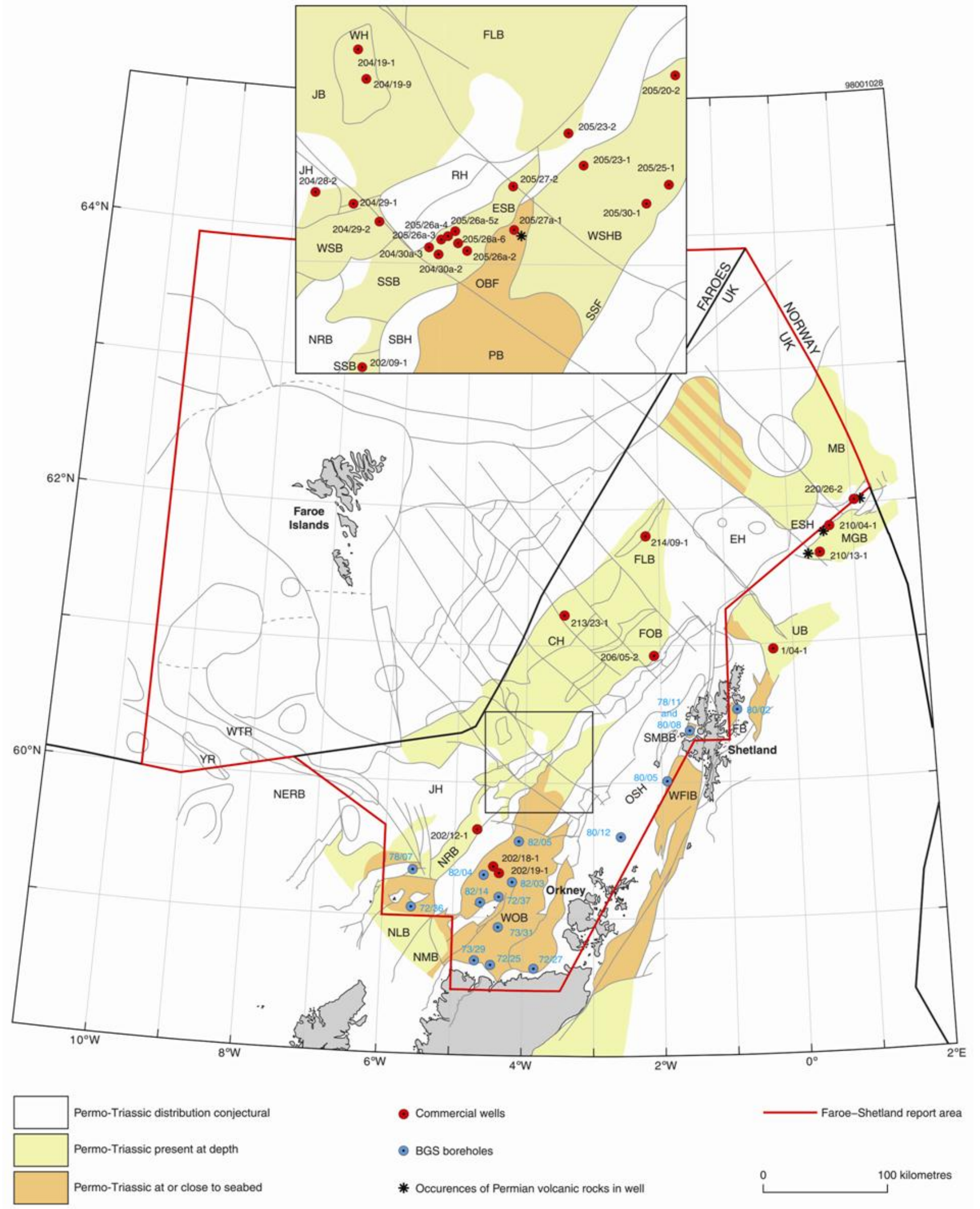

Fig 6-3. Distribution of Devonian Strata in the Faroe-Shetland region. CH=Corona High, EH=Erlend High, ESH=East Shetland High, FLB=Flett Subbasin, FOB=Foula Subbasin, JH=Judd High, MB=Møre Basin, MGB=Magnus Basin, NLB=North Lewis Basin, NMB=North Minch Basin, NRB=North Rona Basin, NERB=NorthEast Rockall Basin, OSH=Orkney-Shetland High, SMBB=St. Magnus Bay Basin, UB=Unst Basin, WFIB=West Fair Isle Basin, WOB=West Orkney Basin, WTR=Wyville-Thomson Ridge, YR=Ymir Ridge. Outline of present day structural elements outlined in grey. From Smith and Ziska (2010).

It has been demonstrated that segmentation of rift basins by rift-oblique lineaments may be controlled by the development of transfer zones or accommodation zones (Faulds & Varga 1998). Transfer zones are defined as discrete zones of sub-vertical

strike-slip and oblique-slip faulting that trend near-parallel to the extension direction, facilitating the transfer of strain between two rift domains (Faulds & Varga 1998). Accommodation zones are defined as regions of overlapping fault terminations where strain is transferred between fault tips through a series of relay structures (i.e. 'soft-linkage'; e.g. Morley et al. 1990; Acocella et al. 1999; Moustafa 2002). The key criteria defining transfer and accommodation zones are that extensional strain is conserved along the length of the segmented rift basin (Gibbs 1984; Morley et al. 1990), and that transfer and accommodation zones do not extend beyond the region of active rifting. Thus, transfer and accommodation zones are second-order features that are inherently related to the rift architecture. They are distinct from the regional-scale strike-slip fault interpretations that have been proposed to explain the NW– SE-trending lineaments on the NE Atlantic margin. An alternative hypothesis, therefore, is that the rift-oblique lineaments observed within the Faroe–Shetland Basin may have originated as transfer or accommodation zones during periods of rifting prior to continental break-up.
Therefore, we propose that the rift-oblique lineaments observed within the Faroe–Shetland Basin (e.g. Rump et al. 1993) may not at any time have been continuous active tectonic features; but rather composed of discrete fragments of opportunistic re-activation of pre-existing, but otherwise inactive, features. When the rift-oblique lineaments are traced as continuous or sub-continuous lineaments in potential field data this may reflect that different parts of a pre-existing feature are reactivated at different times. The apparent continuity of the rift-oblique lineaments may also result from re-crystalisation due to hydrothermal circulation in the tectonic inactive parts of the pre-existing feature or possibly magmatic intrusion.

6.3 Similarities with the Kangerlussuaq area

6.3.1 NW-SE major faults

In the Kangerlussuaq area NW-SE trending faults are represented by the Nansen Fjord Fault and the Kangerlussuaq Fjord Fault. These are inferred to be normal faults in the Late Ctretaceous-Early Paleocene rift stage. During the Middle-Late Paleocene oblique rift the same faults where re-activated as right-lateral and probably also during the Early Eocene breakup stage. Finally, during the inversion of the basin in Late Eocene-Oligocene the two structures where re-activated as reverse faults.
Plate tectonic reconstruction of Late Paleocene using www.gplates.org software shows a good correspondence between the Kangerlussuaq Fjord Fault (Fig.8-2) and the Judd Fault (Fig. 6-4).

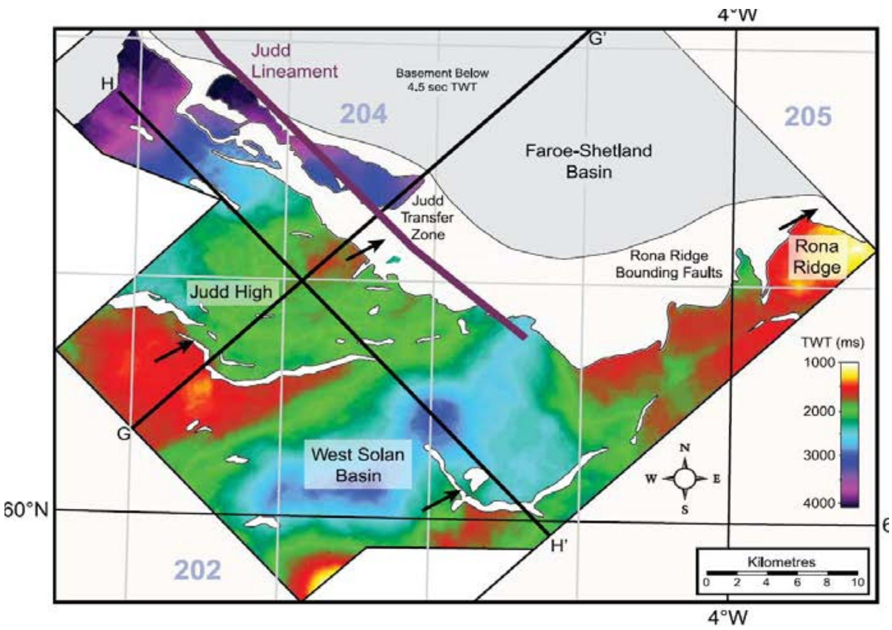

Fig. 6-4. Time–structure map of the top Precambrian basement displaying the West Solan and Faroe–Shetland Basins. (After Moy and Imber 2009).

Comparison between a seismic line across the Judd High and Judd Fault (Fig. 6-5) and a restored geologic cross-section across the Kangerlussuaq Fjord Fault (Fig. 6-6) shows that also the geology of the two faults seems to have many similarities. They have a Cretaceous-Paleocene sequence on the down-faulted side and the Eocene covering the footwall that in turn is represented in both cases by pre-Cambrian basement.

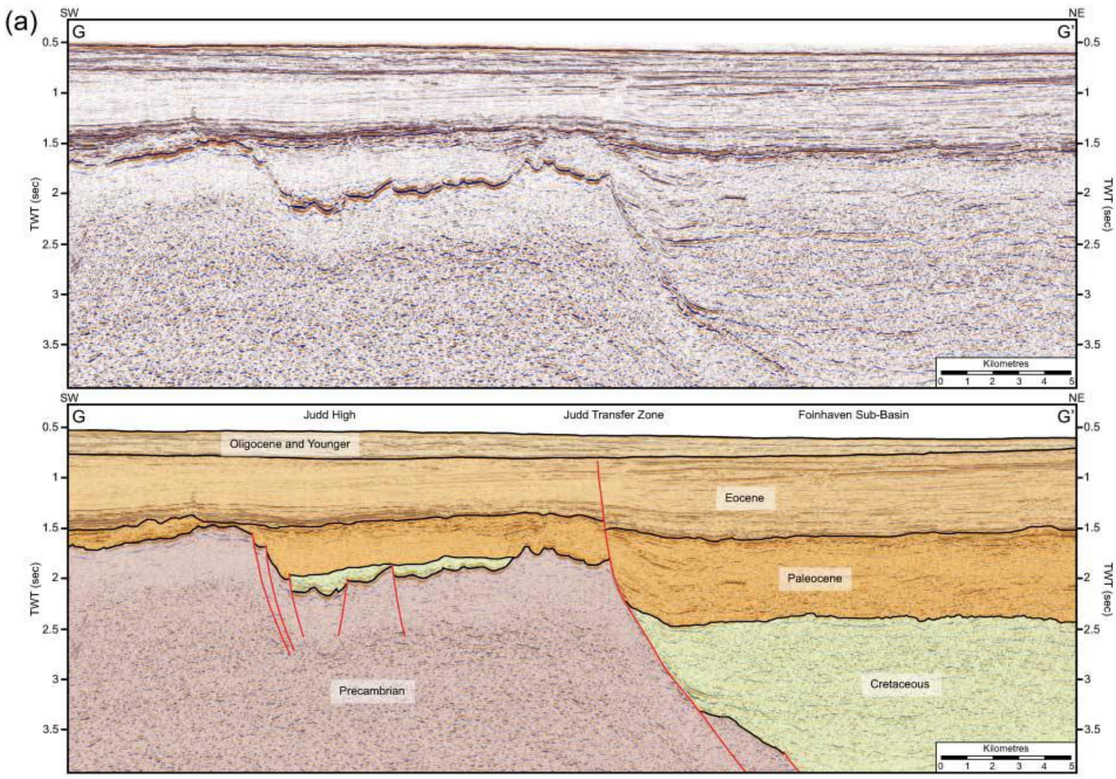

Fig. 6-5. Seismic lines displaying the tectonic style across the Judd Transfer Zone. Line location is shown in Figure 6-4. (After Moy and Imber 2009).

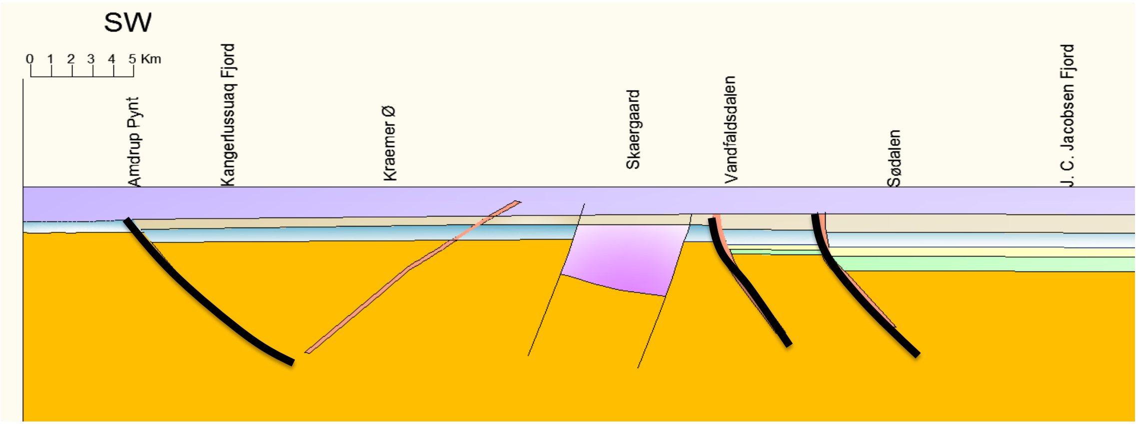

Fig. 6-6. Restored cross-section across the Kangerlussuaq Fjord Fault. (cf. Enclosure 4).

6.3.2 Paleostress orientation

The only two papers handling fault-slip data and paleostress analysis in the Faroese area describe the same paleostress tensor for the pre-breakup tectonic stage (Figs 6-7a/b and 6-8b). The maximum horizontal stress in NE-SW oriented in a strike-slip tectonic setting. This paleostress coincides with the oblique rifting stage described in the previous chapters (Fig. 6-9).

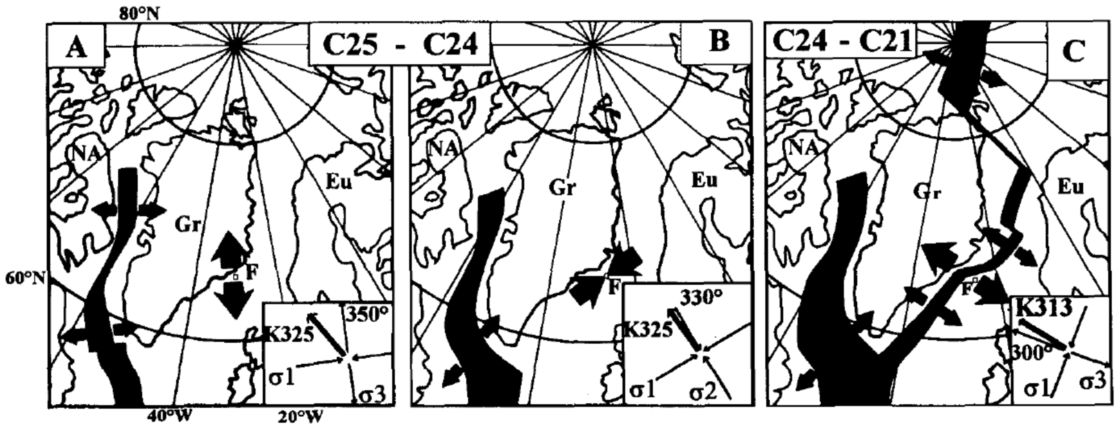

Fig. 6-7. Tectonic events in the Faroe Islands from Chrons 25 to 21 (after Geoffroy et al. 1994)

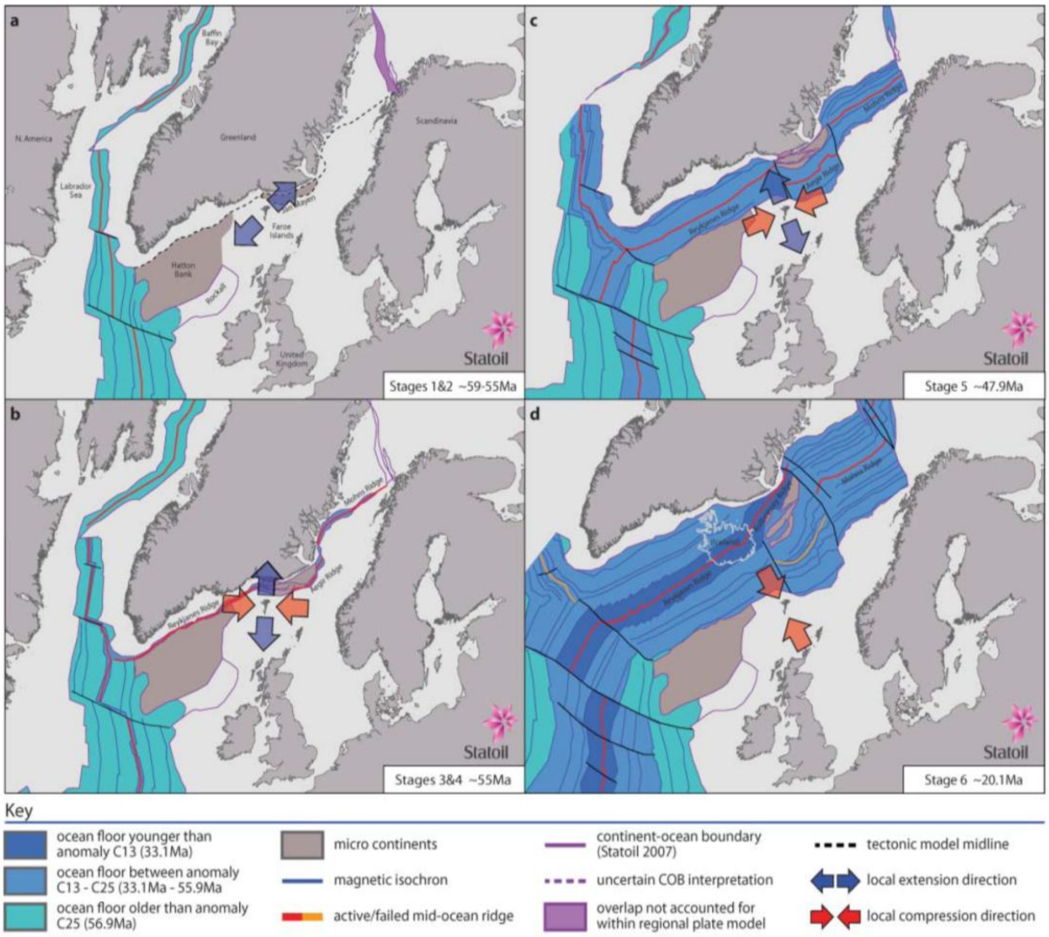

Fig. 6-8. North Atlantic plate reconstructions from the Paleocene to Miocene, focused on the Faroe Islands (after Walker et al. 2011)

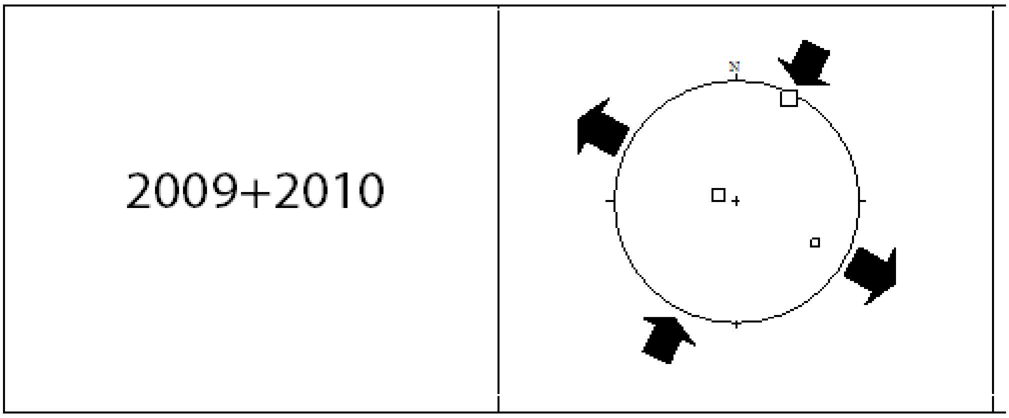

Fig. 6-9. Paleostress tensor from analysis of fault-slip data collected in 2009 and 2010 (cf. Chap. 3) considered to the state of stress during oblique rifting in Middle-Late Paleocene, up to the emplacement of the macrodykes complex at 55.8 Ma.

7. The Kangerlussuaq Fracture Zone

South of the Kangerlussuaq Fjord the coastal dyke swarm is concentrated in a number of zones arranged in a left-stepping en-echelon (the **Agtertia Shear Zone**). This was interpreted as evidence for right-lateral shear by Myers (1980). Klausen and Larsen (2002) suggested that the group of earliest (pre-breakup) dykes defines a regional pattern of intrusion shown with en-echelon geometry similar to the structure envisaged by Myers (1980), by striking NE-SW and slightly oblique to the eventual line of breakup. If this trend was controlled by the regional stress field, the sinistral en echelon pattern would indicate that a dextral transtensional stress field was active during this initial stage between 61-58Ma (Fig. 7-1) (Klausen and Larsen 2002).

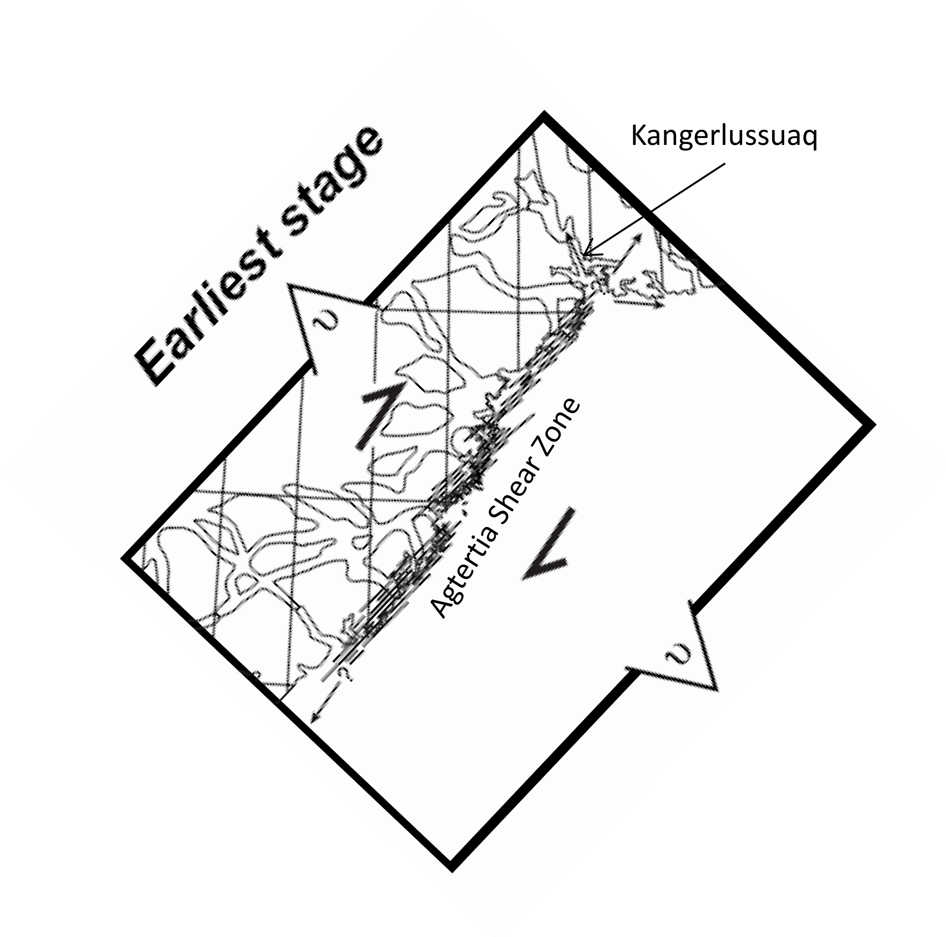

Fig. 7-1. Schematic models of left-stepping en echelon pattern of propagating earliest dikes (after Klausen and Larsen 2002)

North of Kangerlussuaq Fjord the macrodykes complex is arranged in right-stepping en-echelon geometry and interpreted as evidence for oblique rifting in Middle-Late Paleocene (Fig. 7-2) (cf. Chap. 3).

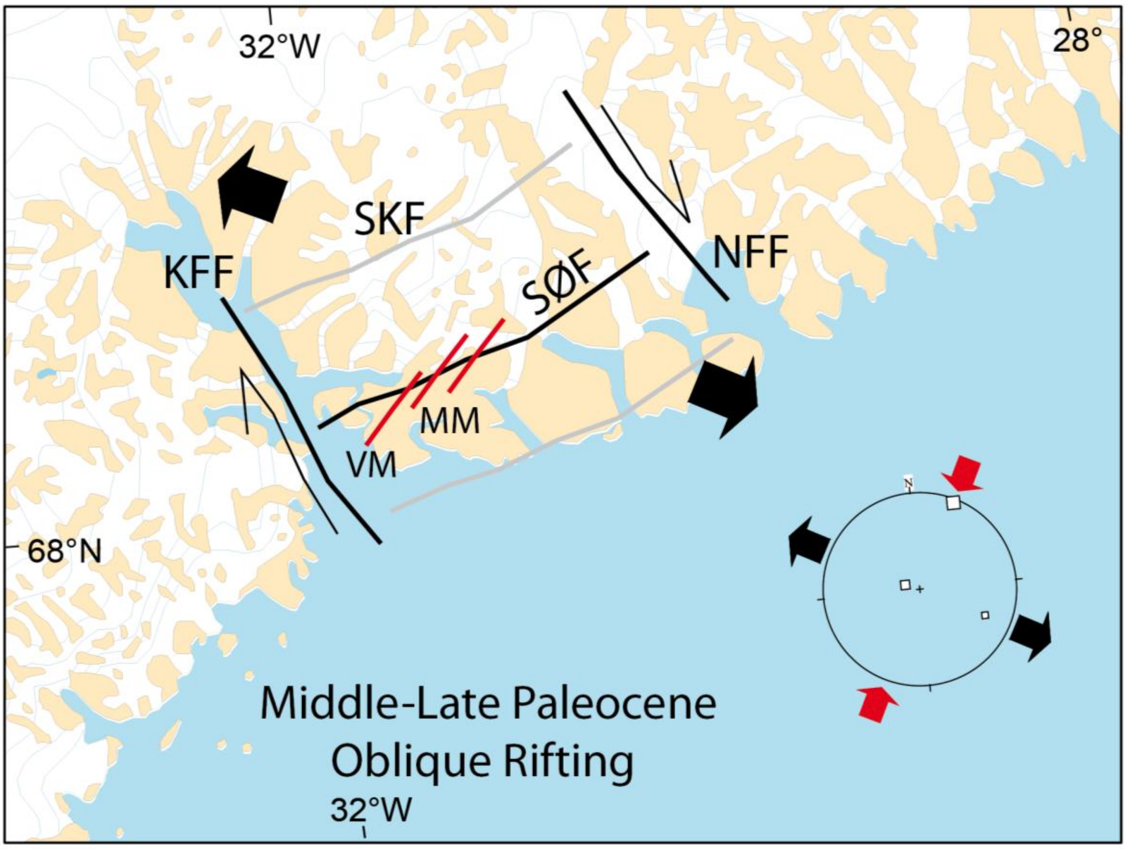

Fig. 7-2. En-echelon geometry of macrodykes and the relationship with the oblique rifting stage.

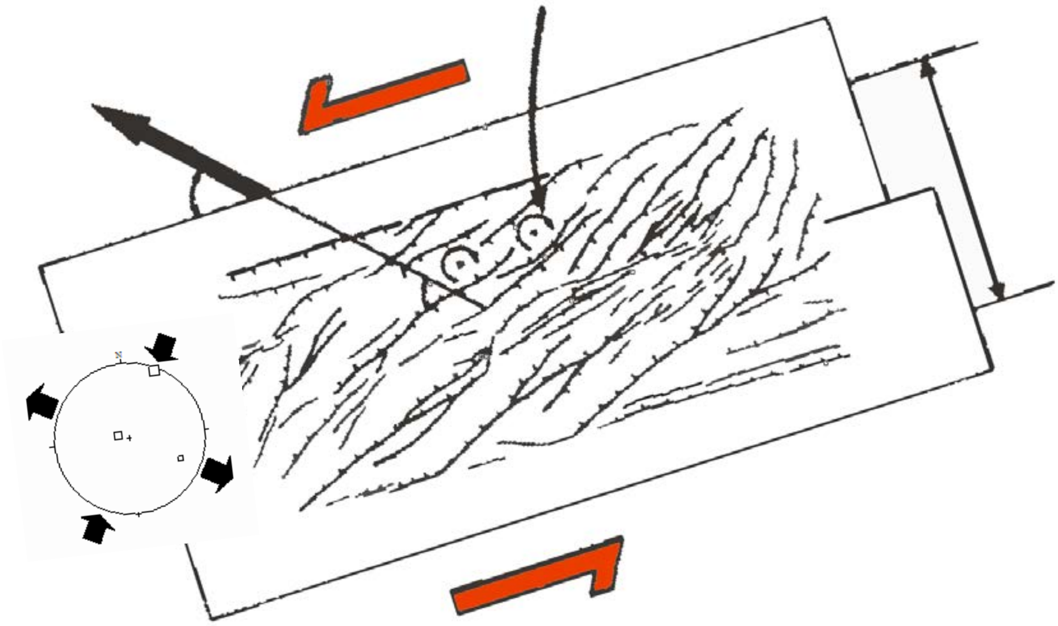

Fig. 7-3. Fault pattern distribution in oblique rifting experiment (Tron and Brun 1991) and the paleostress reconstructed from fault-slip data.

In the experiment performed by Tron and Brun (1991) the extensional features are oriented at an angle of 30º respect to the former discontinuity (Fig. 7-3). In the Kangerlussuaq area the former discontinuity is represented by Sortekap and the Sødalen faults. The latter seems to re-activate an old basement discontinuity as the Watkins Fjord Lineament. Furthermore, the trend of the macrodykes, the strike-slip movements on the faults and the reconstructed paleostress are coherent with an oblique extension applied along the rift faults as depicted in Figure (7-3).

Since the contemporaneous activity of the Nansen Fjord and Kangerlussuaq Fjord faults with right-lateral movements, is possible to hypothesize the presence of other small basins like the Kangerlussuaq one as in Figure (7-4) separated by transfer/transform faults.

Finally, the **Kangerlussuaq Fracture Zone** is an ENE-WSW trending lineament that most probably correspond to an inherited crustal discontinuity in the Archaean basement reactivated as normal fault during the rift phase in Late Cretaceous-Early Paleocene and as left-lateral fault in the oblique rifting stage leading to the initial breakup of the continental crust at 55,8 Ma (Fig. 7-4). After the breakup a strong subsidence caused the coastal flexure accommodating up to 6-7 km of Plateau Basalts probably in relation with a land-ward dipping normal fault enhanced by thermal subsidence and loading of seaward dipping reflectors.

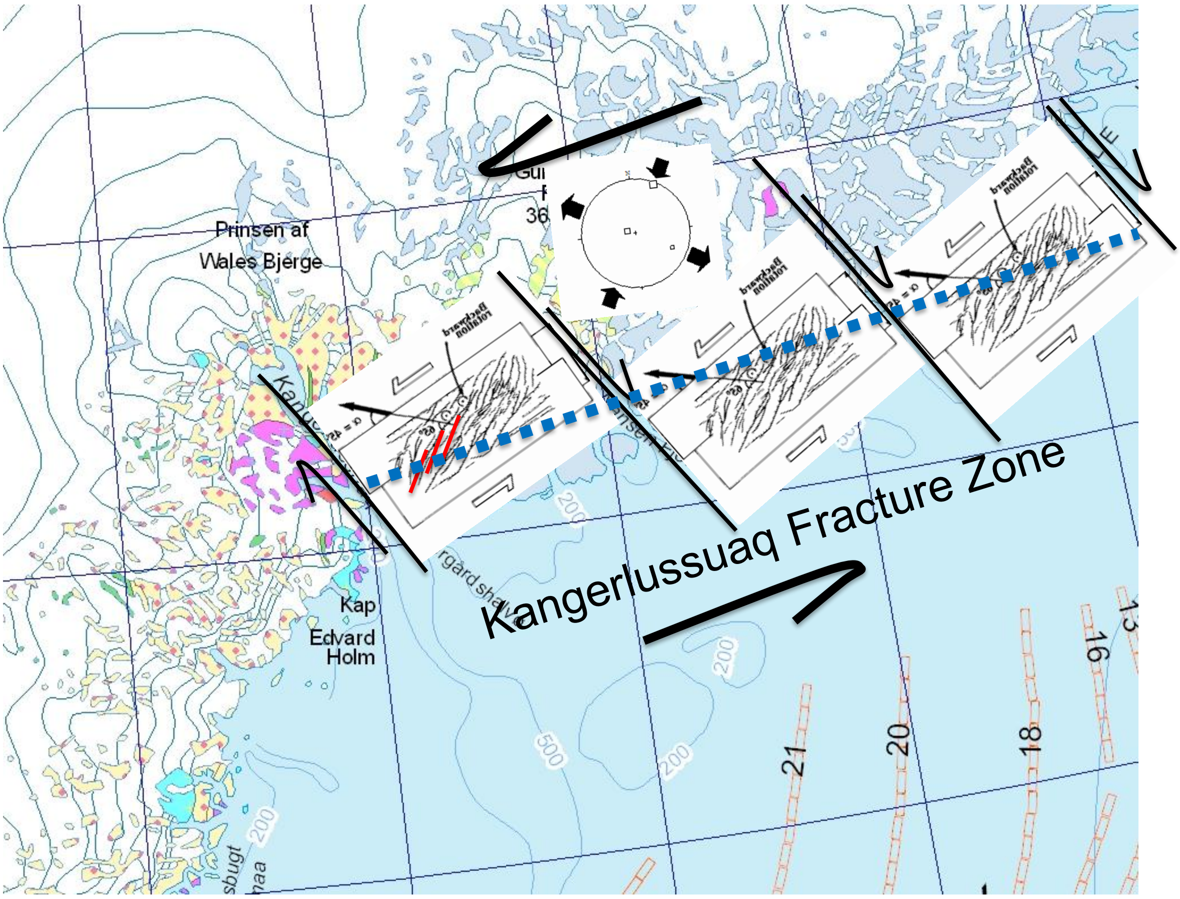

Fig. 7-4. The Kangerlussuaq Fracture Zone and associated transfer zones.

8. Implication for Plate Tectonics

Separation between Greenland and Europe follows a NW-SE vector orthogonal to magnetic anomalies recognizable in the ocean floor. The initial line of breakup (around 55 Ma) is assumed to be parallel to the first reconstructed spreading anomaly corresponding to Chron 24B. Moreover, the rift stage preceding the breakup is considered to be related to the same state of stress with NW-SE oriented extension.

The architecture of the Kangerlussuaq rift and the kinematics of faults clearly show that the rift-to-drift transition, leading to breakup and separation between Greenland and Europe, is not simply related to a continuous extensional regime as it is perceived.

South of Kangerlussuaq (66º to 68º N) the NE-SW trending right-lateral Agtertia Shear Zone (cf. Chap. 7) is probably active since Late Cretaceous-Paleocene and magmatically intruded by the early tholeiitic dykes between 61 to 58 Ma. The contemporaneous rift activity documented in the Kangerlussuaq Basin can be interpreted as related to a pull-apart evolution as depicted in Figure (8-1).

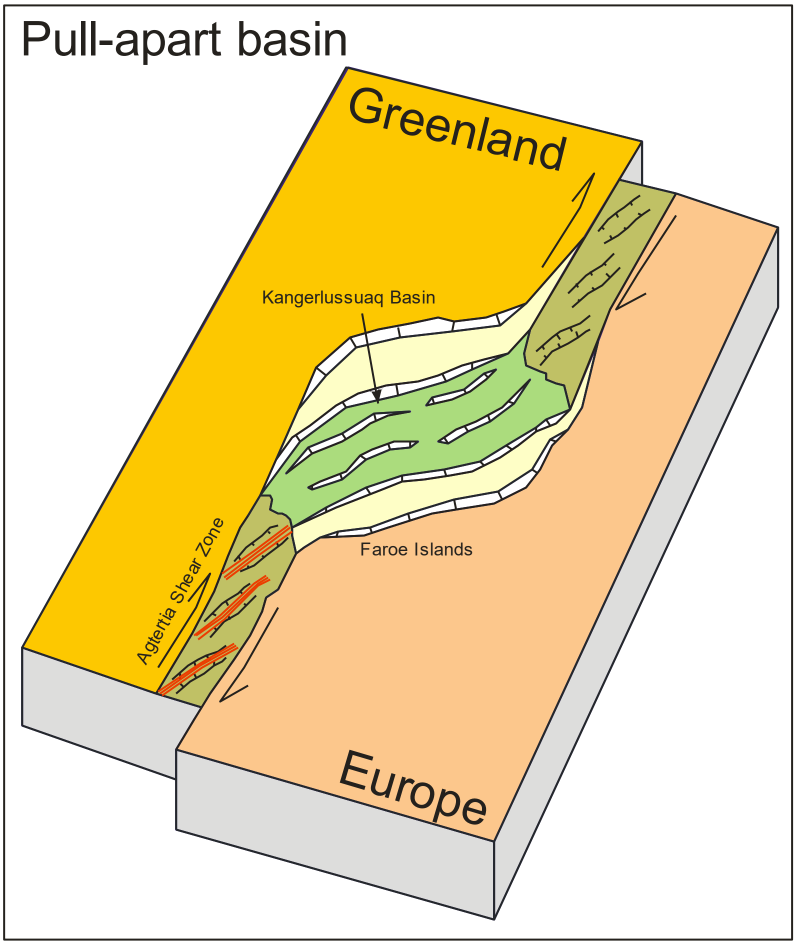

Fig. 8-1. Pull-apart model to explain the initial rift in the Kangerlussuaq basin.

The Late Cretaceous-Early Paleocene tectonics should be related to the opening of the Labrador Sea and the consequent NE-ward rotation of the Greenland plate.

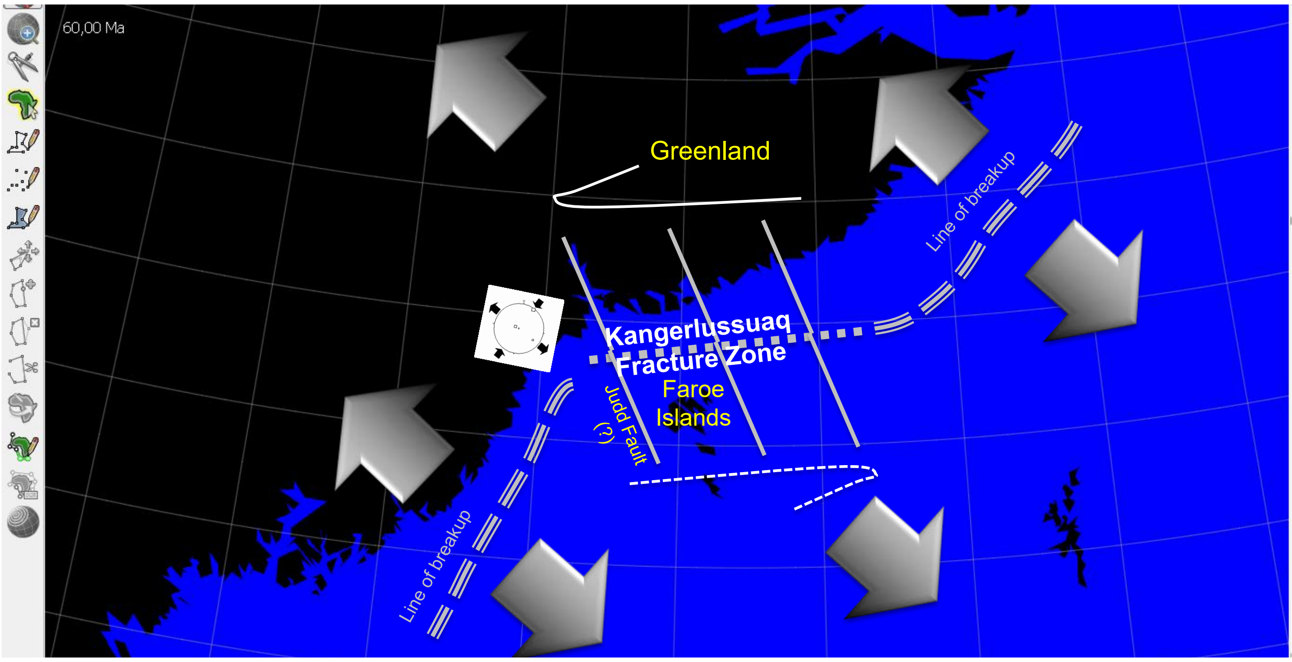

Fig. 8-2. Plate reconstruction at 60Ma from www.gplates.org.

After the initial pull-apart stage of rifting related to a right-lateral movement of the Greenland plates respect to the European one, separation between the two plates becomes NW-SE oriented (Fig. 8-2). The new configuration re-activates previous rift faults in a left-lateral oblique rifting with the development of the Kangerlussuaq Fracture Zone. In this light the NW-SE oriented transfer zones like the Kangerlussuaq Fjord Fault and Nansen Fjord Fault can be traced across the entire basin through the Faroes area with a straightforward correlation between the Judd Fault and the Kangerlussuaq Fjord Fault.

9. Conclusion

The present study, based on structural data collected along major faults in the Kangerlussuaq basin, shows how the complex tectono-magmatic and sedimentary evolution of this area is related to four tectonic stages:

1) The first documented faults activity (achieved from stratigraphic evidence eg. deepening of basin, erosion and major unconformities) is **Late Cretaceous-Early Paleocene**. This stage of rifting corresponds to a pull-apart formation along with NE-SW oriented rift faults and NW-SE transfer faults. The NE-SW oriented maximum horizontal stress derived from fault-slip data inversion together with the evidence of NNE-SSW right-lateral shear along the Agtertia Shear Zone are interpreted in relation with rotation and NE-ward motion of Greenland during the initial opening of the Labrador Sea;
2) During **Middle-Late Paleocene** re-activation of former rift faults with strike-slip component, together with the en-echelon geometry and magmatic segmentation of macrodykes intruded at 55.8 Ma, are interpreted as evidence of oblique rifting during NW-SE extension and the activation of the ENE-WSW Kagerlussuaq Fracture Zone;
3) The **Early Eocene** breakup around 55.4 Ma is associated with coastal flexure and thermal subsidence during the emplacement of a thick sequence of Plateau Basalts. This tectonic stage is associated with intrusion of a sheeted dyke complex parallel to the present-day coastline together with land-ward dipping normal faults that accommodate the NW-SE extension;
4) Post-breakup deformation is related to an E-W maximum horizontal stress. This strike-slip tectonic regime is interpreted as responsible for basin inversion and uplift of the area in **Late Eocene-Early Oligocene** in response to plate reorganization related to separation of the Jan Mayen micro-continent. Seismic data offshore East Greenland shows a prograding wedge of sediments bounded by prominent sequence boundaries. The sedimentary sequence seems to be related to the uplift of the area. This prograding wedge is commonly observed along much of the East Greenland coast is believed to be late Eocene to Oligocene in age.

Finally, the NW-SE trending Kangerlussuaq Fjord Fault can be considered as analogue of the Judd Fault in the Faroe-Shetland area.

10. Enclosures

10.1 Fault-slip data

10.2 Paleostress

10.3 Geological Map of the Kangerlussuaq Basin

10.4 Regional Cross-Sections

GEUS REPORT 2012/63. Pierpaolo Guarnieri, John R. Hopper, Morten S. Andersen. **Enclosure 1 - Fault-slip data**

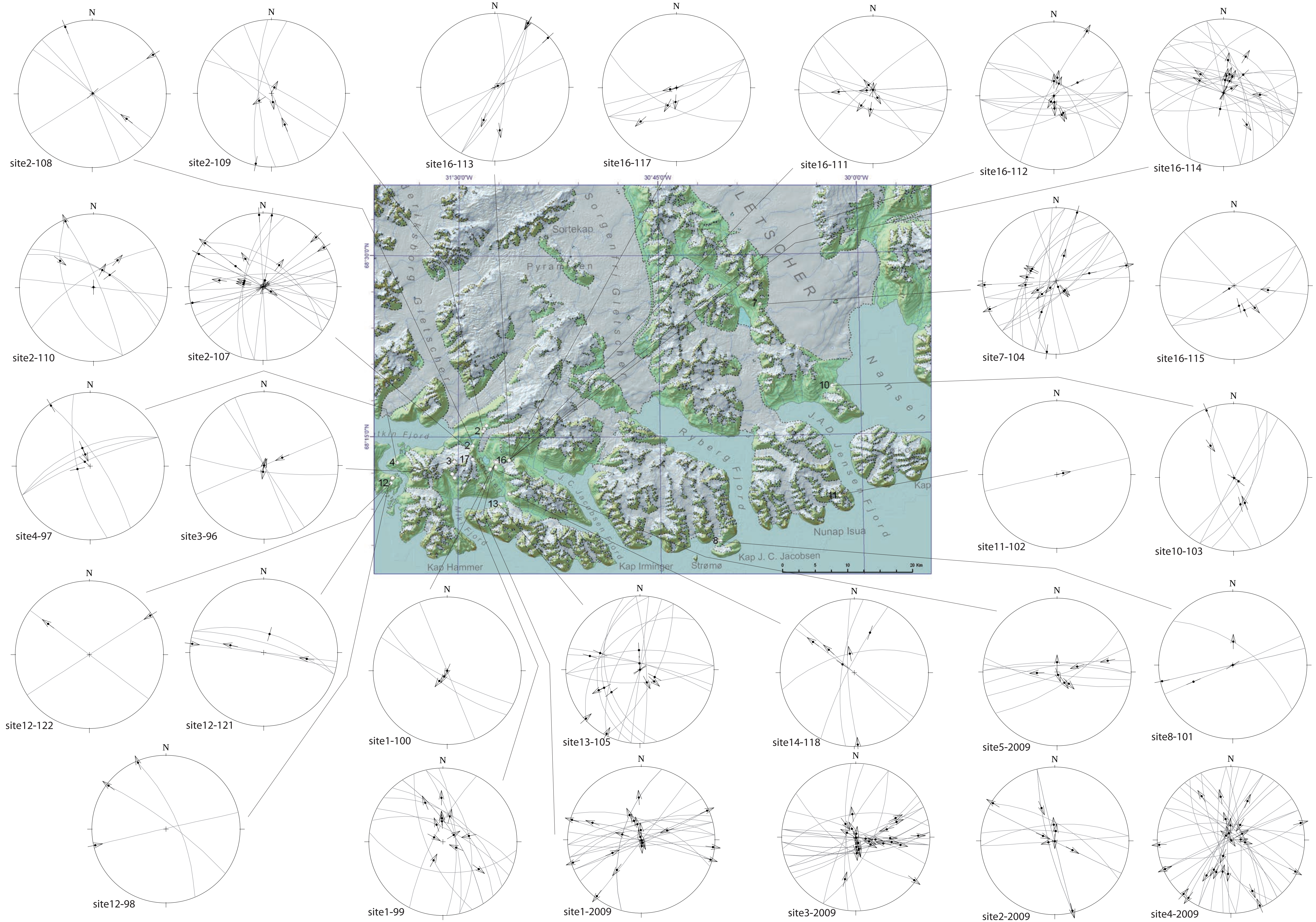

GEUS REPORT 2012/63 Pierpaolo Guarnieri, John R. Hopper, Morten S. Andersen. **Enclosure 2 - Paleostress**

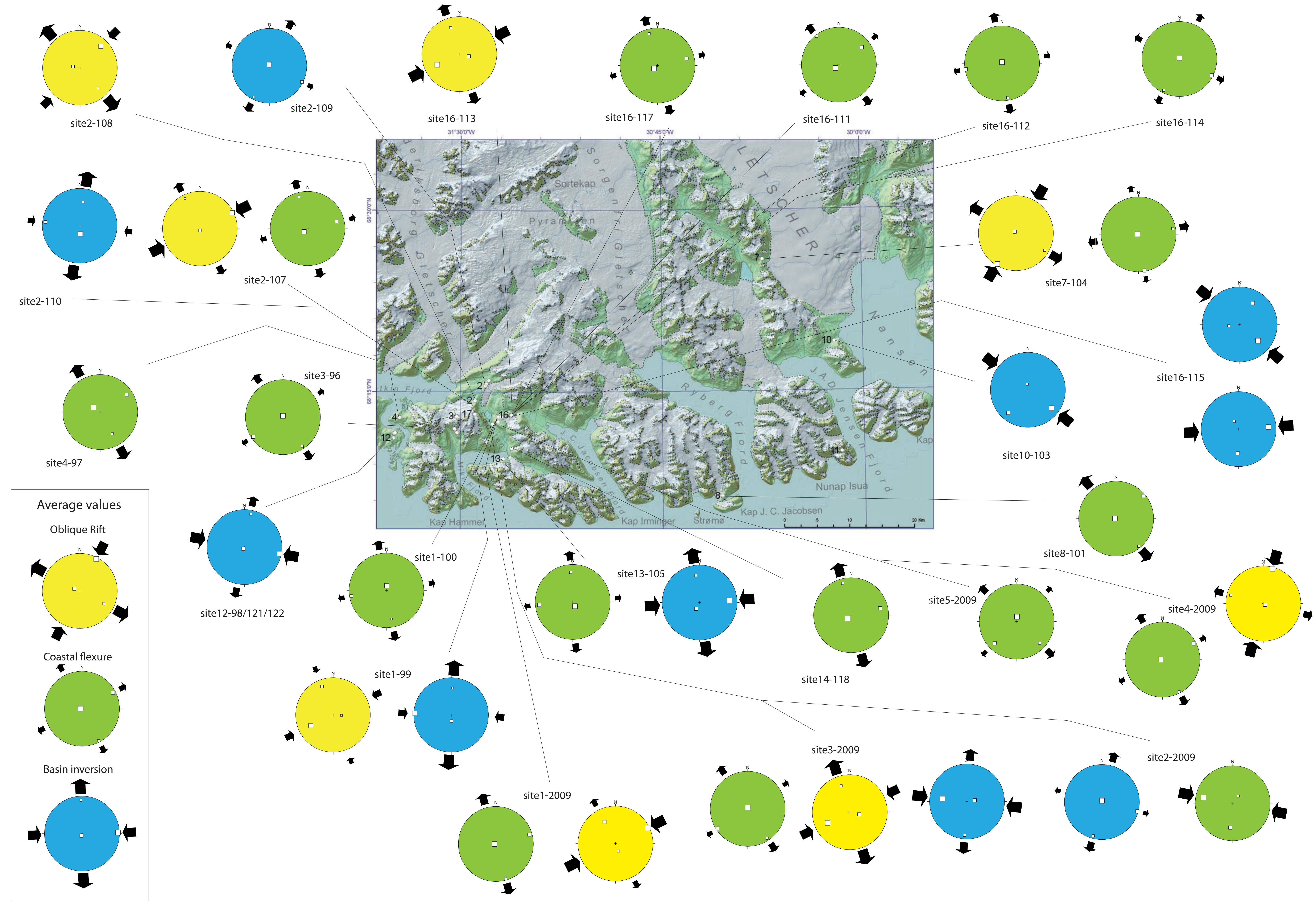

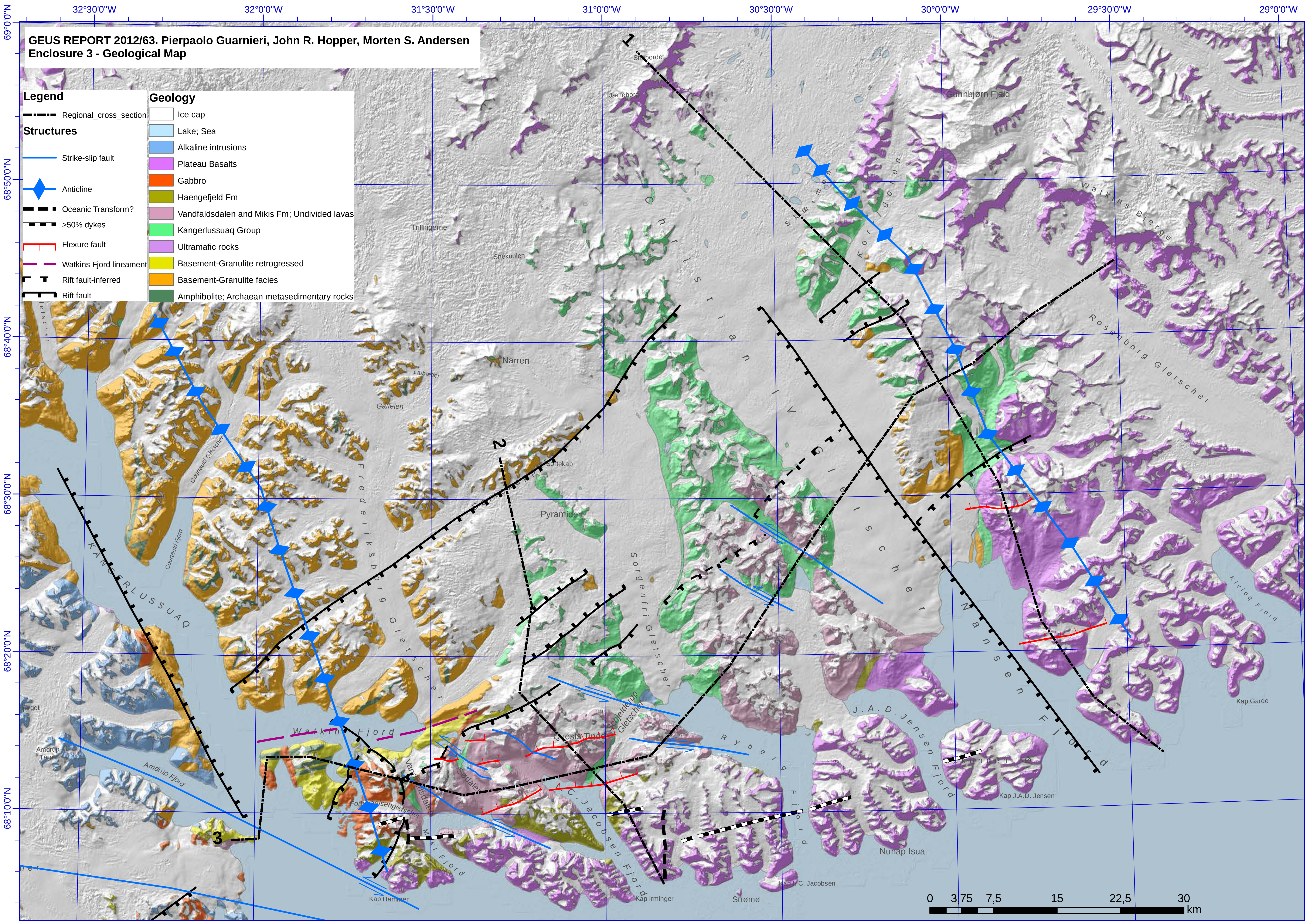

GEUS REPORT 2012/63. Pierpaolo Guarnieri, John R. Hopper, Morten S. Andersen
Enclosure 3 - Geological Map
Legend
Regional_cross_section
Structures
Strike-slip fault
Anticline
Oceanic Transform?
>50% dykes
Flexure fault
Watkins Fjord lineament
Rift fault-inferred
Rift fault
Geology
Ice cap
Lake; Sea
Alkaline intrusions
Plateau Basalts
Gabbro
Haengefjeld Fm
Vandfaldsdalen and Mikis Fm; Undivided lavas
Kangerlussuaq Group
Ultramafic rocks
Basement-Granulite retrogressed
Basement-Granulite facies
Amphibolite; Archaean metasedimentary rocks
32°30'0"W
32°0'0"W
31°30'0"W
31°0'0"W
30°30'0"W
30°0'0"W
29°30'0"W
29°0'0"W
69°0'0"N
68°50'0"N
68°40'0"N
68°30'0"N
68°20'0"N
68°10'0"N
1
2
3
Gunnbjørn Fjeld
Watkins Bjerge
Rosenborg Gletscher
Christian IV Gletscher
Frederiksborg Gletscher
Sorgenfri Gletscher
Nansen Fjord
KANGERLUSSUAQ
Courtauld Gletscher
Courtauld Fjord
Watkins Fjord
Amdrup Fjord
Ryberg Fjord
J.A.D. Jensen Fjord
C. Jacobsen Fjord
Miki Fjord
Kivioq Fjord
Narren
Pyramiden
Trillingerne
Snekuplen
Gabelen
Questa Tinde
Kap Garde
Kap J.A.D. Jensen
Nunap Isua
Kap Hammer
Kap Irminger
Strømø
Kap J.C. Jacobsen
0 3,75 7,5 15 22,5 30
km

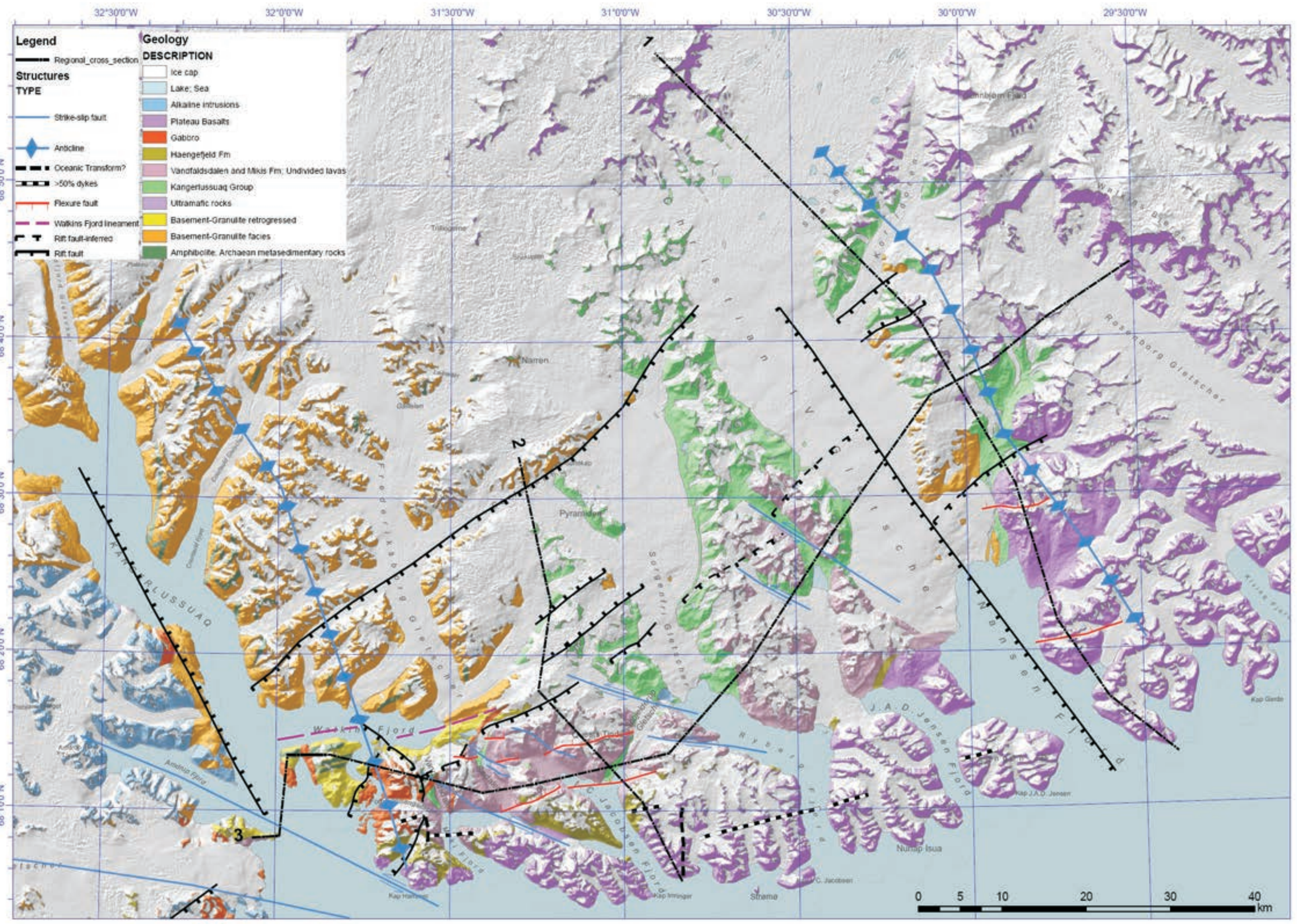
Legend
Regional_cross_section
Structures
TYPE
Strike-slip fault
Anticline
Oceanic Transform?
>50% dykes
Flexure fault
Watkins Fjord lineament
Rift fault-inferred
Rift fault
Geology
DESCRIPTION
Ice cap
Lake; Sea
Alkaline intrusions
Plateau Basalts
Gabbro
Haengefjeld Fm
Vandfaldsdalen and Mikis Fm: Undivided lavas
Kangerlussuaq Group
Ultramafic rocks
Basement-Granulite retrogressed
Basement-Granulite facies
Amphibolite: Archaean metasedimentary rocks
32°30'0"W
32°0'0"W
31°30'0"W
31°0'0"W
30°30'0"W
30°0'0"W
29°30'0"W
1
2
3
0 5 10 20 30 40 km

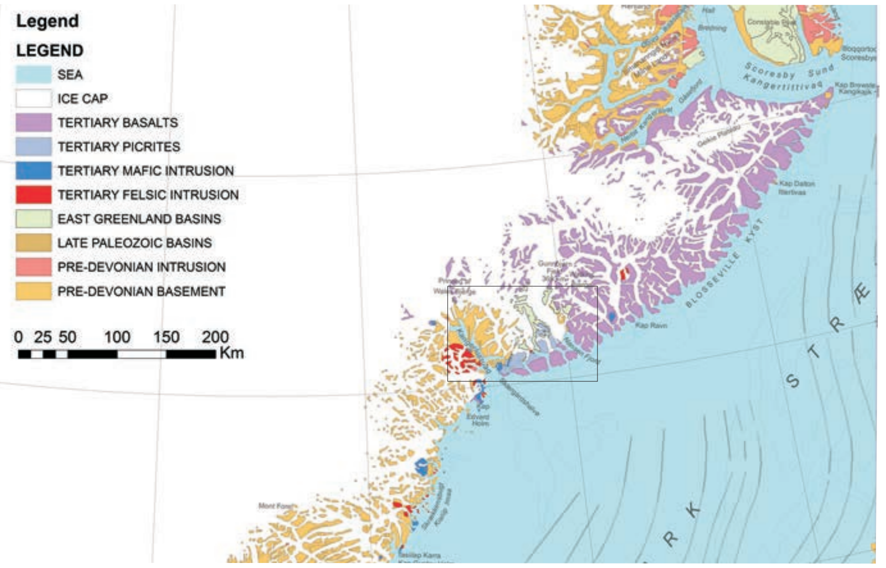
Legend
LEGEND
SEA
ICE CAP
TERTIARY BASALTS
TERTIARY PICRITES
TERTIARY MAFIC INTRUSION
TERTIARY FELSIC INTRUSION
EAST GREENLAND BASINS
LATE PALEOZOIC BASINS
PRE-DEVONIAN INTRUSION
PRE-DEVONIAN BASEMENT
0 25 50 100 150 200 Km

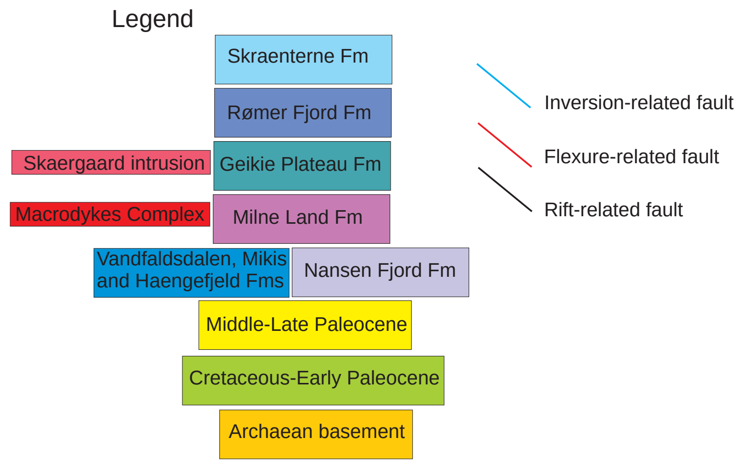
Legend
Skraenterne Fm
Rømer Fjord Fm
Skaergaard intrusion
Geikie Plateau Fm
Macrodykes Complex
Milne Land Fm
Vandfaldsdalen, Mikis and Haengefjeld Fms
Nansen Fjord Fm
Middle-Late Paleocene
Cretaceous-Early Paleocene
Archaean basement
Inversion-related fault
Flexure-related fault
Rift-related fault

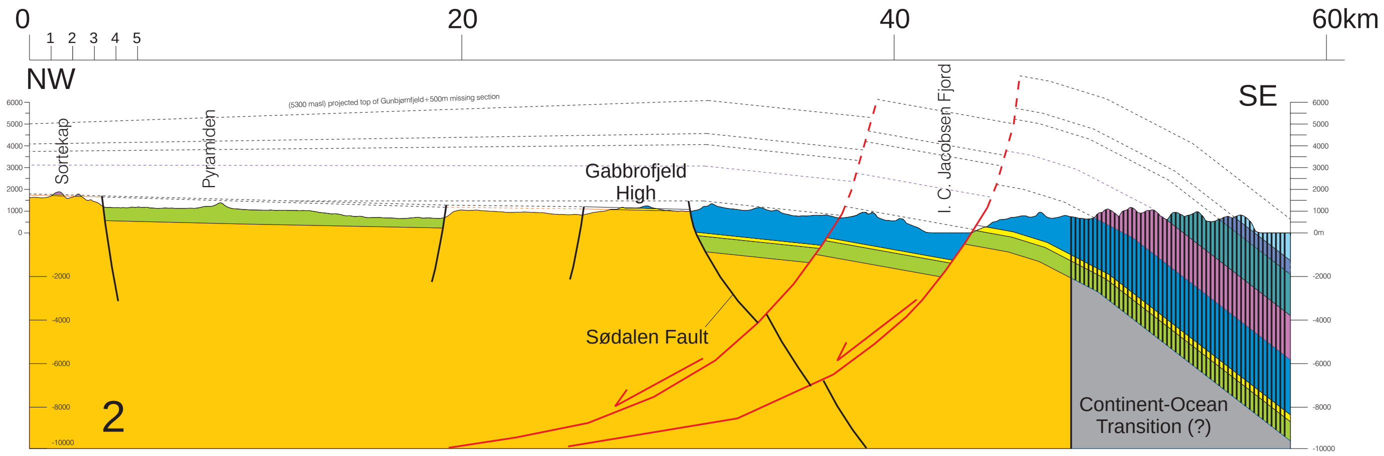
0 20 40 60km
NW
SE
Sortekap
Pyramiden
Gabbrofjeld High
I. C. Jacobsen Fjord
Sødalen Fault
Continent-Ocean Transition (?)
2

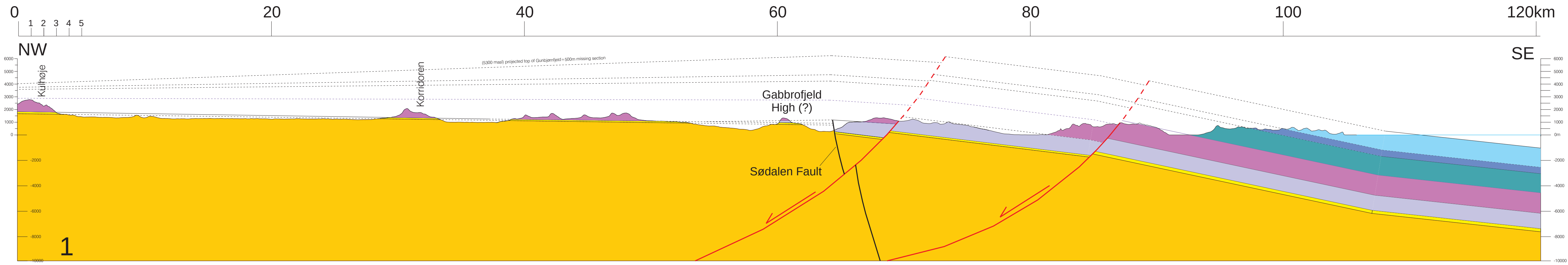
0 20 40 60 80 100 120km
NW
SE
Kulhøje
Korridoren
Gabbrofjeld High (?)
Sødalen Fault
1

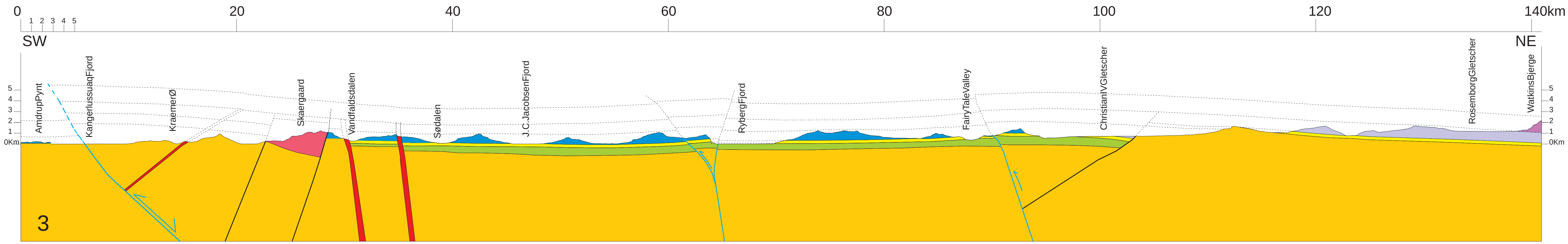
0 20 40 60 80 100 120 140km
SW
NE
AmdrupPynt
KangerlussuaqFjord
KraemerØ
Skaergaard
Vandfaldsdalen
Sødalen
J.C.JacobsenFjord
RybergFjord
FairyTaleValley
ChristianIVGletscher
RosemborgGletscher
WatkinsBjerge
0Km
3

11. Appendix 1 Structural data

Quality: Consistency of the measurement of the direction of slip along the fault. For exam-ple, some faults can be normal or reverse, but kinematic indicators along the fault planes do not allow for reliable estimation of the direction of movement. The following definitions are used: * - the type of the fault is not known; P – probable; S – supposedly; C – cer-tainly.
Kinematics: Interpreted type of movement along the fault. The following definitions are used: N – normal fault; I – reverse fault; D – dextral fault; S – sinistral fault; ? – unknown.
Dip direction: Azimuth of the fault-dip.
Dip angle: Dip of the fault.
Pitch: Angle between the slickenlines on the fault plane and the intersection-line be-tween the fault plane and the horizontal plane.

SITE N.	QUALITY	KINEMATICS	DIP DIRECTION	DIP ANGLE	PITCH
SITE1-99	P	I	297	75	90
	C	S	37	50	40
	P	I	77	50	90
	P	I	87	70	80
	C	S	187	45	40
	C	S	77	70	30
	C	S	47	55	70
	C	N	17	60	80
	C	S	57	70	60
	C	N	27	70	70
	P	I	247	65	70
	C	N	57	70	90
	C	N	57	70	60
SITE1-100	C	N	217	70	90
	*	?	68	90	90
	C	N	207	80	90
SITE2-107	*	?	37	90	40
	*	?	27	90	1
	*	?	37	90	90
	*	?	17	80	90
	C	S	27	60	50
	C	S	357	70	30
	*	?	27	90	90
	C	N	287	60	90
	C	N	277	60	90
	C	N	27	90	90

	*	?	147	90	90
	*	?	347	90	1
	*	?	27	90	1
	C	N	37	50	90
	C	S	12	90	60
	*	?	347	90	1
	*	?	347	90	90
	*	?	97	90	1
	C	S	37	90	1
	C	N	357	90	90
	C	N	167	80	80
	C	D	147	90	1
	C	N	337	90	90
	C	D	137	90	1
	*	?	87	90	1
SITE2-108	C	D	147	89	1
	C	S	37	89	30
	*	?	47	89	90
	*	?	68	89	1
SITE2-109	*	?	282	70	1
	C	N	267	70	80
	C	N	27	80	90
	C	N	217	80	80
	C	S	68	89	40
SITE2-110	*	?	7	89	90
	C	S	247	50	40
	C	N	27	60	90
	*	?	32	60	80
	C	S	67	80	1
	C	D	327	70	40
SITE3-096	P	S	337	90	60
	C	N	187	80	90
	C	N	247	80	90
	C	N	237	80	90
SITE4-097	*	?	337	80	85
	*	?	337	60	90
	*	?	257	70	90
	*	?	57	75	1
	C	I	337	70	90
SITE4-097 rotated	*	?	157	70	89
	*	?	336	90	87
	*	?	264	81	61
	*	?	50	79	32
	C	N	157	80	86

SITE7-104	C	N	137	70	90
	C	N	142	70	90
	C	N	307	50	80
	C	N	307	50	70
	C	N	317	80	60
	C	N	297	50	90
	C	S	107	90	50
	C	D	137	90	60
	*	?	72	90	80
	C	S	357	90	1
	C	S	167	70	1
	*	?	107	90	1
	*	?	277	65	1
	C	N	267	80	80
	C	N	277	45	80
	*	?	347	90	40
	*	?	287	80	40
	C	S	337	90	1
SITE8-101	C	D	147	89	1
	C	S	37	89	30
	*	?	47	89	90
	*	?	68	89	1
SITE10-103	C	I	107	60	60
	*	?	117	60	60
	C	S	257	60	40
	*	?	68	89	1
	*	?	117	89	90
	*	?	127	80	90
S. 11-102	C	N	347	90	80
SITE12-98/121/122	C	D	347	89	1
	C	S	67	70	1
	C	S	37	80	1
	C	D	7	90	1
	C	S	12	90	40
	C	S	17	75	30
	*	?	17	60	90
	C	D	147	90	1
	C	S	37	90	20
SITE13-105	P	S	12	80	20
	P	S	17	80	30
	*	?	357	60	90
	*	?	107	90	90
	*	?	117	65	90

	*	?	97	90	90
	*	?	257	40	70
	C	N	277	30	60
	C	N	87	80	70
	C	N	177	70	70
	*	?	357	80	90
	*	?	267	35	70
	C	D	317	35	1
	C	D	297	55	1
SITE14-118	C	N	347	60	90
	*	?	277	70	80
	C	S	37	90	20
	C	D	267	80	1
	*	?	297	80	30
	C	S	42	90	40
SITE16-111	C	N	317	80	90
	C	S	357	90	80
	C	N	187	60	90
	C	N	197	80	80
	C	S	357	90	40
	C	N	217	60	90
	C	N	47	90	90
	*	?	17	90	90
SITE16-112	C	N	152	60	90
	C	N	177	80	90
	C	N	178	70	90
	C	N	179	60	80
	*	?	357	90	90
	C	N	207	80	90
	C	N	22	70	90
	C	S	27	70	80
	C	S	57	70	70
	*	?	337	85	50
	*	?	297	80	1
SITE16-113	*	?	137	90	1
	C	N	337	90	85
	C	D	117	80	40
	C	D	92	75	30
	C	D	117	90	1
	C	D	117	70	1
SITE16-114	*	?	27	90	90
	C	N	27	70	90
	C	D	167	70	40
	C	N	37	30	85

	*	?	17	90	90
	*	?	19	90	90
	C	N	17	80	80
	C	N	297	50	90
	C	S	17	70	50
	*	?	192	65	90
	*	?	42	90	90
	C	D	77	60	40
	C	N	17	60	90
	C	N	342	70	70
	*	?	47	50	90
	*	?	77	90	90
	C	N	347	65	80
	C	S	67	60	50
	C	N	7	70	90
SITE16-115	C	N	47	90	80
	*	?	147	90	81
	*	?	157	50	90
	*	?	147	60	80
	C	S	187	90	40
SITE16-117	*	?	337	90	90
	C	N	207	60	90
	C	D	157	50	30
	C	S	347	90	80
	C	N	157	70	80

12. References

Acocella, V., Faccenna, C., Funiciello, R. & Rossetti, F. 1999. Sand-box modelling of basement-controlled transfer zones in extensional domains. Terra Nova, 11, 149–156.

Bird, D.K., Rosing, M.T., Manning, C.E. & Rose, N.M. 1985: Geologic fi eld studies of the Miki Fjord area, East Greenland. Bulletin of the Geological Society of Denmark 34, 219–236.

Blichert-Toft, J., Lesher, C.E. & Rosing, M.T. 1992: Selectively contaminated magmas of the Tertiary East Greenland macrodike complex. Contributions to Mineralogy and Petrology 110, 154–172.

Booth, J., Swiecicki, T. & Wilcockson, P. 1993. The tectono-stratigraphy of the Solan Basin, West of Shetland. In: Parker, J.R. (ed.) Petroleum Geology of Northwest Europe: Proceedings of the 4th Conference. Geological Society, London, 987–998.

Brekke, H. 2000. The tectonic evolution of the Norwegian Sea continental margin, with emphasis on the Vøring and Møre basins. In: Nøttvedt, A. (ed.) Dynamics of the Norwegian Margin. Geological Society, London, Special Publications, 167, 327–378.

Brooks, C.K. 1979: Geomorphological observations at Kangerdlugssuaq, East Greenland. Meddelelser om Grønland, Geoscience 1, 1–21.

Brooks, C.K. 1985a: Vertical crustal movements in the Tertiary of central East Greenland: a continental margin at a hot spot. Zeitschrift für Geomorphologie Supplement 54, 101–117.

Brooks, C.K. 2011: The East Greenland rifted volcanic margin. Geol. Surv. Den. Green. Bull. 24, 96 pp.

Corti G. 2008: Control of rift obliquity on the evolution and segmentation of the main Ethiopian rift. Nature Geoscience 1, 258-262.

Cox, K.G. 1993: Continental magmatic underplating. Philosophical Transactions of the Royal Society (London) 342, 155–166.

Coward, M.P. 1990. The Precambrian, Caledonian and Variscan framework to NW Europe. In: Hardman, R.F.P. & Brooks, J. (eds) Tectonic Events Responsible for Britain's Oil and Gas Reserves. Geological Society, London, Special Publications, 55, 1–34.

Coward, M. P., Dewey, J. F., Hempton, M., and Holroyd, J., 2003, Tectonic Evolution, in Evans, D., Graham, C., Armour, A. R., and Bathurst, J., eds., The Millenium Atlas: petroleum geology of the central and northern North Sea, Geological Society of London.

Davies, R., Cloke, I., Cartwright, J., Robinson, A. & Ferrero, C. 2004. Postbreakup compression of a passive margin and its impact on hydrocarbon prospectivity: An example from the Tertiary of the Faeroe-Shetland Basin, United Kingdom. AAPG Bulletin, 88, 1–20.

Dean, K., McLachlan, K. & Chambers, A. 1999. Rifting and the development of the Faeroe–Shetland Basin. In: Fleet, A.J. & Boldy, S.A.R. (eds) Petroleum Geology of Northwest Europe: Proceedings of the 5th Conference. Geological Society, London, 533–544.

Dewey, J. F., and Strachan, R. A., 2003, Changing Silurian-Devonian relative plate motion in the Caledonides: sinistral transpression to sinistral transtension: Journal of the Geological Society, v. 160, p. 219-229.

Dore´, A.G., Lundin, E.R., Fichler, C. & Olesen, O. 1997. Patterns of basement structure and reactivation along the NE Atlantic margin. Journal of the Geological Society, London, 154, 85–92.

Dore´, A.G., Lundin, E.R., Jensen, L.N., Birkeland, Ø., Eliassen, P.E. & Fichler, C. 1999. Principal tectonic events in the evolution of the northwest European Atlantic margin. In: Fleet, A.J. & Boldy, S.A.R. (eds) Petroleum Geology of Northwest Europe: Proceedings of the 5th Conference. Geological Society, London, 41–61.

Dore´, A.G., Lundin, E.R., Kusznir, N.J. & Pascal, C. 2008. Potential mechanisms for the genesis of Cenozoic domal structures on the NE Atlantic margin: pros, cons and some new ideas. In: Johnson, H., Dore´ , A.G., Gatliff, R.W., Holdsworth, R.E., Lundin, E.R. & Ritchie, J.D. (eds) The Nature and Origin of Compression in Passive Margins. Geological Society, London, Special Publications, 306, 1–26.

Duindam, P. & van Hoorn, B. 1987. Structural evolution of the West Shetland continental margin. In: Brooks, J. & Glennie, K. (eds) Petroleum Geology of North West Europe. Graham and Trotman, London, 765–773.

Eldholm, O., & Grue, K. 1994: North Atlantic volcanic margins: dimensions and production rates. Journal of Geophysical Research 99, 2955–2968.

Ellis, D., Jolley, D.W., Passey, S.R. & Bell, B.R. 2009. Transfer zones: The application of new geological information from the Faroe Islands applied to the offshore exploration of intra basalt and sub-basalt strata. In: Ziska, H. & Varming, T. (eds) Faroe Islands Exploration Conference: Proceedings of the 2nd Conference. Annales Societatis Scientarum Faroensis Supplement 50, 205–226.

Escher J. C. and Pulvertaft T. C. R. 1995 Geological Map of Greenland 1:2500000. Copenhagen. Geological Survey of Greenland

Faulds, J.E. & Varga, R.J. 1998. The role of accommodation zones and transfer zones in the regional segmentation of extended terranes. In: Faulds, J.E. & Stewart, J.H. (eds) Accommodation Zones and Transfer Zones: The Regional Segmentation of the Basin and Range Province. Geological Society of America, Special Papers, 323, 1–45.

Færseth, R.B. & Lien, T. 2002. Cretaceous evolution in the Norwegian Sea: a period characterized by tectonic quiescence. Marine and Petroleum Geology, 19, 1005–1027

Gaina C., Gernigon L. and Ball P. 2009. Paleocene Recent plate boundaries in the NE Atlantic and the formation of the Jan Mayen microcontinent. Journal of the Geological Society. 166, 601-616.

Gibbs, A.D. 1984. Structural evolution of extensional basin margins. Journal of the Geological Society, London, 141, 609–620.

Gill, R.C.O., Nielsen, T.F.D., Brooks, C.K. & Ingram, G.A. 1988: Tertiary volcanism in the Kangerdlugssuaq region, East Greenland: trace element geochemistry of the lower lavas and tholeiitic dyke swarms. In: Morton, A.C. & Parson, L.M. (eds): Early Tertiary Volcanism and the Opening of the NE Atlantic. Geological Society Special Publications (London) 39, 161–179.

Geist, D. & White, C. 1994: Assimilation and fractionation in adjacent parts of the same magma chamber: Vandfaldsdalen macrodike, East Greenland. Contributions to Mineralogy and Petrology 116, 92–107.

Geoffroy, L. 2005. Volcanic passive margins. Comptes Rendus de l'Académie des Sciences, Série II Fascicule A: Sciences de la Terre et ses Planétes, 337, 1395–1408.

Geoffroy, L., Bergerat, F. & Angelier, J. 1994. Tectonic evolution of the Greenland–Scotland ridge during the Palaeogene: new constraints. Geology, 22, 653–656.

Gleadow, A.J.W. & Brooks, C.K.1979: Fission track dating, thermal histories and tectonics of igneous intrusions in East Greenland. Contributions to Mineralogy and Petrology 71, 45–60.

Guarnieri, P. 2011: Analysis of Palaeogene strike-slip tectonics along the southern East Greenland margin (Sødalen area). Geological Survey of Denmark and Greenland Bulletin 23, 65–68.

Guarnieri P. Vosgerau H. J., Hansen R. W., Larsen M., Dennehy C. J., Booth Y, Knudsen C. 2009. 3D-modeling of intra-basaltic, shallow marine sandstones in East Greenland, analogue for the volcanic play of the Faroes and UK (Rosebank). Abstract Volume, The 3rd Faroe Islands Exploration Conference, Tórshavn 2009

Hanghøj K, Storey M. and Stecher O. 2003. An Isotope and Trace Element Study of the East Greenland Tertiary Dyke Swarm: Constraints on Temporal and Spatial Evolution during Continental Rifting. Journal of Petrology. 44/11, 2081-2112.

Hansen, K. 1992: Post-orogenic tectonic and thermal history of a rifted continental margin: the Scoresby Sund area, east Greenland. Tectonophysics 216, 309–326.

Hansen, K. 1996: Th ermotectonic evolution of a rifted continental margin: fi ssion track evidence from the Kangerlussuaq area, SE Greenland. Terra Nova 8, 458–469.

Hansen, K. 2000: Tracking thermal history in East Greenland: an overview. Global and Planetary Change 24, 303–309.

Hansen, K. & Brooks, C.K. 2002: Th e evolution of the East Greenland margin as revealed from fi ssion track studies. Tectonophysics 349, 93–111.

Hansen, H. & Nielsen, T.F.D. 1999: Crustal contamination in Palaeogene East Greenland flood basalts: plumbing system evolution during continental rifting. Chemical Geology 157, 89–118.

Hansen, K. & Reiners, P.W. 2006: Low temperature thermochronology of the southern East Greenland continental margin: evidence from apatite (U-Th)/He and fi ssion track analysis and implications for intermethod calibration. Lithos 92, 117–136

Harding, T.P. 1990. Identification of wrench faults using subsurface structural data—criteria and pitfalls. AAPG Bulletin, 74, 1590–1609

Herries, R., Poddubiuk, R. & Wilcockson, P. 1999. Solan, Strathmore and the back basin play, West of Shetland. In: Fleet, A.J. & Boldy, S.A.R. (eds) Petroleum Geology of Northwest Europe: Proceedings of the 5th Conference. Geological Society, London, 693–712.

Hirschmann, M.M., Renne, P.R. & McBirney, A.R. 1997: 40Ar/39Ar dating of the Skaergaard intrusion. Earth and Planetary Science Letters 146, 645–658.

Hitchen, K. & Ritchie, J.D. 1987. Geological review of the West Shetland area. In: Brooks, J. & Glennie, K. (eds) Petroleum Geology of North West Europe. Graham and Trotman, London, 737–749.

Holbrook, W. S., H. C. Larsen, J. Korenaga, T. Dahl-Jensen, I. D. Reid, P. B. Kelemen, J. R. Hopper, G. M. Kent, D. Lizarralde, S. Bernstein, and R. S. Detrick, 2001, Mantle Thermal Structure and Active Upwelling during Continental Breakup in the North Atlantic, Earth and Planet. Sci. Lett., 190, 251-266.

Hopper, J. R., D. Lizarralde and H. C. Larsen, 1998, Seismic Investigations Offshore South-East Greenland, Geology of Greenland Survey Bulletin, 145-151.

Jolley, D.W., Whitham, A.G., 2004. A stratigraphical and palaeoenvironmental analysis of the sub-basaltic Palaeogene sediments of East Greenland. Petroleum Geoscience 10, 53–60.

Karson, J.A. & Brooks, C.K. 1999: Structural and magmatic segmentation of the Tertiary East Greenland volcanic rifted margin. In: MacNiocail, C. & Ryan, P.D. (eds): Continental tectonics. Geological Society Special Publications (London) 164, 313–338.

Klausen, M.B. & Larsen, H.C. 2002: East Greenland coast-parallel dike swarm and its role in continental break-up. In: Menzies, M.A. et al. (eds): Volcanic rifted margins. Geological Society of America Special Paper 362, 133–158.

Korenaga, J., W.S. Holbrook, G.M. Kent, P.B. Kelemen, R.S. Detrick, H.C. Larsen, J.R. Hopper. and T. Dahl-Jensen, 2000, Crustal Structure of the Southeast Greenland Margin from Joint Refraction and Reflection Seismic Tomography, J. Geophys. Res., 105, 21591- 21615.

Larsen, H.C. 1978: Off shore continuation of East Greenland dike swarm and North Atlantic formation. Nature 274, 220–223.

Larsen, H.C., 1985, Project NAD - East Greenland: An integrated aeromagnetic and marine geophysical project off the east coast of Greenland, GEUS Report file no. 27546.

Larsen, H. C. 1990. The East Greenland Shelf. In Grantz A., Johnson L. and Sweeney J. F. Eds., The Arctic Ocean region: Boulder, Colorado, Geological Society of America, The Geology of North America, Vol. L, 185-210.

Larsen, H.C. & Duncan, R.A. 1996: Introduction: Leg 163 background and objectives. In: Duncan, R.A. et al. (eds): Proceedings of the Ocean Drilling Program, Initial Reports 163, 1–5.

Larsen, H.C., R.A. Duncan, J.F. Allan, C.K. Brooks, et al., 1999, Proceedings of the Ocean Drilling Pro-gram, Scientific Results, Leg 163, Ocean Drilling Program, College Station, Tex.

Larsen, H.C., and S. Jakobsdottir, 1988, Distribution, crustal properties and significance of seawards-dipping sub-basement reflectors off E Greenland, in Early Tertiary Volcanism and the Opening of the NE Atlantic, Geological Society Special Publ. No. 39, edited by A.C. Morton and L.M. Parson, pp. 95-114.

Larsen, H. C. & Saunders, A. D. 1998. Tectonism and volcanism at the SE Greenland rifted margin: a record of plume impact and later continental rupture. In: Larsen, H. C., Saunders, A. D. & Wise, S. W., Jr (eds) Proceedings of the Ocean Drilling Program, Scientific Results 152. College Station, TX: Ocean Drilling Program, 503-533.

Larsen, L. M., Watt, W. S. & Watt, M. 1989. Geology and petrology of the Lower Tertiary plateau basalts of the Scoresby Sund region, East Greenland. Geological Survey of Greenland Bulletin. 157, 1-164.

Larsen, L.M., R. Waagstein, A.K. Pedersen, and M. Storey, 1999, Trans-Atlantic correlation of the Paleogene volcanic successions in the Faeroe Islands and East Greenland, J. Geol. Soc. London, 156, 1081-1095.

Larsen, M., Hamberg, L., Olaussen, S., Nørgaard-Pedersen, N. & Stemmerik, L. 1999: Basin evolution in sourthern East Greenland: an outcrop analog for the Cretaceous–Paleogene basins on the North Atlantic volcanic margin. American Association of Petroleum Geologists, Bulletin 83, 1236–1261.

Larsen, M., Nøhr-Hansen, H., Whitham, A. G. & Kelly, S. R. A. 2005: Stratigraphy of the pre-basaltic sedimentary succession of the Kangerlussuaq Basin. Volcanic basins of the North Atlantic. Danmarks og Grønlands Geologiske Undersøgelse Rapport 2005/62, 141p

Larsen, M. & Whitham A.G. 2005: Evidence for a major sediment input point into the Faroe–Shetland basin from the Kangerlussuaq region of southern East Greenland. In: Doré, A.G. & Vining, B.A. (eds): Petroleum geology: North-West Europe and global perspectives. Proceedings of the 6th Petroleum Geology Conference, 913–922. London: Geological Society.

Lavwer L.A., Muller R.D., Srivastava S.P. and Roest W. 1990. The opening of the Arctic Ocean. In: U. Bleil and J. Thiede, Editors, Geological history of the Polar Oceans: Arctic versus Atlantic, Kluwer Academic Press, Amsterdam, 29–62.

Lundin, E.R. & Dore´, A.G. 1997. A tectonic model for the Norwegian passive margin with implications for the NE Atlantic: Early Cretaceous to break-up. Journal of the Geological Society, London, 154, 545–550.

Lundin E and Doré A. G. 2002. Mid-Cenozoic post-breakup deformatione in the “passive” margin bordering the Norwegian-Greenland sea. Marine and Petroleum Geology, 19, 79-93.

Lundin, E.R. & Dore´, A.G. 2005. NE Atlantic break-up: a re-examination of the Iceland mantle plume model and the Atlantic–Arctic linkage. In: Dore´, A.G. & Vining, B.A. (eds) Petroleum Geology: North-West Europe and Global Perspectives—Proceedings of the 6th Petroleum Geology Conference. Geological Society, London, 739–754.

McBirney, A.R. 1989: Geological Map of the Skaergard intrusion, Souther East Greenland, 1:50000 scale.

McClay, K. R., Norton, M. G., Coney, P., and Davis, G. H., 1986, Collapse of the Caledonide Orogen and the Old Red Sandstone: Nature, v. 323, no. 6084, p. 147-149.

Momme, P. & Wilson, R. 2002: Th e Kraemer Island macrodyke, East Greenland: solidifi cation of a fl ood basalt conduit. Geological Magazine 139, 171–190.

Morley, C.K., Nelson, R.A., Patton, T.L. & Munn, S.G. 1990. Transfer zones in the East African Rift System and their relevance to hydrocarbon exploration in rifts. AAPG Bulletin, 74, 1234–1253.

Moustafa, A.R. 2002. Controls on the geometry of transfer zones in the Suez rift and northwest Red Sea: Implications for the structural geometry of rift systems. AAPG Bulletin, 86, 979–1002.

Moy M. J. and Imber J. 2009. A critical analysis of the structure and tectonic significance of rift-oblique lineaments (‘transfer zones’) in the Mesozoic–Cenozoic succession of the Faroe–Shetland Basin, NE Atlantic margin. Journal of the Geological Society, London, Vol. 166, 2009, pp. 831–844.

Mudge, D.C. & Rashid, B. 1987. The geology of the Faeroe Basin area. In: Brooks, J. & Glennie, K. (eds) Petroleum Geology of North West Europe. Graham and Trotman, London, 751–763.

Myers, J.S. 1980: Structure of the coastal dyke swarm and associated plutonic intrusions of East Greenland. Earth and Planetary Science Letters 46, 407–418.

Naslund, H.R. 1989: Petrology of the Basistoppen sill, East Greenland: a calculated magma diff erentiation trend. Journal of Petrology 30, 299–319.

Naylor, P.H., Bell, B.R., Jolley, D.W., Durnall, P. & Fredsted, R. 1999. Palaeogene magmatism in the Faeroe–Shetland Basin: influences on uplift history and sedimentation. In: Fleet, A.J. & Boldy, S.A.R. (eds) Petroleum Geology of Northwest Europe: Proceedings of the 5th Conference. Geological Society, London, 545–558.

Nielsen, T.F.D. 1975: Possible mechanism of continental breakup in the North Atlantic. Nature 253, 182–184.

Nielsen, T. F. D. (1978). The Tertiary dike swarms of the Kangerlugssuaq area, East Greenland; an example of magmatic development during continental break-up. Contributions to Mineralogy and Petrology. 67, 63-78.

Nielsen, T.F.D. 2004: The shape and volume of the Skaergaard intrusion, Greenland: implications for mass balance and bulk composition. Journal of Petrology 45, 507–530.

Nielsen, T. F. D. & Brooks, C. K. 1981: The E Greenland rifted continental margin: an examination of the coastal flexure. Journal of Geological Society, London 138, 559–568.

Nielsen, T. F. D., Soper, N. J., Brooks, C. K., Faller, A. M., Higgins, A. C. & Matthews, D. W. 1981: The pre-basaltic sediments and the Lower Basalts at Kangerdlugssuaq, East Greenland: Their stratigraphy, lithology, palaeomagnetism and petrology. Meddelelser om Grønland, Geoscience 6, 3–25.

Nielsen T. F. D. 2002. Palaeogene intrusions and magmatic complexes in East Greenland, 66 to 75º N. Geological Survey of Denmark and Greenland Rapport, 2002/113, pp. 249.

Nielsen, T. K., and J. R. Hopper, 2002, Formation of volcanic rifted margins: are temperature anomalies required?, Geophysical Research Letters , 29 , doi: 10.1029/2002GL015,681.

Nielsen, T. K., and J. R. Hopper, 2004, From rift to drift: mantle melting during continental breakup, Geochemistry Geophysics Geosystems , 5 , doi: 10.1029/2003GC000,662.

Nunns A. G. 1983. Plate tectonic evolution of the Greenland Scotland Ridge and surrounding regions. In: M.P.H. Bott, S. Saxon, M. Talwani and J. Thiede, Editors, Structure and development of the Greenland Scotlands Ridge, new methods and concepts, Plenum Press, New York, 11–30.

Nøhr-Hansen, H. 2012: Palynostratigraphy of the Cretaceous–lower Palaeogene sedimentary succession in the Kangerlussuaq Basin, southern East Greenland. Review of Palaeobotany and Palynology 178, 59-90.

Olesen, O., Gellein, J., Håbrekke, H., Kihle, O., Skilbrei, J. R., & Smethurst, M. A. 1997. Magnetic anomaly map, Norway and adjacent ocean areas. Scale 1:3 million, Geological Survey of Norway.

Peate, I.U., Larsen, M. & Lesher, C.E. 2003: Th e transition from sedimentation to fl ood volcanism in the Kangerlussuaq Basin, East Greenland: basaltic pyroclastic volcanism during initial Palaeogene continental break-up. Journal of the Geological Society (London) 160, 759–772, http://dx.doi.org/10.1144/0016-764902-071

Pedersen, A. K., Watt, M., Watt, W. S. & Larsen, L. M. 1997: Structure and stratigraphy of the Early Tertiary basalts of the Blosseville Kyst, East Greenland. Journal of the Geo-logical Society, London 154, 565–570.

Quinn, M., and Ziska, H., 2010, Permian and Triassic, in Ritchie, J. D., Ziska, H., Johnson, H., and Evans, D., eds., Geology of the Faroe-Shetland Basin and adjacent areas.: Keyworth, Nottingham, UK, British Geological Survey, p. 92-102.

Ritchie, J.D. & Darbyshire, D.P.F. 1984. Rb–Sr dates on Precambrian rocks from marine exploration wells in and around the West Shetland Basin. Scottish Journal of Geology, 20, 31–36.

Ritchie, J.D., Johnson, H. & Kimbell, G.S. 2003. The nature and age of Cenozoic contractional deformation within the NE Faroe–Shetland Basin. Marine and Petroleum Geology, 20, 399–409.

Ritchie, J.D., Johnson, H., Quinn, M.F. & Gatliff, R.W. 2008. The effects of Cenozoic compression within the Faroe–Shetland Basin and adjacent areas. In: Johnson, H., Dore´ , A.G., Gatliff, R.W., Holdsworth, R.E., Lundin, E.R. & Ritchie, J.D. (eds) The Nature and Origin of Compression in Margins. Geological Society, London, Special Publications, 306, 121–136.

Roberts, D.G., Thompson, M., Mitchener, B., Hossack, J., Carmichael, S.M.M. & Bjørnseth, H.M. 1999. Palaeozoic to Tertiary rift and basin dynamics: mid-Norway to the Bay of Biscay: a new context for hydrocarbon prospectivity in the deep water frontier. In: Fleet, A.J. & Boldy, S.A.R. (eds) Petroleum Geology of Northwest Europe: Proceedings of the 5th Conference. Geological Society, London, 7–40.

Rosing, M.T., Lesher, C.E. & Bird, D.K. 1989: Chemical modifi -cation of East Greenland Tertiary magmas by two-liquid interdiffusion. Geology 17, 626–629.

Rumph, B., Reaves, C.M., Orange, V.G. & Robinson, D.L. 1993. Structuring and transfer zones in the Faeroe Basin in a regional tectonic context. In: Parker, J.R. (ed.) Petroleum Geology of Northwest Europe: Proceedings of the 4th Conference. Geological Society, London, 999–1009.

Saunders, A. D., Fitton, J. G., Kerr, A. C., Norry, M. J. & Kent, R. W. (1997). The North Atlantic Igneous Province. In: Mahoney, J. J. & Coffin, M. L. (eds) Large Igneous Provinces. Washington, DC: American Geophysical Union, 45-93.

Saunders, A.D., H.C. Larsen, S. Wise, et al., 1998, Proceedings of the Ocean Drilling Program, Scientific Results, Leg 152, Ocean Drilling Program, College Station, Tex.

Smallwood, J.R. & Gill, C.E. 2002. The rise and fall of the Faroe–Shetland Basin: evidence from seismic mapping of the Balder Formation. Journal of the Geological Society, London, 159, 627–630.

Smith, K., and Ziska, H., 2010, Devonian and Carboniferous, in Ritchie, J. D., Ziska, H., Johnson, H., and Evans, D., eds., Geology of the Faroe-Shetland Basin and adjacent areas.: Keyworth, Nottingham, UK, British Geological Survey, p. 79-91.

Soper, N. J., higgens, A. C., Dowie, C., Matthews, D. W. & Brown, P. E. 1976: Late Cretaceous-early Tertiary stratigraphy of the Kangerlussuaq area, east Greenland, and the age of the opening of the north-east Atlantic. Journal of Geological Society, London 130, 85–104.

Storey, M., Duncan R.A. & Tegner, C. 2007b: Timing and duration of volcanism in the North Atlantic Igneous Province: implications for geodynamics and links to the Iceland hotspot. Chemical Geology 241, 264–281, Stoker, M.S., Praeg, D., Shannon, P.M., et al. 2005. Neogene evolution of the Atlantic continental margin of NW Europe (Lofoten Islands to SW Ireland): anything but passive. In: Dore´ , A.G. & Vining, B.A. (eds) Petroleum Geology: North-West Europe and Global Perspectives: Proceedings of the 6th Petroleum Geology Conference. Geological Society, London, 1057–1076.

Taylor, B., and Huchon, P. 2002: Active continental extension in the western Woodlark Basin: a synthesis of Leg 180 results. In Huchon, P., Taylor, B., and Klaus, A. (Eds.), Proc. ODP, Sci. Results, 180, 1–36

Talwani M. and Eldholm O. 1977. Evolution of the Norwegian–Greenland Sea. Geological Society of America Bulletin **88**, 969–999.

Tegner, C., Duncan, R. A., Bernstein, S., Brooks, C. K., Bird, D. K. & Storey, M. 1998. 40Ar-39Ar geochronology of Tertiary mafic intrusions along the East Greenland rifted margin: relation to flood basalts and the Iceland hotspot track. Earth and Planetary Science Letters 156, 75-88.

Thy, P., Lesher, C.E., Larsen, H.C., et al., Proceedings of the Ocean Drilling Program, Initial Reports, Leg 163X, Ocean Drilling Program, College Station, Tex.

Torsvik T., Mosar J. and Eide E. . 2001. Cretaceous-Tertiary geodynamics: a North Atlantic excercise. Geophysical Journal International. **146**, 1–23.

Tron V. and Brun JP 1991: Experiments on oblique rifting in brittle-ductile systems. Tectonophysics, 188, 71-84

Turner, J.D. & Scrutton, R.A. 1993. Subsidence patterns in western margin basins: evidence from the Faeroe–Shetland Basin. In: Parker, J.R. (ed.) Petroleum Geology of Northwest Europe: Proceedings of the 4th Conference. Geological Society, London, 975–983.

Ukstins Peate I., Larsen M., Lesher C. E. 2003. The transition from sedimentation to flood volcanism in the Kangerlussuaq basin, East Greenland: basaltic pyroclastic volcanism during initial Palaeogene continental break-up. Journal of the Geological Society, 160, 759-772.

Vogt, P. R. 1986. Geophysical and geochemical signatures in plate tectonics. In Hurdle, B. G. (Ed.), The Nordic Seas, Springer-Verlag, New York, pp. 413–662.

Vosgerau, H., Guarnieri, P., Weibel, R., Larsen, M., Dennehy, C., Sørensen, E.V. & Knudsen, C. 2010: Study of a Palaeogene intrabasaltic sedimentary unit in southern East Greenland: from 3-D photography to micropetrography. Geological Survey of Denmark and Greenland Bulletin 20, 75–78.

Wager, L. R. (1935). Geological investigations in East Greenland. Part II. Geology of Kap Dalton. Meddelelser om Grùnland 105(3), 1-32.

Wager, L. R. (1947). Geological investigations in East Greenland. Part IV. The stratigraphy and tectonics of Knud Rasmussens Land. Meddelelser om Grùnland 134(5), 1-64.

Wager, L.R. & Deer, W.A. 1939: Geological investigations in East Greenland. Part III: Th e petrology of the Skaergaard intrusion, Kangerdlugssuaq, East Greenland. Meddelelser om Grønland 105(4), 352 pp.

Waight, T.E. & Lesher, C.E. 2010: Pb isotopes during crustal melting and magma mingling – a cautionary tale from the Miki Fjord macrodike, central east Greenland. Lithos 118, 191–201

Walker R. J., Holdsworth R. E., Imber J. & Ellis D.: Onshore evidence for progressive changes in rifting directions during continental break-up in the NE Atlantic. Journal of the Geological Society, London, Vol. 168, 2011, pp. 27–48.

White, R. & McKenzie, D. 1989. Magmatism at rift zones: the generation of volcanic continental margins and flood basalts. Journal of Geophysical Research, Solid Earth and Planets, 94, 7685–7729.

White, C.M., Geist, D.J., Frost, C.D. & Verwoerd, W.J. 1989: Petrology of the Vandfaldsdalen macrodike, Skaergaard region, East Greenland. Journal of Petrology 30, 271–299.